EFFECT OF ELECTROLYTE/SULFUR RATIO IN THE CATHODE ON THE ELECTROCHEMICAL PERFORMANCE OF Li-S BATTERIES

A THESIS SUBMITTED TO
THE GRADUATE SCHOOL OF NATURAL AND APPLIED SCIENCES
OF
MIDDLE EAST TECHNICAL UNIVERSITY

BY

NUR BER EMERCE

IN PARTIAL FULFILLMENT OF THE REQUIREMENTS
FOR
THE DEGREE OF MASTER OF SCIENCE
IN
CHEMICAL ENGINEERING

JANUARY 2019

Approval of the thesis:

EFFECT OF ELECTROLYTE/SULFUR RATIO IN THE CATHODE ON THE ELECTROCHEMICAL PERFORMANCE OF Li-S BATTERIES

submitted by **NUR BER EMERCE** in partial fulfillment of the requirements for the degree of **Master of Science in Chemical Engineering Department, Middle East Technical University** by,

Prof. Dr. Halil Kalıpçılar
Dean, Graduate School of **Natural and Applied Sciences** _____

Prof. Dr. Pınar Çalık
Head of Department, **Chemical Engineering** _____

Prof. Dr. Görkem Külah
Supervisor, **Chemical Engineering Dept., METU** _____

Asst. Prof. Dr. Damla Eroğlu Pala
Co-Supervisor, **Chemical Eng. Dept., Boğaziçi University** _____

Examining Committee Members:

Prof. Dr. Tayfur Öztürk
Metallurgical and Materials Engineering Dept., METU _____

Prof. Dr. Görkem Külah
Chemical Engineering Dept., METU _____

Asst. Prof. Dr. Damla Eroğlu Pala
Chemical Engineering Dept., Boğaziçi University _____

Asst. Prof. Dr. Burak Ülgüt
Chemistry Dept., Bilkent University _____

Asst. Prof. Dr. Harun Koku
Chemical Engineering Dept., METU _____

Date: 23.01.2019

I hereby declare that all information in this document has been obtained and presented in accordance with academic rules and ethical conduct. I also declare that, as required by these rules and conduct, I have fully cited and referenced all material and results that are not original to this work.

Name, Surname: Nur Ber Emerce

Signature:

ABSTRACT

EFFECT OF ELECTROLYTE/SULFUR RATIO IN THE CATHODE ON THE ELECTROCHEMICAL PERFORMANCE OF Li-S BATTERIES

Emerce, Nur Ber
M.Sc., Department of Chemical Engineering
Supervisor: Prof. Dr. Görkem Külah
Co-Supervisor: Asst. Prof. Dr. Damla Eroğlu Pala

January 2019, 141 pages

In this study, the effect of electrolyte to sulfur (E/S) ratio in the cathode, which is an important cell design parameter, on the electrochemical and cell- and system-level performance of a Lithium-Sulfur (Li-S) battery is investigated through modeling efforts. First, a 1-D electrochemical model is developed for an isothermal, constant-current discharge of a Li-S cell to predict the voltage at 60% discharge depth. In the model, cathode exchange current density is defined as a linear function of the electrolyte amount. Increasing the E/S ratio improves the electrochemical performance at different current densities. Next, cell- and system-level performance models based on the developed electrochemical model are proposed. In these models, the cathode specific capacity is either defined as a linear function of the E/S ratio or taken constant. The model, in which the cathode specific capacity depends on the E/S ratio, predicts that increasing E/S ratio increases the cell- and system-level specific energy and energy density until 10 mL g_{sulfur}^{-1}. However, when the cathode specific capacity is kept constant at 1200 mAh g_s^{-1} in the model, the specific energy and energy density at the cell and system level decrease significantly with increasing electrolyte amount. In the cell- and system-level performance analysis, the effect of other critical cell parameters such as the cathode thickness, carbon to sulfur ratio, S loading and excess Li amount are also considered. As a result, Li-S batteries with high cell- and system-level performance can be designed with the optimum E/S ratio and specified cell design parameters.

Keywords: Lithium-sulfur battery, electrolyte to sulfur ratio, electrochemical modeling, cell and system level performance

ÖZ

KATOTTA ELEKTROLİTE SÜLFÜR ORANININ LİTYUM-SÜLFÜR BATARYALARININ ELEKTROKİMYASAL PERFORMANSINA ETKİSİ

Emerce, Nur Ber
Yüksek Lisans, Kimya Mühendisliği Bölümü
Tez Danışmanı: Prof. Dr. Görkem Külah
Ortak Tez Danışmanı: Yrd. Doç. Dr. Damla Eroğlu Pala

Ocak 2019, 141 sayfa

Bu çalışmada, Li-S bataryalarında önemli bir hücre tasarım parametresi olan katotta elektrolite sülfür (E/S) oranının elektrokimyasal ve hücre- ve sistem-düzeyi performansa etkisi modellenmiştir. Öncelikle Li-S hücresinin izotermal ve sabit-akım deşarjı için tek-boyutlu bir elektrokimyasal model geliştirilerek hücrenin %60 deşarj derinliğindeki voltajı öngörülmüştür. Katottaki tek kinetik parametre olan katot değişim akım yoğunluğu modelde elektrolit miktarının lineer bir fonksiyonu olarak tanımlanmıştır. Model artan E/S oranının hücrenin elektrokimyasal performansını akım yoğunluğundan bağımsız olarak geliştirdiğini öngörmektedir. Önerilen bu elektrokimyasal model kullanılarak hücre- ve sistem-düzeyi performans modelleri de geliştirilmiştir. Bu modellerde katottaki spesifik kapasite, ya E/S oranının lineer bir fonksiyonu olarak belirlenmiş ya da 1200 mAh g_s^{-1} olarak sabit tutulmuştur. Katottaki spesifik kapasitenin elektrolit miktarına bağlı olarak tanımlandığı model, artan E/S oranının hücrenin ve bataryanın spesifik enerji ve enerji yoğunluğunu 10 mL gs^{-1} oranına kadar arttırdığını öngörmektedir. Modelde spesifik kapasitenin sabit tutulduğu durumda ise hücre- ve sistem-düzeyi spesifik enerji ve enerji yoğunluğunun artan E/S oranıyla düştüğü görülmüştür. Hücre- ve sistem-düzeyi performans analizlerinde, katot kalınlığı, katotta karbona sülfür oranı, S yükleme oranı ve anotta fazla Li miktarı gibi diğer önemli hücre parametrelerinin

etkisi de göz önünde bulundurulmuştur. Sonuç olarak, yüksek hücre- ve sistem-düzeyi performansa sahip Li-S bataryaların optimum E/S oranı ve belirlenen diğer hücre parametreleri ile elde edilebileceği sonucuna varılmıştır.

Anahtar Kelimeler: Lityum-sülfür batarya, elektrolitin sülfüre oranı, elektrokimyasal modelleme, hücre ve sistem düzeyi performans

To My Family

ACKNOWLEDGEMENTS

I would like to present my deepest appreciations to my co-advisor Asst. Prof. Dr. Damla Eroğlu Pala for her unbroken guidance, supports and patience throughout my study. Since my undergraduate education, her wisdom and encouragements motivated me and I am very happy to graduate as her master student. Also, I would like to give special thanks to my supervisor Prof. Dr. Görkem Külah for her support and advice during my thesis study.

I would like to thank the Scientific and Technological Research Council of Turkey (TUBITAK), Grant No: 116M574 for financially supporting. This study was also supported in part by ENDAM, Center for Energy Materials and Storage Devices, Middle East Technical University.

I thank my lovely friends, Nisa Erişen, Yağmur Çulhacıoğlu, Aslı Karausta, Beril Dumanlılar, Soner Yaşar, Selin Şahin, Almira Çaldıklıoğlu, Fatma Şahin, Merve Sarıyer, Merve Özkutlu, Ezgi Yavuzyılmaz, Seda Sivri, Zeynep Karakaş and Berrak Erkmen and Ezgi Gözde for their friendship, helps and precious advices. Also, I would like to express my special thanks to Can Yıldırım for his moral support. I am so glad to have them in my life.

Last but not the least, I want to give my deepest gratitude to my family; Gülistan Emerce, Beril Emerce, Arzu Cülcül, Şeyda Aydoğdu, and rest of my family for their unconditional love and support.

TABLE OF CONTENTS

LIST OF TABLES

TABLES

LIST OF FIGURES

FIGURES

LIST OF SYMBOLS

a	Superficial area in cm^{-1}
A_{cell}	Cell area in cm^2
A_{layer}	Layer area in cm^2
A_{pack}	Pack area in cm^2
ASI	Area-Specific Impedance
ASI_{cc+}	Positive collector ASI in Ω cm^2
ASI_{cc-}	Negative collector ASI in Ω cm^2
ASI_{cell}	Total ASI of the cell in Ω cm^2
ASI_{ne}	Anode ASI in Ω cm^2
ASI_{pe}	Cathode ASI in Ω cm^2
ASI_{sep}	Separator ASI in Ω cm^2
$ASI_{total\ ,p}$	Total ASI of the cell at rated power in Ω cm^2
$ASI_{total\ ,e}$	Total ASI of the cell at rated energy in Ω cm^2
BatPac	Battery Performance and Cost
BET	Brunauer-Emmett-Teller analysis
c	Specific capacity in Ah cm^{-2}
C	Discharge rate in Ah g_s^{-1}
c_{ne}	Negative electrode capacity in Ah cm^{-3}
c_{pe}	Positive electrode capacity in Ah cm^{-3}
$c_{pos,act}$	Positive active material capacity in Ah g_s^{-1}
$c_{neg,act}$	Negative active material capacity in Ah g_s^{-1}
DOD	Depth of Discharge
DOL:DME	Dioxolane: Dimethoxy ethane
E	Battery pack energy in kWh
EV	Electric vehicles
E/S	Electrolyte/Sulfur Ratio in mL g_s^{-1}
F	Faraday constant

$H_{batt.\ pack}$	Height of battery pack in mm
H_{module}	Height of module in mm
$i_{o,ne}$	Anode exchange current density in A cm^{-2}
$i_{0,pe}$	Cathode exchange current density in A cm^{-2}
i_1	Current density of matrix phase in the cathode
i_2	Current density of electrolyte phase in the cathode
I	Current density in A cm^{-2}
Ie	Average current density in A cm^{-2}
Ip	Pulse power current density in A cm^{-2}
L_{anode}	Anode thickness in mm
L_{cc^-}	Positive current collector thickness in mm
L_{cc^+}	Negative current collector thickness in mm
L_{pe}	Cathode thickness in mm
L_{sep}	Thickness of separator in mm
$L_{pos.\ electrode}$	Thickness of positive electrode in mm
$L_{cell\ edge}$	Thickness of cell edge from positive elect. to outside of fold in mm
L_{cell}	Thickness of cell in mm
$L_{cc\ tabs}$	Thickness of current collector tabs in mm
L_{module}	Thickness of module in mm
L_{term}	Thickness of terminal in mm
$L_{cooling\ fin}$	Thickness of cooling fin in mm
$L_{coolant\ space}$	Thickness of coolant space above and below modules in mm
$L_{battery\ pack}$	Thickness of battery pack in mm
$L_{total\ battery\ jacket}$	Thickness of total battery jacket in mm
$LiNO_3$	Lithium nitrate
Li-S	Lithium-Sulphur
LiTFSI	Lithium bis(trifluoro methane sulfonyl)imide
m_b	Binder loading in the cathode in g cm^{-2}
m_c	Carbon loading in the cathode in g cm^{-2}
m_{cc+}	Positive current collector mass in g cm^{-2}

m_{cc-}	Negative current collector mass in g cm^{-2}
m_e	Electrolyte loading in the cathode in g cm^{-2}
m_{ne}	Negative electrode mass in g_{ne} cm^{-2},
m_{pe}	Positive electrode mass in g_{pe} cm^{-2}
m_s	Sulfur loading in the cathode in g cm^{-2}
m_{sep}	Separator mass in g_{sep} cm^{-2}
$m_{module\ SOC\ reg.}$	Module SOC regulator assembly mass in g
$m_{balance\ of\ mod.}$	Balance of module material mass in kg
$m_{mod.\ term.}$	Module terminal mass in kg
$m_{pos.\ term.\ assem.}$	Positive terminal assembly mass in g
$m_{neg.\ term.\ assem.}$	Negative terminal assembly mass in g
$m_{cell\ container}$	Cell container mass in g
$m_{each\ mod.\ inter.}$	Each module interconnect mass in kg
$m_{mod.\ comp.\ plates\ steel\ strap}$	Module compression plates and steel straps mass in g
$[L/W]_{pos.\ elect.}$	Length to width ratio for positive electrode
N/P	Negative-to-positive capacity ratio
OCV	Open-circuit voltage
P	Battery pack power in kW
PET	Polyethylene terephthalate
PP	Polypropylene
PS	Polysulfides
PVDF	Polyvinylidene difluoride
Q	Cell capacity in Ah cm^{-2}
R	Gas constant
SEI	Solid-Electrolyte Interphase
T	Temperature in kelvin
t_{cell}	Thickness of cell thickness in mm
$t_{cell\ container\ Al\ layer}$	Thickness of Aluminum layer of cell container in μm
$t_{cell\ edge\ from\ pos.elect.\ to\ outside\ fold}$	Thickness of cell edge from positive electrode to outside fold in mm

$t_{neg.\ foil}$	Thickness of negative foil in mm
$t_{pos.\ foil}$	Thickness of positive foil in mm
$t_{pos.\ elect.\ at\ adj.\ OCV}$	Thickness of positive electrode at adjusted OCV in mm
$t_{neg.\ elect.\ at\ adj.\ OCV}$	Thickness of negative electrode at adjusted OCV in mm
t_{sep}	Thickness of separator in mm
t_{pouch}	Thickness of pouch in mm
$t_{cell\ container}$	Thickness of cell container in µm
t_{term}	Thickness of terminal in mm
$t_{module\ wall}$	Thickness of module wall in mm
$t_{module\ compr.\ plate}$	Thickness of module compression plate in mm
$t_{total\ battery\ jacket}$	Thickness of total battery jacket in mm
$t_{battery\ pack\ insulation}$	Thickness of battery pack insulation in mm
U	Open-circuit voltage of the cell in V
V_b	Binder volume value per cm^{-2} in $cm^3\ cm^{-2}$
VBA	Visual Basic for Applications
V_c	Carbon volume value per cm^{-2} in $cm^3\ cm^{-2}$
V_{cc+}	Positive current collector volume in $cm^3\ cm^{-2}$
V_{cc-}	Negative current collector volume in $cm^3\ cm^{-2}$
V_e	Electrolyte volume value per cm^{-2} in $cm^3\ cm^{-2}$
Ve	Voltage at rated energy in V
V_{cell}	Cell voltage in V
V_{ne}	Negative electrode volume in $cm^3\ cm^{-2}$
Vp	Voltage at rated power in V
V_s	Sulfur volume value per cm^{-2} in $cm^3\ cm^{-2}$
V_{sep}	Separator volume in $cm^3\ cm^{-2}$
v_b	Binder volume fraction in the cathode
v_c	Carbon volume fraction in the cathode
v_e	Electrolyte volume fraction in the cathode

v_s	Sulfur volume fraction in the cathode
$w_{pe,act}$	Sulfur weight fraction in the cathode
$w_{ne,act}$	Lithium weight fraction in the anode
$W_{pos.\ elect.}$	Weight of positive electrode in mm
W_{cell}	Weight of the cell in mm
W_{term}	Weight of the terminal in mm
W_{module}	Weight of the module in mm
$W_{total\ bat.\ jacket}$	Weight of total battery jacket in mm

Greek Symbols

α_{ne}	Transfer coefficient
ε_{dis}	Discharged volume fraction in mAh cm^{-3}
η_{cc+}	Positive collector overpotential in V
η_{cc-}	Negative collector overpotential in V
η_{cell}	Total overpotential of the cell in V
η_{ne}	Anode overpotential in V
η_{pe}	Cathode overpotential in V
η_{sep}	Separator overpotential in V
$\eta_{total,e}$	Total overpotential of the cell at rated energy in V
$\eta_{total,p}$	Total overpotential of the cell at rated power in V
κ_{eff}	Effective ionic conductivity in S cm^{-1}
$\kappa_{eff,sep}$	Effective ionic conductivity of the separator in S cm^{-1}
ρ_{Al}	Aluminum density in g cm^{-3}
ρ_b	Binder density in g cm^{-3}
ρ_c	Carbon density in g cm^{-3}
ρ_{cc+}	Positive current collector density in g cm^{-2}
ρ_{cc-}	Negative current collector density in g cm^{-2}
ρ_{Cu}	Copper density in g cm^{-3}

ρ_{SS}	Stainless steel density in g cm^{-3}
ρ_{e}	Electrolyte density in g cm^{-3}
ρ_{s}	Sulphur density in g cm^{-3}
$\rho_{coolant}$	Coolant density in g cm^{-3}
$\rho_{ne,total}$	Negative electrode density in g cm^{-3},
$\rho_{pe,total}$	Positive electrode density in g cm^{-3}
ρ_{sep}	Separator density in g cm^{-3}
ϕ_{1}	Potential of matrix phase in the cathode
ϕ_{2}	Potential of electrolyte phase in the cathode
σ_{Cu}	Copper conductivity in $\Omega^{-1}cm^{-1}$
σ_{Al}	Aluminum conductivity in $\Omega^{-1}cm^{-1}$
σ_{eff}	Effective electronic conductivity in S cm^{-1}

CHAPTER 1

INTRODUCTION

As the global energy consumption continues to increase, the demand for fossil fuels also increases. However, increasing fossil fuel usage causes higher greenhouse gas emissions especially in transportation. According to a study, in the U.S. conventional gasoline cars comprise approximately 27% of the total greenhouse gas emissions [1]. Therefore, by replacing the fossil fuels by the renewable sources such as wind, solar etc. air pollution and global warming can be prevented. For example, by using renewable sources in transportation, CO_2 emission can be reduced significantly. Consequently, developing efficient and cost friendly energy storage systems is very important. Li-ion batteries, which was first commercialized by Sony in 1991, have been used in many applications such as in portable devices and EVs because of their high energy density [2, 3]. However, with developing technologies, improvements in the energy, safety, durability and cost of the Li-ion batteries are required [4]. For instance, Li-ion batteries cannot meet the requirements for the current EVs. For example, advanced EVs, which have a 300 mile range, need a battery with 350-400 Wh kg^{-1} cell level specific energy [5]. However, Li-ion batteries can provide 80-150 Wh kg^{-1} [1, 6]. As a result, researchers work on new battery chemistries with higher specific capacities. Lately, Li-S batteries have gained significant attention because of their high theoretical specific energy. Li-S batteries were first introduced in 1960s but, the progress has been slow due to the improvements in Li-ion batteries [7]. In 2009, Li-S batteries have regained interest as a result of improved cycling performance by Nazar et al. [8]. Sulfur as an active material is advantageous for the rechargeable batteries because sulfur has high theoretical specific capacity of 1675 mAh g_s^{-1}. In addition, sulfur is a non-toxic, naturally abundant and low cost material [9–14]. Li-S battery has a higher energy storage ability compared to a Li-ion battery, as given in Table 1.1.

Table 1.1. The comparison of cell voltage, specific energy and energy density of Li-S batteries and Li-ion batteries [3,5,8–10,12,15–18]

Battery	Working Voltage (V)	Theoretical Specific Energy (Wh kg^{-1})	Theoretical Energy Density (Wh L^{-1})
Li-ion	3.8	387	1015
Li-S	2.2	2567	2199

The U.S. Department of Energy projects that the future battery for EV will have greater than 250 Wh kg^{-1} specific energy and 400 Wh L^{-1} energy density in 2020 [19]. In commercialized batteries, usually 25-40 % of the theoretical specific energy can be used [20, 21]. Li-ion batteries can only supply 200-250 Wh kg^{-1} specific energy, whereas Li-S batteries can satisfy the future EV battery requirements with a prototype specific energy of 200- 400 Wh kg^{-1}. For instance, Sion Power and Oxis Energy companies produced Li-S prototypes with approximately 350-400 Wh kg^{-1} specific energy [16, 17, 22–25]. However, their batteries have only approximately 700 Wh L^{-1}. Since for EV applications energy density is more important, improving the energy density of the Li-S battery has become critical.

The Li-S battery contains a sulfur-carbon composite porous cathode, organic electrolyte, a porous separator and a lithium anode [10, 13]. The schematic configuration of a typical Li-S battery is given in Figure 1.1 and the overall redox reaction is shown in Equation 1.1.

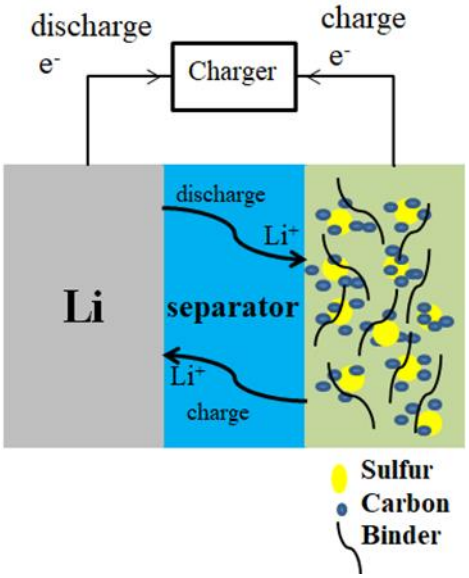

Figure 1. 1. A typical Li-S battery

$$16\,Li + S_8 \rightarrow 8Li_2S \qquad (1.1)$$

Sulfur is used in S_8 form which is the most stable type among its 30 allotropes [13]. In the battery, discharge and charge processes occur with multi-step redox reactions. During the discharge, S_8 is reduced to Li_2S via multistage redox reactions from long chain to short chain polysulfides. The redox steps and the cell voltage profile during discharge and charge are given in Equations 1.2-1.6 and Figure 1.2, respectively [3, 4, 12, 26].

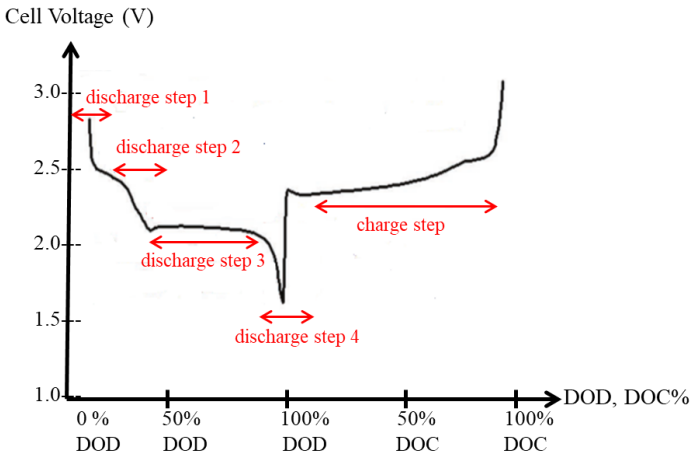

Figure 1. 2. The voltage profile of a Li-S battery during discharge and charge

Discharge step 1: sulfur reduces to high-order polysulfides which have high solubility in the electrolyte

$$S_{8(s)} + 2Li^+ + 2e^- \rightarrow Li_2S_8 \quad (1.2)$$

Discharge step 2: high order polysulfides reduce to low order polysulfides

$$Li_2S_8 + 2Li^+ + 2e^- \rightarrow 2Li_2S_4 \quad (1.3)$$

Discharge step 3: low order polysulfides reduce to insoluble solid Li_2S_2 and Li_2S mixture. This liquid to solid transition comprises the major part of the cathode capacity.

$$Li_2S_4 + 2Li^+ + 2e^- \rightarrow 2Li_2S_{2(s)} \quad (1.4)$$

$$Li_2S_4 + 6Li^+ + 6e^- \rightarrow 4Li_2S_{(s)} \quad (1.5)$$

Discharge step 4: Li_2S_2 converts to Li_2S slowly because of solid to solid transition.

$$Li_2S_{2(s)} + 2Li^+ + 2e^- \rightarrow 2Li_2S_{(s)} \quad (1.6)$$

Despite their advantages, Li-S batteries suffer from major challenges related to both the sulfur and the lithium electrode. These challenges are poor electrode conductivity, polysulfide shuttle mechanism and instability of the lithium anode surface [9, 10, 17, 18, 27, 28]. Firstly, both sulfur ($5x10^{-30}$ S cm^{-1} conductivity [18]) and its end products, Li_2S and Li_2S_2, have insulating natures. Therefore, accumulation of these on the cathode surface causes lower sulfur utilization in the cell [7,9,17,29]. Secondly, polysulfide shuttle mechanism, which is unique to Li-S batteries, may occur because of the diffusion of high and low order polysulfides within the electrodes. During discharge, high order polysulfides have a high concentration in the cathode and, due to the concentration difference between the two electrodes, they can diffuse to the anode. There they are converted into either low order polysulfides or Li_2S and Li_2S_2. Then, low order polysulfides can diffuse back to the cathode again to create high order polysulfides. This circulation called

the polysulfide shuttle mechanism leads to fast capacity fade and low coulombic efficiency in the cell [12, 15–17, 19, 30–32]. Another challenge in the cell is the instability of the lithium surface electrolyte interphase (SEI), which is the interphase film formed by a side reaction of the Li metal with the electrolyte. This side reaction may result in Li metal or electrolyte depletion in the cell. Moreover, as mentioned before, polysulfides and non-conducting products, Li_2S and Li_2S_2, can accumulate on the anode because of the shuttle mechanism. Accumulation of these on the anode surface due to the absence of a stable SEI may cause corrosion on the anode surface in addition to an increase in the cell resistance [14, 16, 26, 29].

In Li-S batteries, there are important design parameters at the cell-level that influence the materials level properties such as the reaction and degradation mechanisms greatly. In addition, these design parameters also determine the cell level performance (cycle life, sulfur utilization and useable specific capacity) and system level performance (energy density, specific energy and original equipment manufacturer (OEM) cost) significantly [10]. These design parameters are explained below.

The cell level design parameters:

- Excess lithium amount in the anode (in other words negative electrode capacity to positive electrode capacity ratio (N/P ratio)): Since SEI film on the lithium surface is unstable, it consumes lithium and electrolyte continuously. Therefore, excess lithium is typically needed to improve the cyclability of the cell [17]. However, excess amount of lithium influences the cell and system level energy density and specific energy negatively via increasing the cell mass and volume.
- Specific capacity of the cell: Cathode specific capacity, or discharge capacity in other words, is the amount of charge delivered per unit sulfur mass in the electrode (mAh g_s^{-1}). High and retainable specific capacities are critical to obtain good cell and system level performance since specific capacity is also a measure of the sulfur utilization in the cell.

- Electrolyte amount (in other words electrolyte to sulfur ratio (E/S)): Electrolyte amount in the cathode directly affects the polysulfide concentration on the cathode surface, and thus plays a critical role in reaction and polysulfide shuttle mechanisms. Increasing electrolyte amount improves the reaction kinetics thus the specific capacity and the cyclability of the cell. On the other hand, it has a negative impact on the energy density and specific energy.
- Carbon to sulfur ratio (C/S): Because of the insulating nature of sulfur, carbon, which has a good electronic conductivity, is typically needed in the cell in excess amounts. Carbon amount increases both the electrochemically active area and the electronic conductivity in the cathode and thus improves the cathode kinetics. Therefore, it improves the discharge capacity and the cyclability of the cell. However, increasing carbon content may decrease the cell and system level energy density after a point since it is an inactive material in the cell.
- Sulfur loading: S loading, which depends on the cathode thickness, is critical as it determines the areal specific capacity in the cell. As the cathode thickness, and thus the active material loading, increases, the energy density of the cell increases remarkably. However, due to the transport limitations in thicker electrodes, the discharge capacity and cycle life of the cell could be affected inversely.
- Current density: It affects both the specific capacity and the capacity retention of the cell. Typically, cell kinetics is improved at lower current densities as transport limitations become less significant. C-rate is a measure of the current density normalized for the cell capacity. For instance, a C-rate of C/5 means that the cell is discharged at a current density at which the cell will be discharged entirely at 5 h.

These cell level design parameters are critical for the performance of a Li-S battery because that they influence the reaction and degradation mechanisms by means of the material level parameters such as the surface area for electron transfer and polysulfide concentration in the cell. A detailed literature survey of the experimental

and modeling studies about the effect of these design parameters is given in Chapter 2.

1.1 Scope of Current Work

The E/S ratio is a critical design parameter of the cell because it affects the electrochemical performance of the cell by means of the precipitation and dissolution reaction and polysulfide shuttle mechanisms. For example, higher electrolyte amount provides better wettability of the electrode and therefore, an easier ion transport within the cell. In addition, it prevents incomplete sulfur utilization and also the polysulfide shuttle mechanism. However, when the E/S ratio is too high, it causes a decrease in the columbic efficiency and the capacity, which affects the specific energy and energy density of the cell. On the other hand, if the ratio is too low, the cell has poor capacity retention. Therefore, the amount of the E/S ratio should be selected carefully. In the literature, there are many experimental studies on the E/S ratio effect on the electrochemical performance of the cell. However, the modeling effort on investigating the effect of this key design parameter is very limited. Therefore, a simple model predicting the effect of E/S ratio on the cell- and system-level performance of a Li-S battery is required in the literature.

In this thesis, the effect of E/S ratio in the cell on the electrochemical and cell- and system level performance of a Li-S battery was investigated. For this purpose, a 1-D electrochemical model was developed for constant current, isothermal discharge of a Li-S cell. The proposed model assumes that there are no concentration gradients or shuttle mechanism within the cell. Another major assumption of the model is that there is a single reaction in each of the two discharge voltage plateaus. In the model, Butler-Volmer equation is used at the negative electrode, Ohm's Law is used at the separator and the Porous Electrode Theory is used at the positive electrode [34]. In the second part of this study, cell and system level performance models were developed using the proposed electrochemical model to predict the performance of a Li-S battery as a function of the E/S ratio. Each of these models is described in Chapter 3. In the electrochemical model, the cathode exchange current density was

defined as a function of the electrolyte amount. As a result of this novel approach, the model can capture the trend seen for the experimental studies. An additional novelty of the study is that the specific capacity of the cell was described as a function of the E/S ratio in the cell and system level performance models. The impact of the E/S ratio on the performance of the battery was discussed also as a function of other critical design parameters such as cathode thickness, carbon to sulfur (C/S) ratio in the cathode, excess Li% in the anode (N/P ratio), sulfur loading, current density and cathode specific capacity. Based on these implications, electrochemical and cell- and system- level performances of the Li-S battery with varying E/S ratio were determined and the results are given in Chapter 4.

CHAPTER 2

LITERATURE SURVEY

In this thesis, the effect of E/S ratio on the electrochemical performance and cell and system level performance of the Li-S was modeled as a function of other important design parameters such as C/S ratio, sulfur loading, N/P ratio, current density, cathode thickness and specific capacity. Therefore, in this part, the literature research for the experimental studies on the effect of these important design parameters as well as previous modeling studies about Li-S batteries are discussed.

2.1 Previous Studies on the Effect of Electrolyte to Sulfur Ratio on the Cell Performance

Choi et al. [35] investigated the dependence of cycle life on the electrolyte amount at 4, 12, 30 μL. Even though, higher electrolyte amounts provide better wetting of the electrode and thus easier Li^+ transportation, less electrolyte amount is better to reduce the cell mass area. According to the results, 30 μL of electrolyte provided the highest specific capacity which corresponds approximately to 85% of sulfur utilization. This is because electrolyte carries the lithium ions to the cathode and with higher amount more sulfur is utilized. When the other electrolyte amounts were analyzed, similar capacities were obtained. However, cycle life of the cells gave different results. At 30 μL of electrolyte specific capacity decreased significantly with cycling. On the other hand, specific capacities of the other cells increased at the earlier cycles.

Zhang [36] determined the capacity changes with cycle number at different E/S ratios. For this purpose, 13.3, 10 and 6.5 mL g_s^{-1} E/S ratios were taken at a C/S ratio of 0.26. At the highest E/S ratio, the highest capacity drop was observed due to increasing polysulfide shuttle mechanism. 6.5 mL g_s^{-1} E/S ratio resulted in a more stable capacity, but its cycle life was limited. This is because that the electrolyte

amount was too low resulting in concentrated polysulfide solutions on the electrode surface which decreases the sulfur utilization. Therefore, 10 mL g_s^{-1} E/S ratio was found to be the optimum ratio; at this ratio, the capacity remained approximately constant and the cycle life was not as short as in 6.5 mL g_s^{-1} E/S ratio.

Zheng et al. [37] reported the effect of S/E ratio on the cell performance at approximately 1-2 mg cm^{-2} sulfur loading, C/S ratio of 0.125 and 0.2 C-rate. The lower S/E ratio means the higher electrolyte amount and, the ratios were changed between 15 g L^{-1} and 100 g L^{-1}. At the lowest S/E ratio (highest E/S ratio), polysulfide shuttle mechanism was observed due to high electrolyte amount; specific capacity dropped significantly with cycling. However, with increasing S/E ratio (decreasing E/S ratio) up to 30 g L^{-1}, shuttle effect starts to reduce and also, specific capacity starts to decrease gradually. At 50 g L^{-1} S/E ratio, the best cycling performance was observed. At higher S/E ratios the capacity diminishes and the cell experiences wetting problems. Therefore, in this study 50 g L^{-1} was reported as the optimum S/E ratio.

Urbonaite and Novak [27] studied the impact of the binder and electrolyte type and electrolyte amount on the cell performance. When the electrolyte amount in the cell was changed as 30, 50 and 100 μL, it was found that although the initial specific capacity of the highest electrolyte amount was the highest, with increasing cycle number its capacity decreases more rapidly than others. This result was seen for all different binder and electrolyte types.

According to Hagen et al. [38], while E/S ratio improves the cycle life and sulfur utilization, it may decrease the energy density of the cell; hence, it should be optimized. In the study, different E/S ratios as 3:1, 4:1, 5:1, 6:1, 7:1 and 8:1 mL g_s^{-1} were used and, the effect of E/S ratio on the cell voltage was determined at 6.6 mg cm^{-2} sulfur loading, C/S ratio of 2 and 0.67 mA cm^{-2}. According to the study, 7:1 mL g_s^{-1} is the optimum E/S ratio for the cell because at lower E/S ratios capacity diminishes significantly (especially at E/S ratio of 3:1). The main reason for this is that increasing polysulfide concentration in the electrolyte leads to higher electrolyte resistance in the cell and thus faster capacity fade. On the other hand, increasing

electrolyte too much, such as 8:1 mL g_s^{-1} E/S ratio, may cause a sudden stop in the discharge capacity.

Ding et al [2] studied the effect of electrolyte amount on the cell voltage and specific capacity at a constant sulfur loading and current density. For this purpose, electrolyte amount was taken as 20, 40 and 80 μL at 2.4 mg cm^{-2} sulfur loading, 0.5 C/S ratio and 56.6 μA cm^{-2} current density. It was observed that, increasing electrolyte amount from 20 to 40 μL increased the specific capacity of the cell by 71 mAh g_s^{-1}. This was explained by a better wetting of the electrode. The improvement in the specific capacity with increasing electrolyte amount after this point was less significant. As a result, 1066 mAh g_s^{-1} of specific capacity was obtained from the cell with 80 μL of electrolyte. When the cells were compared based on their capacity retention, the cells with 20 and 40 μL electrolyte retained approximately the same capacities in the first 25 cycles. However, the cell with 80 μL of electrolyte had high initial capacity loss; this was explained such that excessive increase in the electrolyte amount speeds up the transportation of the polysulfides from the cathode to the anode causing fast capacity fade. When the electrolyte amount (μL) is converted into E/S ratio (μL mg_s^{-1}) using the sulfur loading (mg cm^{-2}) and the area of the electrode (cm^2), approximately 4.72, 9.45 and 18.9 μL mg_s^{-1} E/S ratios were calculated respectively for 20, 40 and 80 μL. According to the results, 9.45 μL mg_s^{-1} E/S ratio gave the best performance among them.

Yan et al. [4] studied the effect of E/S ratio on the electrochemical performance (cycle life and sulfur reaction kinetics) and the capacity fade of the Li-S cell. Moreover, the effect of E/S ratio on the cell resistance was examined via electrochemical impedance spectroscopy (EIS) method. The change of discharge capacity with cycle number at different E/S ratios as 5, 8, 12 μL mg^{-1} were analyzed. It was found that the cell with 5 μL mg^{-1} gave the lowest initial capacity, however it remained constant during the cycling. On the other hand, the cell with 12 μL mg^{-1} had the highest initial discharge capacity but, its capacity diminishes throughout cycling. When the sulfur utilization and capacity fade percentages were considered, similar conclusions were obtained. For the sulfur utilization, the cell with 12 μL mg^{-1} started at 97.7% but dropped till 38%. The cells with 5 μL mg^{-1} and 8 μL mg^{-1} ended

up with similar sulfur utilization percentages after 100 cycles. Likewise, capacity fade percentage was the highest for the cell with 12 μL mg^{-1}. Based on the discharge capacity, sulfur utilization percentage and capacity fade percentage of the cells, 8 μL mg^{-1} was reported as the optimum ratio for good cycling. When the sulfur reaction kinetics was studied as a function of the E/S ratio, it was seen that the cell voltage was the highest for the cell with 12 μL mg^{-1} since higher electrolyte amounts improve the reaction kinetics. Moreover, EIS was used at different E/S ratios in order to observe the electrochemical reaction behaviors. At a fully discharged state, two depressed semicircles and an inclined line were seen in the EIS result. These two depressed semi circles were observed at high and medium frequency regions referring to the charge transfer at carbon interface and to the charge transfer of solid Li_2S_2 and Li_2S formation, respectively. Semi-circle of the charge transfer at the lowest E/S ratio showed the largest impedance because that sufficient amount of electrolyte leads to easier charge transfer.

Kolosnitsyn et al. [20] investigated the effect of electrolyte amount and lithium salt type on the cell voltage. For all the lithium salt types, similar trends were observed at different electrolyte amounts. In addition, the trends were as expected based on the typical cell voltage behavior of the Li-S batteries. Electrolyte amounts were taken 1, 1.5, 2, 3, 4 μL per 1 mAh cathode capacity and 4 μL gave the highest discharge capacity.

Fan and Chiang [39] analyzed the effect of E/S ratio on the Li_2S electrodeposition kinetics of the cell via cell voltage and capacity results. Li_2S electrodeposition in the cathode is an important process for the cell capacity. High concentrations of polysulfides due to low electrolyte amounts in the cell lead to slow Li_2S deposition. This increases the polarization while decreasing the cell capacity. In the study, 7.9, 4.2 and 2.4 mL g_s^{-1} E/S ratios were used at a C/S ratio of 0.88 and C/4 rate. According to the results, increasing E/S ratio increased the specific capacity as expected. At 4.2 mL g_s^{-1} E/S ratio, capacity was similar with that of 7.9 mL g_s^{-1} E/S ratio. However, the polarization was more significant causing a sudden decrease in the cell voltage. At 2.4 mL g_s^{-1} E/S ratio, the second voltage plateau was not observed. This may be because that the electrolyte amount may not be enough to

dissolve sulfur, which raises the resistance of the cell since sulfur restricts the effective conductive cathode area.

Lacey [40] analyzed the dependence of the internal cell resistance on the E/S ratio. This is mainly because that internal resistance can show the physical and chemical changes occurring in the cell such as varying reaction kinetics. Therefore, the effect of changing E/S ratio on the cell performance can be represented by the cell resistance data. In order to observe that effect, the capacity and resistance changes of the cell with 4, 4.5, 5, 6, 8 $\mu L\ mg_s^{-1}$ E/S ratios at both discharge and charge were taken. It was seen that during discharge, the resistance shows a peak at every E/S ratio from 19 $\Omega\ cm^2$ to 107 $\Omega\ cm^2$. The cell with 4 $\mu L\ mg_s^{-1}$ E/S ratio had the highest resistance peak because that excess polysulfide concentration with less amount electrolyte causes harder solubility and easier blocking of the cathode pores increasing the cell resistance. Moreover, when the resistance change with cycling was considered, it was seen that the resistance increased continuously with cycling, especially at low electrolyte amounts. These results were in consistent with the others discussing the effect of E/S ratio on the cell performance.

2.2 Previous Studies on the Effect of Critical Design Parameters on the Cell Performance

Cheon [41] et al. discussed the electrochemical performance of a Li-S battery with changing current density and cathode thickness. Higher C-rates influenced the sulfur utilization negatively because that current density raises the overpotential of the cell and decreases the cell voltage and capacity. Furthermore, increasing the cathode thickness (15, 30 and 60μm) diminished the sulfur utilization. For example, at 15 μm of cathode thickness, 80% sulfur utilization was achieved whereas at 30 μm of thickness approximately 65% sulfur utilization was observed. The reason for this is that at a thicker cathode there is a thicker Li_2S layer causing larger diffusional resistance. Therefore, higher cathode thicknesses and discharge rates decrease the specific capacity of the Li-S battery.

Kang et al. [18] observed how specific capacity changed with cycling at different sulfur loadings and E/S ratios. The effect of sulfur loading on the energy density of the cell with cycling was also investigated. For these studies, cells with different sulfur loadings (0.99, 2.98, 6.8 $mg_s\ cm^{-2}$) were prepared by varying the cathode thickness. At the same time, electrolyte amount was arranged to examine the specific capacity changes with cycling. According to the results, at 0.99 $mg_s\ cm^{-2}$ of sulfur loading, specific capacity was higher than that of other sulfur loadings. In addition, E/S ratio of 10 $\mu L\ g_s^{-1}$ gave the best capacity retention with cycling. Therefore, 0.99 $mg_s\ cm^{-2}$ of sulfur loading and 10 $\mu L\ g_s^{-1}$ of E/S ratio was decided to be the optimum condition for the best specific capacity results. In addition to the specific capacity of the cell, energy density values were also calculated from the specific capacity, voltage and weight of the cell ($capacity \times voltage/weight$). It was observed that 2.98 $mg_s\ cm^{-2}$ of sulfur loading gave the highest energy density results throughout cycling. As a conclusion, the lowest amount of sulfur loading did not show the highest energy density although it gave the highest specific capacity, because of the low amount of active material present in the cell.

Lv et al. [29] studied the performance of a Li-S battery with carbon nanoparticles integrated into the cathode. For this purpose, the changes in the specific capacity at different C-rates were observed. The results were as expected based on the other studies. 0.1, 0.2 and 2C rates were used and it was observed that increasing C-rate decreased the specific capacity. Especially at 2C, this impact could be seen more easily; at 0.1 C and 0.2 C specific capacities were close to each other as 1100 and 900 mAh g_s^{-1} but at 2C specific capacity could reach only to 500 mAh g_s^{-1}. Therefore, it was concluded that very high current densities affect the electrochemical performance of the battery poorly.

Chen et al. [42] determined the effect of carbon to sulfur ratio on the specific capacity of sulfur and capacity retention with cycling. For this purpose, 40%, 50% and 70% of sulfur weight percentages in the cathode were used at a constant electrolyte amount. It was examined that the lowest C/S ratio, which had 70wt% sulfur, gave an average sulfur specific capacity of approximately 1400 mAh g_s^{-1} but, it provided a better capacity retention with cycling compared to the results of other

C/S ratios. On the other hand, the cell with the highest C/S ratio resulted in a specific capacity close to the theoretical capacity of the sulfur electrode, however, the cell had the worst capacity retention behavior during cycling because of the increasing inactive material in the cathode.

Lu et al. [43] studied the effect of E/S ratio and sulfur loading on the cell energy density (Wh kg^{-1}) in addition to the effect of cathode thickness on the cell voltage. For this purpose, sulfur loadings of 4-8 mg cm^{-2} and E/S ratios of 1-10 μL mg^{-1} were used. It was observed that increasing E/S ratio decreased the energy density whereas higher sulfur loadings resulted in higher energy density values. With lower than 3 μL mg^{-1} of E/S ratio and higher than 4 mg cm^{-2} sulfur loading, current Li-ion energy density value, that is approximately 300 Wh kg^{-1}, could be obtained. Moreover, in order to show the importance of good electrode wetting, 60, 80 and 120 μm thick cathodes were used and their discharge capacities and cell voltages were examined. At each thickness value, approximately the same specific capacity was obtained. However, when the cell was compressed to 60 μm, significant drop in the cell voltage was observed.

2.3 Previous Studies on the Modeling of Electrochemical Performance of a Li-S Cell

Mikhaylik and Akridge [30] proposed a model for observing the shuttle mechanism effect on the cell performance. Firstly, the discharge profile of a Li-S cell was defined using two redox reactions for each of the two discharge plateau as given in Equations 2.1 and 2.2. The reaction kinetics for both high and low discharge plateau are treated with the Nernst equation shown in Equation 2.3. The model predicts the standard potentials, E_H^0 and E_L^0 , as 2.33 V and 2.18 V at low currents, respectively.

$$S_8{}^0 + 4e^- = 2S_4{}^{2-} \tag{2.1}$$

$$S_4{}^{2-} + 4e^- = 2S^{2-} + S_2{}^{2-} \tag{2.2}$$

$$E_L = E_L^0 + \frac{RT}{n_L F} \ln \frac{[S_4{}^{2-}]}{[S^{2-}]^2 [S_2{}^{2-}]} \tag{2.3}$$

The shuttle effect was considered in the model by taking into account the change of high order polysulfide concentration with time. This is because that these polysulfides diffuse to the lithium anode where they become low order PS and then, they go back to the cathode where they become high order polysulfides again. Therefore, their concentration affects the shuttle mechanism significantly. The relation of the shuttle mechanism with the polysulfide concentration proposed in the model is given in Equation 2.4. Moreover, the charge and discharge profiles of the Li-S cell as a function of the discharge current were also predicted in the study.

$$\frac{d[S_H]}{dt} = \frac{I}{q_H} - k_s[S_H] \tag{2.4}$$

where $[S_H]$ is the concentration of high order polysulfides, t is the time, I is the current of charge or discharge, q_H is the specific capacity of sulfur at high discharge plateau and k_s is the shuttle constant.

Kumaresan et al. [44] developed a detailed mathematical model accounting for the concentration changes of different species ($Li^+, S_{8(l)}$, S_8^{2-}, S_6^{2-}, $S_4^{2-}, S_2^{2-}, S^{2-}$ and A^- (anion of lithium salt in electrolyte)) with time and position in the cell. In the model, dissolution and precipitation reactions were also considered in addition to the electrochemical reactions as given below [44].

$$Li \leftrightarrow Li^+ + e^- \tag{2.5}$$

$$\frac{1}{2}S_{8(l)} + e^- \leftrightarrow \frac{1}{2}S_8^{2-} \tag{2.6}$$

$$\frac{3}{2}S_8^{2-} + e^- \leftrightarrow 2S_6^{2-} \tag{2.7}$$

$$S_6^{2-} + e^- \leftrightarrow \frac{3}{2}S_4^{2-} \tag{2.8}$$

$$\frac{1}{2}S_4^{2-} + e^- \leftrightarrow S_2^{2-} \tag{2.9}$$

$$\frac{1}{2}S_2^{2-} + e^- \leftrightarrow S^{2-} \quad (2.10)$$

$$S_{8(l)} \leftrightarrow S_{8(s)} \quad (2.11)$$

$$2Li^+ + S_8^{2-} \leftrightarrow Li_2S_{8(s)} \quad (2.12)$$

$$2Li^+ + S_4^{2-} \leftrightarrow Li_2S_{4(s)} \quad (2.13)$$

$$2Li^+ + S_2^{2-} \leftrightarrow Li_2S_{2(s)} \quad (2.14)$$

$$2Li^+ + S^{2-} \leftrightarrow Li_2S_{(s)} \quad (2.15)$$

Marinescu et al. [45] developed a 0-D electrochemical model to observe the voltage profiles during discharging and charging. In the model, the cathode reactions were taken as in the study of Mikhaylik and Akridge. Therefore, the model included 2 redox reactions in the cathode, a single reaction for each of the two voltage plateaus. The reaction kinetics was treated by the Butler-Volmer equation in the model. In addition, the shuttle mechanism was also considered in the model through a shuttle rate constant. Moreover, the impact of precipitation reactions was added into the model via a precipitation rate constant. The cell voltage results were obtained at two different current densities and, in order to understand the effect of overpotential and precipitation on the model predictions, the model was run at 3 different ways: (1) in the absence of both the precipitation and B-V equations, (2) in the absence of only the precipitation equation and (3) in the presence of both the precipitation and B-V equations. It was indicated that cases (1) and (2) had similar trends but, when the model did not include the precipitation equation (2), lower voltage values were predicted. As different from these two cases, when both precipitation and B-V equations were included in the model, a dip formed between the two discharge plateaus was predicted.

In addition to these electrochemical models, there are several other modeling studies in the literature discussing the reaction kinetics, polysulfide shuttle mechanism,

transport and precipitation limitations, charge and discharge behaviors etc. in a Li-S cell [21, 46–56]. However, only a few of these models in the literature considered the impact of significant cell design parameters on the cell performance.

2.4 Previous Studies on the Modeling of Cell and System Level Performance of a Li-S Cell

Eroglu et al. [10] developed a techno-economic model to investigate the effect of critical cell design parameters on the cell and system level performance of Li-S batteries designed for EV applications. For this purpose, BatPac (Battery Performance and Cost) model, which calculates the battery mass, volume and cost for the Li-ion batteries to be used in EVs, became a basis for the model.

As apart from the other performance models, this model considered the impact of key cell level parameters on the cell and pack design. In the model, voltage calculations were done assuming isothermal and concentration independent conditions at a constant current discharge. Moreover, the model used a single kinetic parameter, the cathode exchange current density, in the cathode. For the cell and system level performance, total pack energy and power were specified to determine the cell and pack area and cell capacity. Table 2.1 shows the parameters specified in the techno-economic model.

Table 2.1. The parameters used in the cell- and system- level performance model calculations [10]

Total Pack Energy (kWh)	118
Total Pack Power (kW)	80
Average Battery Voltage (V)	360
Average Cell Voltage (V)	2.2
Maximum Cathode Thickness (μm)	150
Sulfur Utilization (mAh g_s^{-1})	600-1672
Electrolyte Volume Fraction (%)	50-90
S:C Weight Fraction (%)	80:10-40:50
Cathode Exchange Current Density (A cm^{-2})	10^{-8}-10^{-6}

In the cell level performance model, the effect of electrolyte volume fraction and excess lithium in the anode on the specific energy and energy density of a Li-S cell were determined. As in the other cell level models, increasing the electrolyte amount decreased the specific energy and energy density of the cell significantly. Likewise, increasing excess lithium amount had a negative effect on the cell level performance of the cell.

In the system level performance model, firstly, the system specific energy and energy density with varying specific capacity were calculated. It was seen that increasing the specific capacity improved the system level performance of a Li-S battery; capacities greater than 1000 mAh g^{-1} are typically required for good system properties [3,29,57]. Then, the effect of E/S ratio was investigated. As in the cell level performance, increasing E/S ratio reduced the specific energy and energy density. The model predicts that electrolyte amounts smaller than approximately

70% electrolyte volume fraction, or 1.9 mL g^{-1} E/S ratio, gave better results. This is mainly because that higher E/S ratios cause increasing inactive materials in the pack in addition to the high electrolyte volume and therefore, the system performance of

the battery drops significantly. After that, the influence of the cathode exchange current density as the kinetic parameter in the model was indicated. According to the results, increasing cathode exchange current density had a positive impact on the specific energy and energy density since the reaction kinetics can change the pack level performance greatly by means of area specific impedance values. These values are affected by the cell resistances, which are due to the charge transfer and transport limitations that play an important role in the concentrations of the reactants and the rate constants of the reactions. Therefore, one of the main outputs of this study was that the electrolyte amount, which controls the reactant concentrations in the cell via the dissolving polysulfides, has a critical impact on the reaction kinetics. Lastly, the influence of the carbon content in the battery was observed. Up to a point, increasing carbon content improved the system level performance of the battery. However, after this point, increasing carbon amount dropped the specific energy and energy density. The reason of this trend is explained as such. Increasing carbon content raises the electrical conductivity and thus improves the cathode kinetics however, excess carbon leads to an increase in the inactive materials in the cell. Therefore, it drops the performance of the battery once the kinetic limitations in the cell are not significant anymore.

In another study, McCloskey [57] studied the effect of E/S ratio and sulfur loading on the cell level specific energy and energy density of a Li-S cell with simple calculations as showed in Equation 2.16.

$$E_g = \frac{V \times m_A \times C}{\sum W_i}, E_v = \frac{V \times m_A \times C}{\sum \frac{W_i}{\rho_i}} \tag{2.16}$$

where E_g and E_v are the specific energy and energy density at the cell level in Wh kg^{-1} and Wh L^{-1}, respectively, V is average cell voltage in V, m_A is active material loading in g cm^{-2}, C is active material capacity in mAh g^{-1}, W_i is the weight of each component in the cell in g cm^{-2} and ρ_i is the density of each component in the cell in g cm^{-3}.

In the calculations, kinetic and transport limitations were not considered; an average cell voltage and a constant sulfur utilization were used in the model. The study was

conducted for both an ideal case -100 wt% sulfur in the cathode and 100% sulfur utilization- and a more realistic case -75 wt% sulfur and 60% sulfur utilization-. The parameters used in the model are given in Table 2.2.

Table 2.2. The parameters used in the cell level performance calculations [57]

Thickness of Al current collector (μm)	10
Thickness of Cu current collector(μm)	4
Separator weight (mg)	12
Carbon wt% in cathode (%)	20
Binder wt% in cathode (%)	5
Li metal excess (%)	20
S utilization (mAh g^{-1})	1000
Thickness of separator (μm)	40
Average operating voltage (V)	2

At different sulfur loadings between 0.5 and 15 mg cm^{-2}, total mass per cm^{-2} was calculated using each E/S ratio and so, the effect of sulfur loading and E/S ratio on the specific energy and energy density at the cell level was found. Although the ideal case predicted higher specific energy and energy density values than that of the real cell, the same trend was observed for both of them. Increasing sulfur loading improved the specific energy and energy density whereas, increasing E/S had an adverse effect on the cell level performance.

Deng et al. [1] examined the life cycle assessment (LCA) of a Li-S battery for EV applications. For this purpose, a LCA model for a 320 km drive in every charge with 120 kW power was investigated. The model includes a kinetic model that was created based on the BatPac method calculating the ASI and the overpotential of the cell as a function of the current density. The required kinetic parameters were taken from the experimental part of the study.

$$ASI\ (i)=ASI_{cathode}+ASI_{anode}+ASI_{separator} \quad (2.17)$$

The calculations for the thickness and area of the cell, module and battery, for the cooling system and the battery mass and volume were also calculated in the study based on the battery pack configuration part in the BatPaC model.

$$L_{anode}=L_{cathode}\times N/P\times \frac{C_{sulfur}}{C_{lithium}} \quad (2.18)$$

$$L_{cathode}=\frac{C_{cell}}{(\rho_{cathode}\times A\times S\%\times C_{sulfur})} \quad (2.19)$$

where $L_{cathode}$ and L_{anode} is the thicknesses of cathode and anode, C_{sulfur}, $C_{lithium}$ and $C_{cell}$are active material capacities of cathode and anode electrodes and cell capacity.

Finally, the required energy and mass for the EV were calculated. According to the model calculations, 279 kg battery mass, 220 Wh kg^{-1} specific energy, 298 Wh L^{-1} energy density, and 61.3 kWh capacity were found for a battery achieving a 320 km drive in one charge. As a conclusion, this study stated that the Li-S batteries could be a future energy storage system for EV applications with decreasing life cycle environmental effects.

Lastly, Xue et al. [17] studied the modeling of energy density based on a current prototype Li-S cell and the effect of different cell parameters on the energy density was investigated. In the model, only the current collector, anode, separator and cathode parts were included in order to simplify the calculations; therefore, the contribution of the materials for packaging were not considered. Additionally, in the calculations thicknesses of the aluminum and copper current collectors were taken as half since commercialized cells are typically coated in double sides. Moreover, it is assumed that there is electrolyte only in cathode and separator in the cell. Based on these assumptions, energy density values were calculated using Equation 2.20.

$$E_v=\frac{V\times m_A\times C_s}{\frac{\left(\sum \frac{m_i}{\rho_i}\right)}{\varepsilon}+\frac{m_l}{\rho_l}+\sum d_i\times S} \quad (2.20)$$

where E_v is volumetric energy density in Wh L^{-1}, V is average cell voltage in V, m_A is mass of active material in mg, C_s is specific capacity in mAh g^{-1}, m_i is the mass of sulfur, carbon and binder in mg , ρ_i is the density of sulfur, carbon and binder in g cm^{-3}, ε is the cathode porosity, m_l is the mass of lithium in mg, ρ_l is the density of lithium in g cm^{-3}, d_i is the density of current collectors and separator in cm and S is the unit area in cm^{-2}.

In the model, sulfur specific capacity and cell voltage were taken as 1000 mAh g^{-1} and 2.1 V, respectively, whereas other cell parameters were changed at each calculation. At first, the effect of sulfur loading (until 15 mg cm^{-2}) and sulfur content (40, 55, 70, and 85%) on the energy density was investigated at 50% excess lithium and 70% porosity. It was observed that low sulfur loadings such as below 2 mg cm^{-2} gave very low energy density values even though the cell had high sulfur content. Increasing sulfur loading leads to higher energy density but, after a point energy density stayed constant at each sulfur content. Similar to the sulfur loading, increasing sulfur content also raised the energy density. Therefore, it was concluded that high values of sulfur loading and sulfur content improves the cell level performance of the cell via energy density. Next, the effect of porosity on the energy density was examined at 50% excess lithium and 70% sulfur content. It was seen that increasing porosity diminished the energy density of the cell; 30% porosity gave the best result. However, it was discussed that 30% porosity is very low compared to the commercialized Li-S cells. Lastly, the effect of excess lithium amount (20, 50 and 100 %) on the energy density was analyzed at 70% porosity and 70% sulfur content for different sulfur loadings. It was seen that the cell energy density was less sensitive to the excess lithium amount compared to the sulfur loading, porosity and sulfur content results.

As it is seen from the literature, although there are detailed experimental studies on the effect of E/S ratio and thorough electrochemical models for reaction kinetics, there is no study that models the effect of E/S ratio on both the electrochemical performance and the cell- and system- level properties of the Li-S battery.

CHAPTER 3

MODEL DESCRIPTION

In the model description section, electrochemical performance and cell and system level performance models are explained. At first, a one dimensional electrochemical performance model is described and then, cell- and system- level performance models using the developed electrochemical model are defined.

3.1 One Dimensional Electrochemical Performance Model for the Li-S Battery

The model calculation schematic is given in Figure 3.1. In order to investigate the effect of the E/S ratio in the cell on the electrochemical performance of a Li-S battery, a 1-D electrochemical model which shows the current changes with the position is developed [9]. This model is proposed for isothermal and constant-current discharge of the Li-S battery and it determines the relationship between the current and the voltage for each part of the battery.

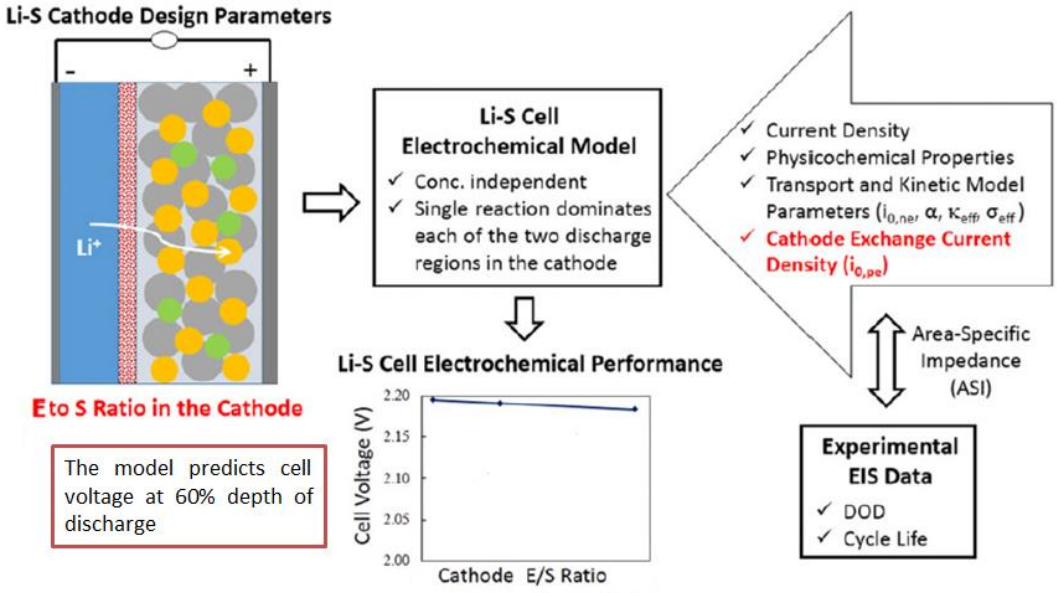

Figure 3. 1.Calculation schematic of the electrochemical model developed for the Li-S cell (adapted from [9])

In the model, the Li-S battery contains a Li-metal anode, a porous separator and a porous cathode which has a porous sulfur and carbon composite, binder and organic electrolyte. The effect of carbon, binder and electrolyte types are not considered in this study so, most typical types used in the literature are chosen. 1M LiTFSI and 2 wt% $LiNO_3$ salts in DOL:DME (1:1 vol%) solvent, which has low viscosity and SEI forming feature, is used as the organic electrolyte [58]. For the binder, polyvinylidene difluoride (PVDF) is chosen due to its high electrochemical constancy and good adhesion features and its amount is kept constant at 10 wt% throughout the study [31]. The super P carbon black is chosen for the cathode and its BET surface area and density values are taken as 650000 $cm^2\ g^{-1}$ and 1.8 g cm^{-3}, respectively [9]. In the model, the following assumptions are made:

- The model is concentration-independent, there is no shuttle mechanism in the cell
- Concentration gradients within the cell are ignored because they are insignificant at low current densities at the lower voltage plateau according to the previous studies in the literature [44, 49]. Therefore, inhomogeneities within the cathode due to the dissolution of lithium polysulfides in the electrolyte are not considered in the model [47, 56].
- There is a single reaction for each of the two discharge plateaus in the cathode. This is the most important assumption in the model and with this single reaction assumption, which is symmetric between charge and discharge, the shuttle effect is also neglected in the model [9, 10, 54].

The model calculates the cell voltage at a given depth of discharge giving the electrochemical performance of the cell. For the calculations, the relation between the current and voltage for the cathode, the separator and the anode in the cell is determined separately as described below.

In the cathode, based on the most important assumption of the model, a 2-step electrochemical reaction scheme is taken for discharge. Generally, Li-S batteries have two -a high and a low- voltage discharge plateaus as discussed in Chapter 1 [30]. When the discharge process starts, at first S_8 rings open to Li_2S_n polysulfides (n=4-8) at the high voltage discharge plateau. Then, these soluble polysulfides turn into insoluble Li_2S_2 and Li_2S at the low voltage discharge plateau. In the proposed model, these multi-step reactions are simplified based on the study conducted by Mikhaylik and Akridge [30] as given in Equations 3.1 and 3.2 for the high and low discharge plateaus, respectively. This single reaction assumption results in a single apparent kinetic parameter in the model for each discharge plateau, which is the cathode exchange current density ($i_{0,pe}$).

$$\frac{1}{4}S_8^{0}+e^{-}\leftrightarrow\frac{1}{2}S_4^{2-} \tag{3.1}$$

$$\frac{1}{4}S_4^{2-}+e^{-}\leftrightarrow\frac{1}{2}S^{2-}+\frac{1}{4}S_2^{2-} \tag{3.2}$$

In the cathode, Porous Electrode Theory by Newman and Tobias is considered [34]. According to the theory, there are two phases, the matrix phase and the electrolyte phase in the cathode, which show continuity over time and position. These phases have current densities as i_1 and i_2 and potentials as $\phi_1$and ϕ_2, respectively. In order to determine the potential difference of the two phases in the cathode-separator and cathode-current collector boundaries, Ohm's law for the matrix phase and the sum of the fluxes of mobile ionic species for the electrolyte phase are used. Detailed governing equations and boundary conditions for the porous electrode theory can be found in Appendix A. In order to determine the current and voltage relation of the electrode, Tafel or linear kinetics is used as given in Equations 3.3 and 3.4, respectively. The detailed derivations of these equations are also given in Appendix A. The model equations are solved using a VBA code.In these equations, the overpotential (η) indicates the deviation of the cell voltage from the theoretical cell potential. In addition, the area-specific impedance (ASI) shows the combination of the resistances in the cell that is caused by the physical and electrochemical changes

such as charge transfer and ohmic resistances [1, 9, 10, 59]. ASI of the cathode is determined as given in Equation 3.5.

Tafel Approximation: $|I|>ai_{0,pe}L_{pe}$

$$\eta_{pe}=\frac{1}{\beta}\left\{(\delta-\varepsilon)\left[\frac{\varepsilon}{\delta}+\frac{2}{\delta}\ln\sec(\theta-\psi)\right]+\frac{2\varepsilon}{\delta}\ln\sec\psi+\ln\left(\frac{2|I|\theta^2}{ai_{0,pe}L_{pe}\delta}\right)\right\} \tag{3.3}$$

Linear Approximation: $|I|<ai_{0,pe}L_{pe}$

$$\eta_{pe}=\frac{I\times Lpe}{\kappa_{eff}+\sigma_{eff}}\left[1+\frac{2+\left(\frac{\sigma_{eff}}{\kappa_{eff}}+\frac{\kappa_{eff}}{\sigma_{eff}}\right)\cosh\nu}{\nu\sinh\nu}\right] \tag{3.4}$$

$$ASI_{pe}=\frac{\eta_{pe}}{I} \tag{3.5}$$

where η_{pe} is the cathode overpotential in V, L_{pe} is the cathode thickness in cm, $i_{0,pe}$ is the cathode exchange current density in A cm^{-2} , a is the superficial area in cm^{-1}, κ_{eff} and σ_{eff} are the effective ionic and electronic conductivities in S cm^{-1} and ASI_{pe} is the cathode ASI in Ω cm^2. Other parameters are defined in Appendix A.

In the porous separator, there is a resistance due to the flow of Li^+ ions causing Ohmic losses. The overpotential and ASI of the separator are calculated using Equations 3.6 and 3.7, respectively.

$$\eta_{sep}=ASI_{sep}\times I \tag{3.6}$$

$$ASI_{sep}=\frac{L_{sep}}{\kappa_{eff,sep}} \tag{3.7}$$

where η_{sep} is the separator overpotential in V, ASI_{sep} is the separator ASI in Ω cm^2, L_{sep} is the thickness of separator in cm, $\kappa_{eff,sep}$ is the effective ionic conductivity of the separator in S cm^{-1}.

In the anode, lithium oxidizes into Li^+ with the reaction shown in Equation 3.8 and its deposition and dissolution kinetics is treated by the Butler-Volmer kinetics. The current and overpotential relation and the ASI of the anode are given in Equations 3.9 and 3.10, respectively.

$$Li^+ + e^- \rightarrow Li^0 \tag{3.8}$$

$$I = i_{o,ne}\left[\exp\left(\frac{\alpha_{ne,a}F}{RT}\eta_{ne}\right) - \exp\left(\frac{-\alpha_{ne,c}F}{RT}\eta_{ne}\right)\right] \tag{3.9}$$

$$ASI_{ne} = \frac{\eta_{ne}}{I} \tag{3.10}$$

where I is the current density of anode in A cm^{-2}, $i_{o,ne}$ is the anode exchange current density in A cm^{-2}, α_{ne} is the transfer coefficient, η_{ne} is the anode overpotential in V, ASI_{ne} is the anode ASI in Ω cm^2, F is the Faraday constant, R is the gas constant, T is temperature.

The total ASI and overpotential of the cell are found using Equations 3.11 and 3.12, respectively. Consequently, the model calculates the cell voltage at a given constant current density via estimating the total ASI and overpotential of the cell as given in Equation 3.13.

$$ASI_{cell} = ASI_{ne} + ASI_{sep} + ASI_{pe} \tag{3.11}$$

$$\eta_{cell} = \eta_{ne} + \eta_{sep} + \eta_{pe} \tag{3.12}$$

$$V_{cell} = U - \eta_{cell} \tag{3.13}$$

where ASI_{cell} is the total ASI of the cell in Ω cm^2, η_{cell} is the total overpotential of the cell, V_{cell} is the cell voltage and U is the open-circuit voltage of the cell in V.

As a conclusion, the effect of E/S ratio in the cathode on the electrochemical performance of the cell is observed by calculating the cell voltage at 60% depth of discharge for different current densities. This depth of discharge is chosen since it corresponds to the second voltage plateau, which is typically used for the battery

design purposes in Li-S batteries. All transport and kinetic parameters used in the model are shown in Table 3.1.

Table 3.1. The parameters in the electrochemical model [9]

Thermodynamic Cell Voltage, U (V)	2.2
Current Density, I (mA cm^{-2})	0.1 – 1.0
C to S Ratio in the Cathode[a]	0.5
Electrolyte Vol% in the Cathode (vol%)[b]	50 – 95
E to S Ratio in the Cathode (mL g^{-1})[c]	0.86 – 16.25
Cathode Thickness, L_{pe} (μm)	50

Exchange Current Density for S Reaction, $i_{0,pe}$(A cm^{-2})	6.28×10^{-7} [9] or $1.81 \times 10^{-5} \times (\varepsilon) - 1.44 \times 10^{-5}$
Transfer Coefficient for S Reaction, $\alpha_{pe,a}$, $\alpha_{pe,c}$	0.5
Electrochemically Active Area in the Cathode, *a* (cm^{-1})[d]	a=650000 cm^{2}g$^{-1}\cdot\rho_C\cdot\varepsilon_C$
Cathode Effective Ionic Conductivity, κ_{eff} (S cm^{-1})[e]	$\kappa_{eff} = \kappa \cdot \varepsilon^{1.5}$
Cathode Effective Electronic Conductivity, σ_{eff} (S cm^{-1})[f]	$\sigma_{eff} = \sigma \cdot \varepsilon_C{}^{1.5}$
Exchange Current Density for Li Deposition/Dissolution, $i_{0,ne}$ (A cm^{-2})	10^{-2}
Transfer Coefficient for Li Deposition/Dissolution, $\alpha_{ne,a}$, $\alpha_{ne,c}$	0.5
Separator Thickness, L_{sep} (μm)	20
Separator Effective Ionic Conductivity, $\kappa_{eff,sep}$ (S cm^{-1})	6.5 x 10^{-4}

[a] The cathode contains 10 wt% binder.

[b] Electrolyte volume fraction in the cathode is equal to the porosity of the cathode, ε.

[c] In the model, E/S ratio and electrolyte volume fraction in the cathode are related through E/S ratio $= \frac{\varepsilon}{\varepsilon_S \times \rho_S}$.

[d] In the model, *a* is defined as a function of the BET surface area (650000 cm^2 g^{-1}), density (ρ_C) and volume fraction of the carbon (ε_C) in the cathode.

[e, f] Effective conductivities for the porous cathode are determined using Bruggeman's expression.

3.2 Cell Level Performance Model for the Li-S Battery

In order to determine the effect of E/S ratio in the cell on the cell level performance of the Li-S battery, a cell level performance model using the electrochemical model described in the previous section is developed. The model calculates the cell level energy density and specific energy of the Li-S battery as a function of the E/S ratio. The calculation schematic for the model is given in Figure 3.2.

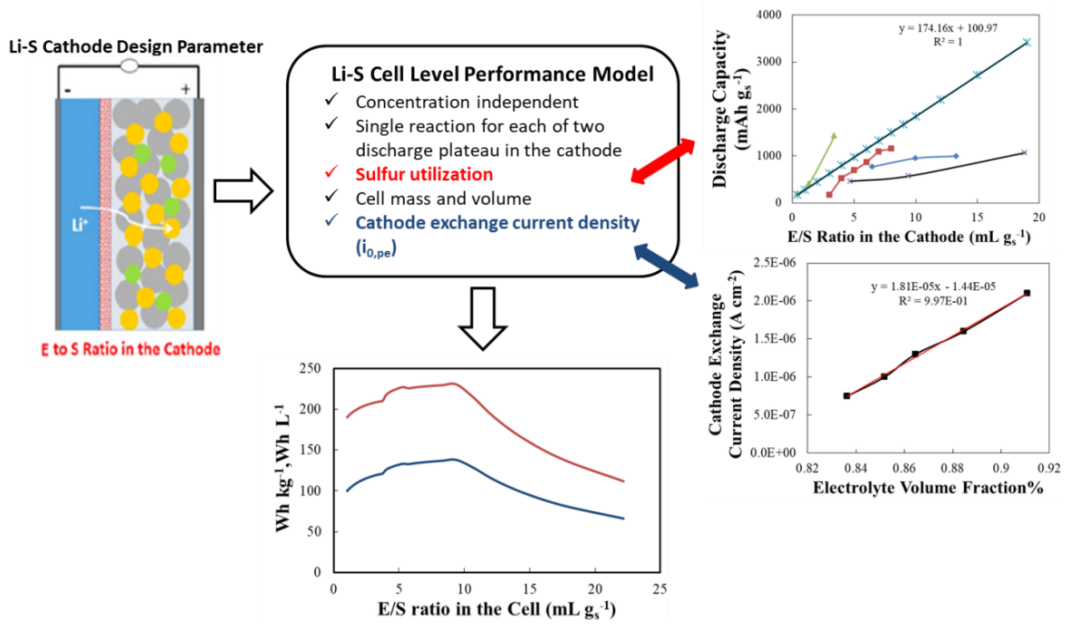

Figure 3. 2.Calculation schematic of the cell level performance model developed for the Li-S cell

In the cell level performance model, positive and negative current collectors are also included as a part of the cell. For energy density and specific energy calculations, volume and mass per area for each cell component and the cell capacity are found. In the performance model, the discharge rate of the Li-S cell is chosen as C/5. C-rate is the discharge current for reaching the full capacity and C/5 means discharge current for discharging the battery entirely in 5 hours. Since C-rate of the battery is kept constant, current density changes as a function of the sulfur loading as given in Equation 3.14.

$$I=\frac{C}{5}\times \text{sulfur loading} \tag{3.14}$$

where I is the current density of the cell in A cm^{-2}, C is the cell capacity in Ah g_s^{-1}, sulfur loading in g_s cm^{-2}.

In the cathode, firstly the positive electrode capacity is calculated as it affects the negative electrode capacity, which determines the anode mass in the model (Equation 3.15). In addition, mass and volume of sulfur, carbon, binder and electrolyte in the cell are calculated in order to procure energy density and specific energy of the cell as given in Equations 3.16-3.18.

$$c_{pe}=c_{pos,act}\times w_{pe,act}\times \rho_{pe,total} \tag{3.15}$$

$$m_{s,c,b}=L_{pe}\times v_{s,c,b}\times \rho_{s,c,b} \tag{3.16}$$

$$m_e=\frac{E}{S}\times m_s\times \rho_e \tag{3.17}$$

$$V_{s,c,b}=\frac{m_{s,c,b}}{\rho_{s,c,b}} \tag{3.18}$$

where c_{pe} is the positive electrode capacity in Ah cm^{-3}, $c_{pos,act}$ is the positive active material capacity in Ah g_s^{-1}, $w_{pe,act}$ is the sulfur weight fraction in the cathode, $\rho_{pe,total}$ is the positive electrode density in g cm^{-3}, m_s, m_c, m_b and m_e are the sulfur, carbon, binder and electrolyte loading in the cathode in g cm^{-2}, L_{pe} is the cathode thickness in cm, v_s , v_c, v_b, v_e are the sulfur, carbon, binder and electrolyte volume fractions in the cathode and ρ_s, ρ_c, ρ_b, ρ_e are sulfur, carbon, binder and electrolyte densities in g cm^{-3}, $\frac{E}{S}$ ratio in mL g_s^{-1}, V_s, V_c, V_b, V_e are the sulfur, carbon, binder and electrolyte volume values per cm^{-2} in cm^3 cm^{-2}.

In the anode, thickness of the electrode is calculated since anode mass depends on the thickness. In the model, cathode thickness is taken constant but, anode thickness changes with the cathode and negative electrode capacities. Anode volume and mass calculation equations are given below.

$$L_{ne}=\frac{L_{pe}\times c_{pe}}{c_{ne}}\times\frac{N}{P} \tag{3.19}$$

$$c_{ne}=c_{ne,act}\times w_{ne,act}\times\rho_{ne,total} \tag{3.20}$$

$$m_{ne}=L_{ne}\times w_{ne,act}\times\rho_{ne,total} \tag{3.21}$$

$$V_{ne}=\frac{m_{ne}}{\rho_{ne}} \tag{3.22}$$

where L_{anode} is the anode thickness in cm, c_{ne} is the negative electrode capacity in Ah $cm^{-3}$and $\frac{N}{P}$ is the negative-to-positive capacity ratio., $w_{ne,act}$ is the negative active material mass fraction , $c_{ne,act}$ is the negative active material capacity in Ah g_s^{-1}, $\rho_{ne,total}$ is the negative electrode density in g cm^{-3}, m_{ne} is the negative electrode mass in g_{ne} cm^{-2}, V_{ne} is the negative electrode volume in cm^3 cm^{-2}.

For the mass and volume of the separator, electrolyte amount in the separator is also considered and the model calculations are given below.

$$m_{\text{sep without electrolyte}}=L_{sep}\times\rho_{sep} \tag{3.23}$$

$$m_{\text{electrolyte in sep}}=L_{sep}\times\rho_{electrolyte}\times\frac{v_{void}}{v_{\text{total sep}}} \tag{3.24}$$

$$m_{total}=m_{\text{sep without electrolyte}}+m_{\text{electrolyte in sep}} \tag{3.25}$$

$$V_{sep}=L_{sep} \tag{3.26}$$

$$V_{\text{electrolyte in sep}}=L_{sep}\times\frac{v_{void}}{v_{\text{total sep}}} \tag{3.27}$$

where m_{sep} is the separator mass in g_{sep} cm^{-2}, $L_{sep}$is the separator thickness in cm, $\rho_{sep}$is the separator density in g cm^{-3} and V_{sep} is the separator volume in cm^3 cm^{-2}.

In the positive and negative current collectors, the contribution of the ASI and overpotential to the cell voltage is also considered as given in Equations 3.28 and

3.29. In addition, mass and volume of the current collectors are calculated for energy density and specific energy of the cell (Equations 3.30 and 3.31).

$$ASI_{cc+,cc-}=\text{resistance} \tag{3.28}$$

$$\eta_{cc+,cc-}=ASI_{cc+,cc-}\times I \tag{3.29}$$

$$m_{cc+,cc-}=L_{cc+,cc-}\times\rho_{cc+,cc-} \tag{3.30}$$

$$V_{cc+,cc-}=\frac{m_{cc+,cc-}}{\rho_{cc+,cc-}} \tag{3.31}$$

where ASI_{cc+} and ASI_{cc-} are the positive and negative collector ASI in Ω cm^2, η_{cc+} and $\eta_{cc-}$is the positive and negative collector overpotential in V, m_{cc+} and m_{cc-} are the positive and negative current collector mass in g cm^{-2}, L_{cc-} and L_{cc+} are the positive and negative current collector thickness in cm, ρ_{cc+} and $\rho_{cc-}$are the positive and negative current collector density in g cm^{-2},$V_{cc+}$and $V_{cc-}$are the positive and negative current collector volume in cm^3 cm^{-2}.

In the last part, total ASI and total overpotential of the cell and thus the cell voltage are calculated as given in Equations 3.32, 3.33 and 3.34. Then, the cell level performance model calculates the specific energy and energy density at the cell level by means of cell capacity, total mass and volume of the cell, which are shown in Equations 3.35- 3.39.

$$ASI_{cell}=ASI_{pe}+ASI_{ne}+ASI_{sep}+ASI_{cc-}+ASI_{cc+} \tag{3.32}$$

$$\eta_{cell}=\eta_{pe}+\eta_{ne}+\eta_{sep}+\eta_{cc-}+\eta_{cc+} \tag{3.33}$$

$$V_{cell}=U-\eta_{cell} \tag{3.34}$$

$$\text{cell mass}=m_s+m_c+m_b+m_e+m_{sep}+m_{ne}+m_{cc-}+m_{cc+} \tag{3.35}$$

$$\text{cell volume}=V_s+V_c+V_b+V_e+V_{sep}+V_{cc-}+V_{cc+} \tag{3.36}$$

$$Q=c_{pos,act}\times\rho_s\times v_s\times L_{pe} \tag{3.37}$$

$$\frac{\text{Wh}}{\text{kg}} = \frac{\text{Q} \times \text{V}_{\text{cell}}}{\text{cell mass}} \tag{3.38}$$

$$\frac{\text{Wh}}{\text{L}} = \frac{\text{Q} \times \text{V}_{\text{cell}}}{\text{cell volume}} \tag{3.39}$$

where ASI_{cell} is the total ASI of the cell in Ω cm^2, η_{cell} is the total overpotential of the cell in V, V_{cell} is the cell voltage in V, U is the open-circuit voltage of the cell in V, Q is the cell capacity in Ah cm^{-2}, $c_{pos,act}$ is the positive active material capacity in Ah g_s^{-1}.

In the cell level performance model, the effect of E/S ratio on the specific energy and energy density of the cell is observed by means of cell voltage and cell mass and volume results. Electrolyte amount affects both the cell voltage and the cell mass and volume. All parameters used in the model are shown in Table 3.2.

Table 3.2. Parameters in the cell level performance model

Current Density, I (mA cm^{-2})	$\frac{C}{5}$ ×sulfur loading
Carbon to Sulfur Wt% in the Cathode (wt%)[a]	30:60
C to S Ratio in the Cathode	0.5
Electrolyte Vol% in the Cathode (vol%)	51 – 96

E to S Ratio in the Cathode (mL g^{-1})[b]	0.89 – 20.5
E to S Ratio in the Cell (mL g^{-1})[c]	1.16-23.85
Cathode Thickness, L_{pe} (μm)	100
Exchange Current Density for S Reaction, $i_{0,pe}$(A cm^{-2})	$1.81\times10^{-5}\times(\varepsilon)-1.44\times10^{-5}$
Exchange Current Density for Li Deposition/Dissolution, $i_{0,ne}$ (A cm^{-2})	10^{-2}
Separator Void Volume Fraction [1]	39%
Specific Capacity (mAh g_s^{-1})	1200 or $174.16\times(E/S)+100.97$

[a] The cathode contains 10 wt% binder.

[b] In the model, $\frac{E}{S}$ ratio in the cathode= $\frac{v_e\%}{v_s\% \times \rho_S}$.

[c] In the model, $\frac{E}{S}$ ratio in the cell= $\frac{V_e}{m_s}$.

3.3 System Level Performance Model for the Li-S Battery

The third part of the thesis is modeling the effect of E/S ratio on the system level performance of the Li-S battery. This part contains the battery modeling that depends on the electrochemical model of the Li-S cell and battery construction design model considering the cell and pack requirements. At the end of this model, specific energy and energy density of the Li-S battery at the system level is observed. The model calculation schematic is given in Figure 3.3.

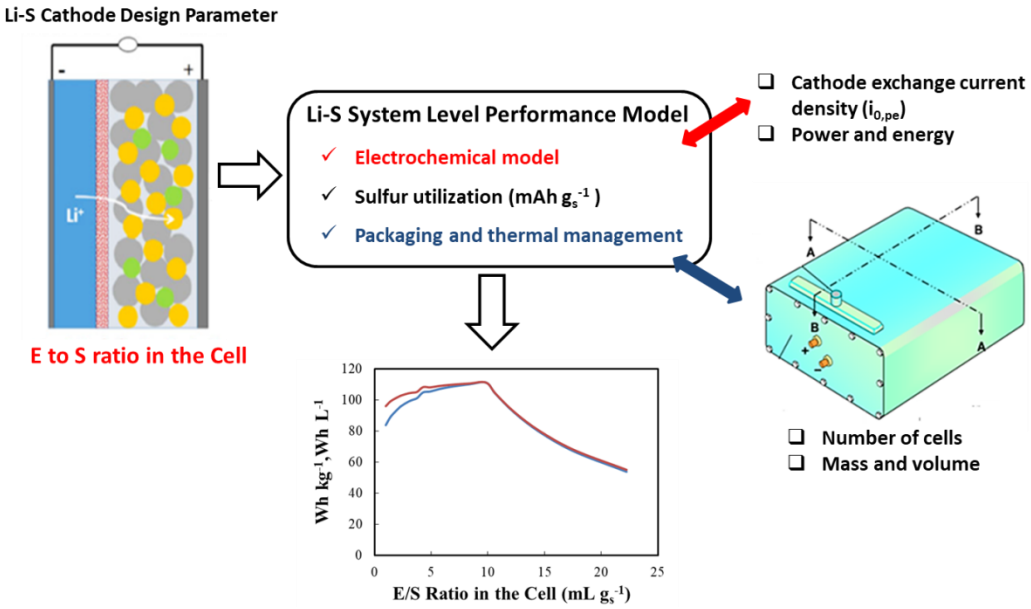

Figure 3. 3. Calculation schematic of the system level performance model developed for the Li-S battery

For the current-voltage relation in the battery, the electrochemical model described previously is used but now, it is more complicated. For the battery pack construction, the Battery Performance and Cost (BatPac) model, which determines the battery design rules for EV applications, becomes the basis of the study [59, 60]. First, the cell considerations are determined with the electrochemical model. Then, the battery design based on these cell considerations are carried out in the battery construction part. Therefore, system level performance model can be divided into two parts as the I-V relation and the battery design.

3.3.1 I-V Relation for System Level Performance Model

For the system level performance, there are some parameters that are needed to be fixed for the battery pack and, the model calculations are done based on them. These requirements are *Energy*, which is used for cell capacity and cathode thickness determinations, *Power*, which calculates cell area, and *Battery Pack Voltage*, which

provides the number of cells in battery. Cell is designed at 80% DOD to provide the rated power and at 50% DOD to provide the rated energy [10, 61]. In the model, all parameters are coupled for rated power and rated energy. Pack design equations based on the current and voltage at rated power (subscript p) and energy (subscript e) are given Equations 3.40-3.50. Detailed overpotential calculations are given in Appendix B.

$$A_{cell}=\frac{P}{\text{number of cell}\times Ip\times Vp} \tag{3.40}$$

$$Q=\frac{E}{\text{number of cell}\times Ve} \tag{3.41}$$

$$L_{pe}=\frac{c}{\varepsilon_{dis}\times v_s} \tag{3.42}$$

$$L_{ne}=\frac{L_{pe}\times\varepsilon_{dis}}{c_{ne}}\times\frac{N}{P} \tag{3.43}$$

$$Ie=\frac{c}{5h} \tag{3.44}$$

$$Vp=0.8\times U \tag{3.45}$$

$$\eta_{total\ p,e}=\eta_{pe,p,e}+\eta_{ne,p,e}+\eta_{sep,p,e}+\eta_{cc-,p,e}+\eta_{cc+,p,e} \tag{3.46}$$

$$ASI_{total\ ,p,e}=ASI_{pe,p,e}+ASI_{ne,p,e}+ASI_{sep,p,e}+ASI_{cc-,p,e}+ASI_{cc+,p,e} \tag{3.47}$$

$$A_{pack}=A_{cell}\times\text{number of cell} \tag{3.48}$$

$$\text{Number of layers per cell}=\text{even}\left(\frac{A_{cell}}{500}\right) \tag{3.49}$$

$$A_{layer}=\frac{A_{cell}}{\text{number of layers per cell}} \tag{3.50}$$

where P is battery pack power in kW, A_{cell} is the cell area in cm^2, Ip is the pulse power current density in A cm^{-2}, Q is the cell capacity in Ah, E is the battery pack energy in kWh, Ve is the voltage at rated energy in V, L_{pe} is cathode thickness in cm, c is specific capacity in Ah cm^{-2}, $\varepsilon_{dis}$is the discharged volume fraction in mAh

cm^{-3}, Ie is the average current density in A cm^{-2}, Vp is the voltage at rated power in V, $\eta_{total,p}$ and $\eta_{total,e}$ are the total overpotential of the cell at rated power and energy in V, $ASI_{total,p}$ and $ASI_{total,e}$ are the total ASI of the cell at rated power and energy in $\Omega\ cm^2$, A_{pack} and A_{layer} are the pack and layer area in cm^2.

3.3.2 I-V Relation with the Maximum Thickness Limitation

The cell area, cell capacity and thickness of the electrode needed for the specified pack energy and power requirements are found using the design equations described above. Typically in the battery design, there is a maximum electrode thickness limitation, a practical limitation in porous electrodes coming from the battery life and performance [10, 60–62]. Therefore, when the model calculates equal or higher thicknesses (Equation 3.51) than the maximum thickness set for the positive electrode, cell area and negative electrode thickness are recalculated based on the maximum positive electrode thickness. Therefore, the I-V relation of the cell is remodeled with some variations. These changed calculations are given in details in Appendix C. The equations which depend on the thickness are summarized below; Li-S battery pack is designed with these equations. The parameters used in I-V relation models are given in Table 3.3.

$$L_{\text{pos. electrode parameter}} = \frac{C}{c_{pe}} \tag{3.51}$$

$$L_{\text{neg. electrode parameter}} = \frac{L_{\text{pos. electrode parameter}} \times c_{pe}}{c_{ne}} \times \frac{N}{P} \tag{3.52}$$

$$L_{\text{pos.electrode at adj OCV\%}} = L_{\text{max pos. electrode}} \quad \left(\text{if } L_{\text{pos. electrode parameter}} > L_{\text{max pos. electrode}}\right) \tag{3.53}$$

$$L_{\text{neg.electrode at adj OCV\%}} = \frac{L_{\text{pos.electrode at adj OCV\%}} \times c_{pe}}{c_{ne}} \times \frac{N}{P} \tag{3.54}$$

$$A_{cell}=\frac{Q}{L_{pos.electrode\ at\ adj\ OCV\%}\times c_{pe}} \tag{3.55}$$

$$\text{Number of layers per cell}=\text{even}\left(\frac{A_{cell}}{500}\right) \tag{3.56}$$

$$A_{layer}=\frac{A_{cell}}{\text{Number of layers per cell}} \tag{3.57}$$

$$A_{pack}=A_{cell}\times\text{number of cell} \tag{3.58}$$

$$Q=\frac{E}{\text{number of cell}\times Ve} \tag{3.59}$$

Table 3.3. Parameters used in the calculation of I-V relations in the system level performance model [10]

Power (kW)	80
Energy (kWh)	118
Average Battery Open-Circuit Voltage, U_{batt} (V)	360
Average Cell Open-Circuit Voltage, U_e (V)	2.2

Target Voltage Efficiency at Rated Power, (V/U)	0.8
Maximum Cathode Thickness, L_{pe} (μm)	150
Negative-to-positive capacity ratio, $\frac{N}{P}$	1.5
Useable SOC (%)	85

3.3.3 Battery Pack Design

As described in the previous part, the cell is designed using the I-V relations to satisfy the energy, power and voltage requirements. After the cell design is completed, a detailed configuration of the battery that depends on the calculated cell capacity, number of cells and cell area is done based on the BatPac model [10, 60]. In this part of the system level performance model, all the essential components for the manufacturing of the Li-S battery pack is considered including the packaging and thermal management. It starts with the cell design, followed by the module design and, finally finishes with the battery pack design. The battery pack is designed for 1 cell in parallel, 8 modules in row, 1 row of module per pack and 1 module in parallel. Required cell and module connections are determined as given in Equations 3.60-3.62. Then, all required dimensions are calculated for the cell, the module and battery pack step by step. Detailed calculations are explained in Appendix D.

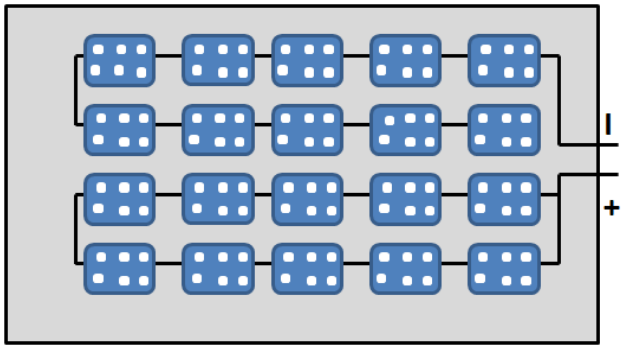

Figure 3. 4. A typical cell and module connections in the battery pack

$$\text{Number of cells per module} = \frac{\left(\frac{U_{battery}}{\text{number of (cells in parallel} \times \text{ modules in parallel} \times U_e)}\right)}{\text{number of modules in row}} \quad (3.60)$$

$$\text{Number of modules per battery pack} = \text{number of (modules in row x rows of modules per battery pack)} \quad (3.61)$$

$$\text{Cells per battery pack} = \text{number of cells per module x number of modules in row} \quad (3.62)$$

In the system level performance model, current and voltage relations obtained for the cell are integrated into the battery design as shown in Equations 3.63-3.66. Finally, using these system values for the batteries the effect of E/S ratio on the specific energy and energy density of the Li-S battery is determined.

$$\text{Usable Energy} = \text{Useable SOC (\%)} \times E \quad (3.63)$$

$$\text{Mass} = \text{Battery mass (all packs)} \quad (3.64)$$

$$\text{Volume} = \text{Battery volume (all packs)} \quad (3.65)$$

$$\text{Specific Energy} = \frac{\text{Usable Energy}}{\text{Mass}} \quad (3.66)$$

$$\text{Energy Density} = \frac{\text{Usable Energy}}{\text{volume}} \tag{3.67}$$

$$\frac{E}{S} = \frac{V_{electrolyte}}{\text{S loading in the cathode}} \tag{3.68}$$

where usable energy in kWh , mass in kg, volume in L, specific energy in Wh kg^{-1}, energy density in Wh L^{-1}, E/S ratio in mL g_s^{-1}.

CHAPTER 4

RESULTS AND DISCUSSION

In this section of the thesis, the model predictions for the effect of the E/S ratio on the Li-S battery performance are explained in detail. This section is divided into three parts as the results of the electrochemical, cell-level and system-level performance models.

4.1 The Effect of E/S Ratio on the Electrochemical Performance of a Li-S Cell

As previously discussed, electrolyte to sulfur ratio is an important design parameter for Li-S cells. Increasing the electrolyte amount provides easier electron transfer and ion diffusion by means of increasing dissolution of polysulfides [4]. However, excess electrolyte amount decreases the energy density of the cell [10]. Therefore, electrolyte to sulfur ratio should be optimized for good electrochemical performance and high energy density. For this purpose, in the electrochemical performance model the effect of E/S ratio on the cathode kinetics is investigated by the cell voltage predictions with varying E/S. The cell performance is examined via cell voltage at 60% depth of discharge corresponding to the second plateau voltage.

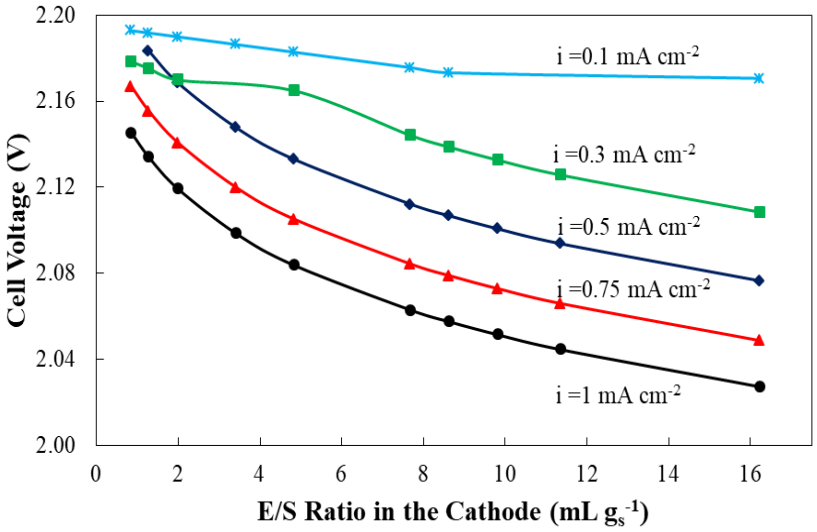

Figure 4. 1. The effect of E/S ratio in the cell on the calculated cell voltage at 60% DOD of a Li-S cell for different current densities. The C/S ratio in the cathode is 0.5, and the cathode exchange current density is i0,pe = 6.28 × 10−7 A cm−2 for all results.

The effect of E/S ratio on the cell voltage with different current densities is determined using the electrochemical performance model as given in Figure 4.1. As it is seen from the figure, increasing E/S ratio in the cathode reduces the cell voltage at each current density. In addition, voltage decreases more sharply with the E/S ratio at higher current densities because that the Tafel kinetics takes over at higher current densities in the model. In the electrochemical model, increasing the E/S ratio in the cathode affects Linear or Tafel kinetics by means of the electrochemically active area, a. Moreover, E/S ratio impacts the Bruggeman's relations defining the effective ionic and electronic conductivities. Rising E/S ratio, or increasing porosity in other words, diminishes a and σ_{eff} and increases κ_{eff} due to the decreasing carbon volume fraction in the cathode. However, this trend seen in Figure 4.1 is unexpected based on other studies in the literature [2, 11, 20, 27, 35–38] because that in the literature increasing electrolyte amount improves the sulfur utilization by dissolving more polysulfides and thus, increases the cell performance.

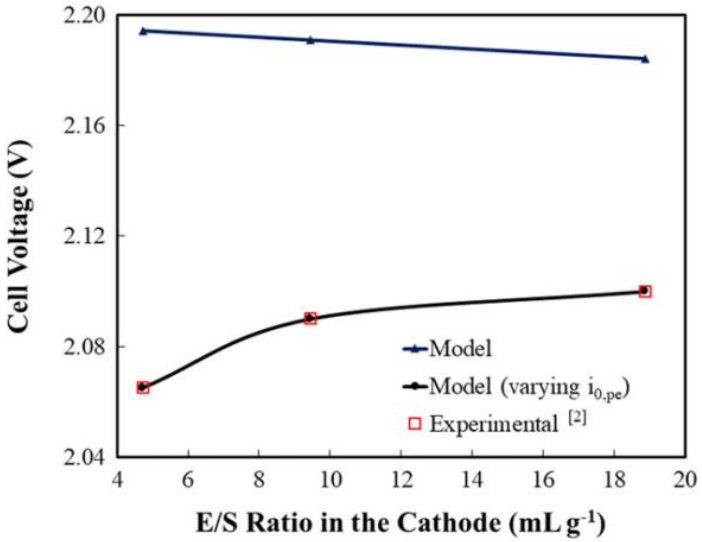

Figure 4. 2. Experimental validation of the effect of E/S ratio in the cell on the calculated cell voltage at 60% DOD of a Li-S cell. The C/S ratio in the cathode is 0.5, the current density is 0.0566 mA cm^{-2}, cathode thickness is 100 μm for all results and the cathode thickness is 100 μm for all results and the cathode exchange current density is $i_{0,pe} = 6.28 \times 10^{-7}$ A cm^{-2} for the blue line and $i_{0,pe}$ is a function of the E/S ratio (7×10^{-9} and 6×10^{-8} A cm^{-2}) for the black line.

The electrochemical model cannot give the same trend with the literature as it is seen from Figure 4.1. In order to validate the model cell voltage predictions, an experimental study by Ding et al. is used [2]. Carbon to sulfur ratio, electrolyte to sulfur ratio, cathode thickness and current density values of the study are fed into the model and the experimental data and the model results are compared at 60% DOD, which is the second plateau region of the cell voltage curve. The comparison of the two studies is given in Figure 4.2. According to the figure, the model cannot capture the experimental trends. In the experimental study, which is shown with the red line in the figure, increasing E/S ratio improves cell voltage as expected. However, the model shows an opposite trend. In addition, the decrease in the cell voltage is modest, indicating that the effect of E/S ratio is not seen so much on the cell voltage. In the model, E/S ratio affects the cell performance via the electrochemically active area; however, the results suggest that E/S has another significant effect that should be considered in the model. From the literature, it is known that the E/S ratio

influences the polysulfide shuttle mechanism and the electrochemical reaction mechanism in the cell. Therefore, it has important role on the reaction kinetics in the cathode [19]. In the model, cathode exchange current density is the only kinetic parameter considering the electrochemical and physical processes occurring in the cathode. For the reason that E/S ratio affects the electrochemical reactions in the cell, $i_{0,pe}$ may be defined as a function of E/S ratio. In the figure, as it is seen from the black line, the model can capture the experimental trend when $i_{0,pe}$ is varied with the E/S ratio between $7x10^{-9}$ and $6x10^{-8}$ A cm^{-2}.

4.1.1 The Effect of E/S Ratio on the Cathode Exchange Current Density

In order to determine the dependence of the cathode exchange current density on the electrolyte amount, the total ASI of the cell obtained by the model (Equation 3.11) can be directly compared with the experimentally measured cell resistances [40, 63, 64]. The data of an experimental study in the literature examining the effect of E/S ratio on the cell resistance is used to define the cathode change current density as a function of the amount of the electrolyte [40]. The experimental current density and C/S and E/S ratios in the cathode are fed into the model and the total area-specific impedance results of the model are compared with the experimentally measured cell resistances at 60% discharge depth (DOD). As shown in Figure 4.3, the ASI results of the model and experimental cell resistance data are matched to determine the dependency of the cathode exchange current density on the electrolyte volume fraction.

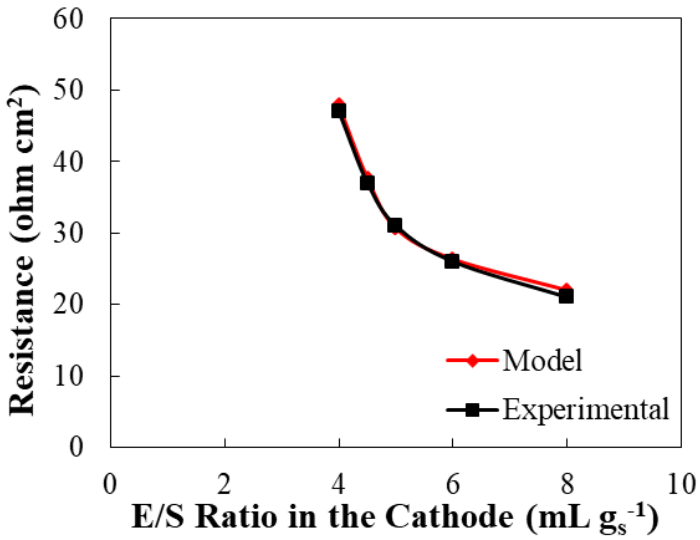

Figure 4. 3. Experimentally measured cell resistances (Figure 5 in the study performed by [40]) in comparison with the total area-specific impedance results calculated at 60% discharge depth as a function of the E/S ratio in the cathode. The current density is 0.4598 mA cm^{-2}, and C/S ratio in cathode is 0.43 for all results.

As mentioned before, the electrolyte amount affects the rate of the electrochemical reactions in the cell through the dissolved polysulfide concentration in the cathode. Therefore, the kinetic parameter cathode exchange current density is influenced by the electrolyte volume fraction in the cathode. Based on Figure 4.3, the relationship between the cathode exchange current density and the electrolyte volume fraction is determined and it is given in Figure 4.4. According to the figure, $i_{0,pe}$ is significantly dependent on the electrolyte volume fraction in the cathode. In addition, this inference verifies Figure 4.2 indicating that increasing E/S ratio improves the cathode kinetics through increasing $i_{0,pe}$. As it is seen from Figure 4.4, $i_{0,pe}$ depends on the electrolyte volume fraction linearly and this relation is given in Equation 4.1. In the equation ε is the electrolyte volume fraction in the cathode, in other words the porosity. The dependence of the kinetic parameter on the electrolyte amount is defined in terms of the porosity in the model rather than the E/S ratio since E/S ratio is also a function of the S loading in the cell. Because this equation gives negative $i_{0,pe}$values in low electrolyte volume fractions ($\varepsilon < 0.8$), in the model $i_{0,pe}$ is kept constant at its value at $\varepsilon = 0.8$ for these lower porosities.

$$i_{0,pe}=1.81\times10^{-5}\times(\varepsilon)-1.44\times10^{-5} \quad (4.1)$$

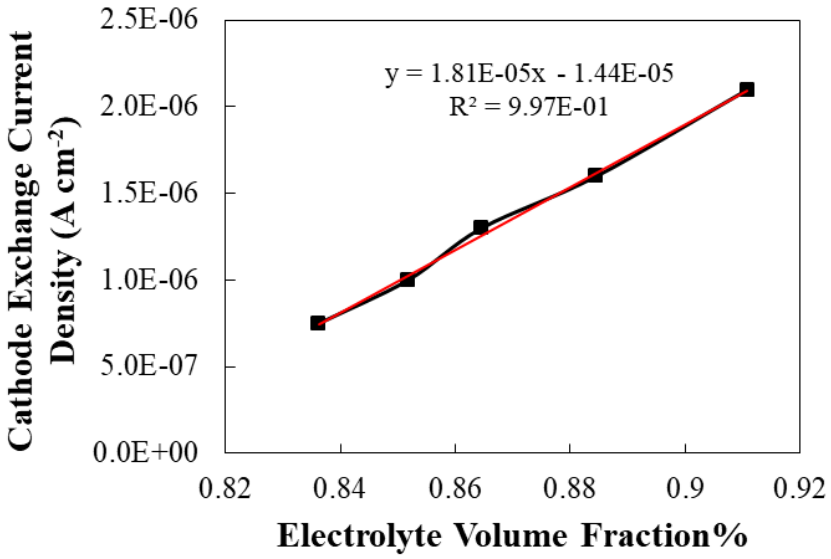

Figure 4. 4. Cathode exchange current density determined as a function of the electrolyte amount.

4.1.2 The Effect of E/S Ratio on the Cell Voltage

In the model, the Tafel and Linear kinetic equations (Equations 3.3. and 3.4.) are modified according to the new cathode exchange current density (Equation 4.1). The effect of E/S ratio in the cathode on the electrochemical performance of a Li-S cell is observed at different current densities as given in Figure 4.5. As it is seen from the figure, increasing E/S ratio in the cell increases cell voltage results at each C-rate; however, the improvement in cell voltage with increasing E/S ratio is less apparent at higher E/S ratios. In addition, cell voltage is more sensitive to the electrolyte amount at higher C-rates, where kinetic limitations are expected to be more obvious. The trends observed in Figure 4.5 is the opposite of the previous predictions of the model (Figure 4.1). It can be concluded that the improved model can capture the experimental trends seen in the literature successfully [2,9,10,27,35,38].

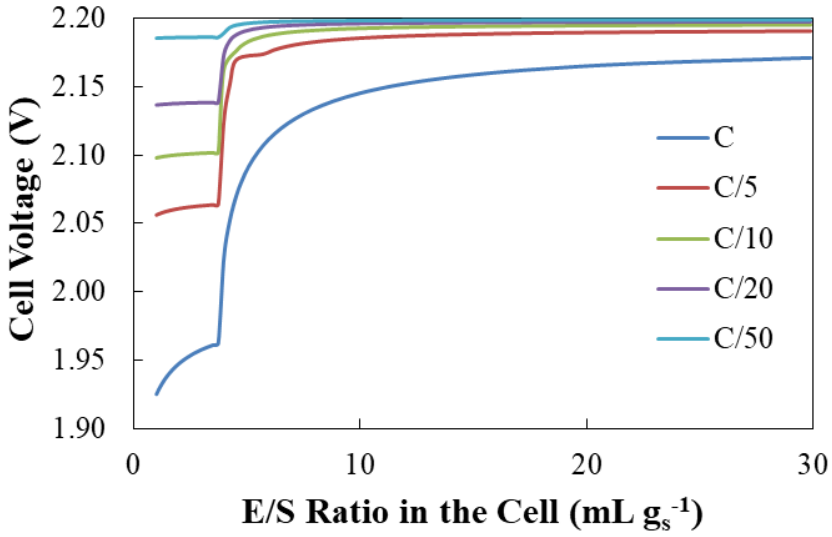

Figure 4. 5. The effect of E/S ratio in the cell on the calculated cell voltage at 60% DOD of a Li-S cell for different current densities. The C/S ratio in the cathode is 0.5, and the cathode thickness is 100μm for all results. The cathode exchange current density is defined as a linear function of the electrolyte volume fraction.

4.2 The Effect of E/S Ratio on the Cell Level Performance of a Li-S Battery

The electrochemical performance model is extended in order to detect the effect of E/S ratio on the cell level performance of a Li-S cell. In the electrochemical performance model, the importance of the electrolyte amount on the cathode exchange current density is realized. However, E/S ratio also plays a significant role on the specific capacity of the cell. Therefore, this effect should be considered in the cell level performance model. There are many experimental studies in the literature about the specific capacity and E/S ratio relation [2, 4, 18, 20, 28, 35, 37, 38]. According to these studies, increasing E/S ratio influences the sulfur utilization thus the discharge capacity of the cell. In order to capture this effect on the cell level performance model, cathode specific capacity, or the discharge capacity in other words, is fed into the model either as a function of the E/S ratio or, as a constant value; specific energy and energy density of the cell are determined accordingly. In addition to the E/S ratio, there are other important design parameters influencing the Li-S cell performance, which are cathode thickness, carbon to sulfur ratio (C/S) in

the cathode, excess lithium amount in the anode (N/P ratio), current density (C-rate) and sulfur loading in the cathode. In the cell level performance model, the dependence of the cell performance on the E/S ratio as a function of these other design parameters is also analyzed as discussed below.

4.2.1 Cell Performance Model with Cathode Specific Capacity Defined as a Function of E/S Ratio in the Cell

4.2.1.1 The Effect of E/S Ratio on the Cathode Specific Capacity

As mentioned before, E/S ratio is an effective parameter in sulfur utilization. An increase in the E/S ratio provides an increase in the initial discharge capacity. This may be explained such that when the electrolyte amount is too low in the cell, polysulfide concentration becomes too high in the cathode decreasing Li-ion and polsulfide diffusion as a result of increasing electrolyte viscosity. Consequently, the capacity of the cell drops [4]. Since modeling the impact of the electrolyte amount on the sulfur utilization is not straight forward, an empirical equation is used in this model. In order to determine the dependence of the specific capacity of the cell on the E/S ratio, experimental data from the literature is used as shown in Figure 4.6 [2, 35, 38]. As it is seen from the Figure 4.6, specific capacity can be defined as a linear function of the E/S ratio. This linear relation, which is based on the average of the experimental data, is shown in Equation 4.2. It is observed that if the E/S ratio is greater than 9 mL g_s^{-1}, which is around 92% porosity, the discharge capacity exceeds the theoretical value of a Li-S cell. Thus, at higher E/S ratios, specific capacity is taken as the theoretical capacity of 1675 mAh g_s^{-1}.

$$c_{pos,act} = 174.16 \times \left(\frac{E}{S}\right) + 100.97 \tag{4.2}$$

which $c_{pos,act}$ is specific capacity in mAh g_s^{-1}, $\frac{E}{S}$ is electroltye to sulfur ratio in the cell in mL g_s^{-1}.

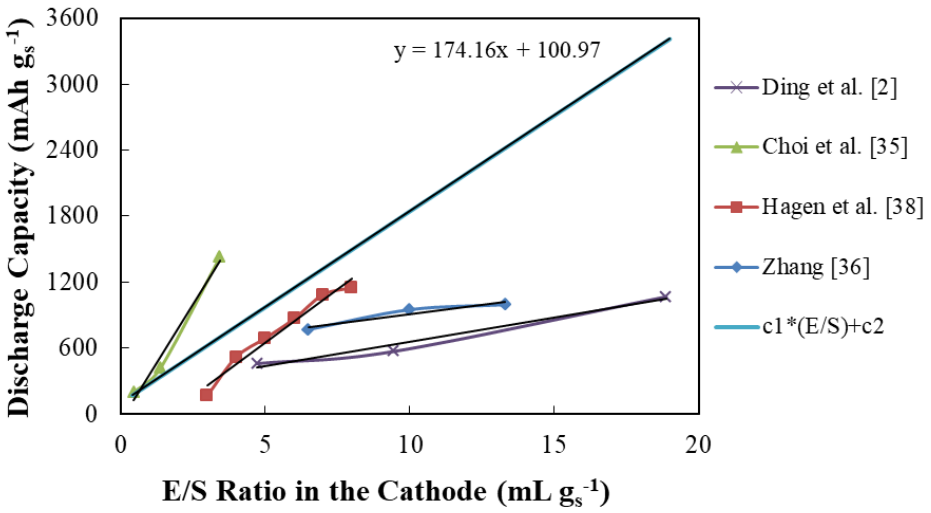

Figure 4. 6. The effect of E/S ratio on the discharge capacity of a Li-S cell for different experimental studies

4.2.1.2 The Effect of E/S Ratio on the Cell Voltage

In the model, in order to observe the effect of E/S ratio on the cell voltage, cathode thickness, C/S ratio, N/P ratio and current density are taken as 100µm, 0.5, 1.5 and C/5 rate, respectively as a baseline and, the result is given in Figure 4.7a. As it is seen from the figure, cell voltage increases sharply around 3.75 mL g_s^{-1} E/S. This sudden rise occurs due to the limitation of the cathode kinetics at low E/S ratios, which may be explained by the relation between the electrolyte amount and the cathode exchange current density discussed in the previous section. After the rise, cell voltage keeps constant at approximately 2.18 V with increasing E/S ratio. At this baseline, The breakdown of ASI and overpotential of the cell components are also given in Figure 4.7b and Figure 4.7c. As it seen from the figures, cathode has the largest portion in the cell ASI and overpotential. Therefore, cathode design affects the current voltage relation for the cell significantly.

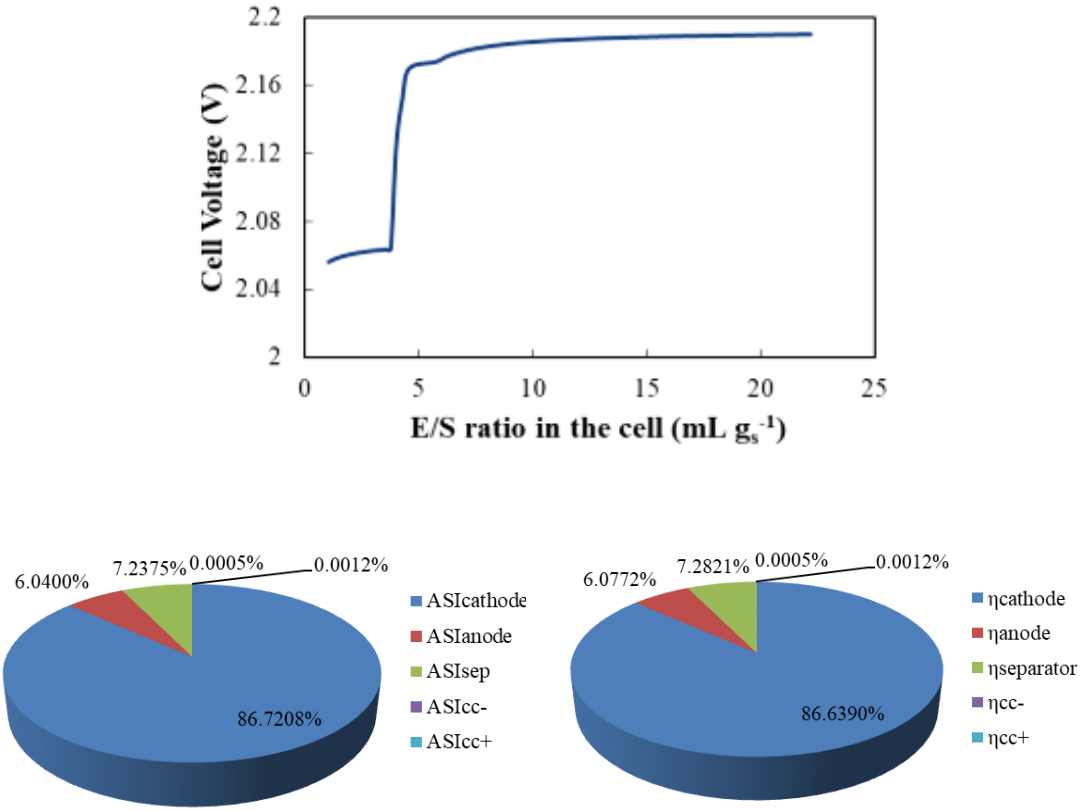

Figure 4. 7. (a)The effect of E/S ratio in the cell on the calculated cell voltage and the breakdown of (b) ASI and (c) overpotential of cell components at 60% depth of discharge of the Li-S cell. The cathode thickness is 100 µm, C/S ratio is 0.5, N/P ratio is 1.5 and current density is C/5.

4.2.1.3 The Effect of E/S Ratio on the Cell Level Specific Energy

The effect of E/S ratio on the cell level specific energy is shown in Figure 4.8. According to the baseline calculations of model, specific energy increases with increasing E/S ratio until approximately 9 mL g_s^{-1}. At this point, the highest specific energy value, which is 138 Wh kg^{-1} is obtained. Then, it starts to decrease continuously. The reason of this trend is that increasing E/S ratio raises the specific capacity and thus the specific energy. However, after the theoretical specific capacity is reached due to the specific capacity limitation in the model, specific energy starts to decrease with increasing E/S ratio. Increasing E/S ratio also improves the cathode kinetics and thus the cell voltage but this effect is less apparent.

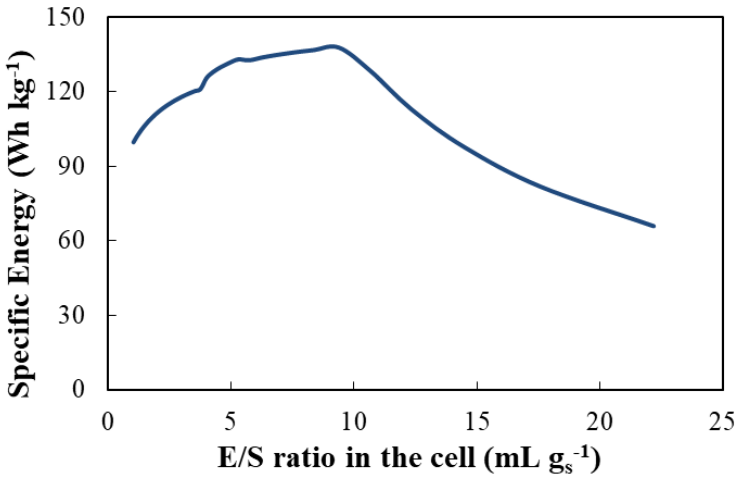

Figure 4. 8. The effect of E/S ratio in the cell on the calculated cell-level specific energy of a Li-S cell. The cathode thickness is 100 µm, C/S ratio is 0.5, N/P ratio is 1.5 and current density is C/5.

4.2.1.4 The Effect of E/S Ratio on the Cell-Level Energy Density

The effect of E/S ratio on the energy density at the cell level is given in Figure 4.9. Similar to the trend seen for the baseline results for the specific energy, energy density also increases with increasing E/S ratio until a point. After approximately 9 mL g_s^{-1} E/S ratio, energy density starts to decrease from the maximum value of 230 Wh L^{-1}. The same discussion is valid here; specific capacity limitation in the model causes this trend.

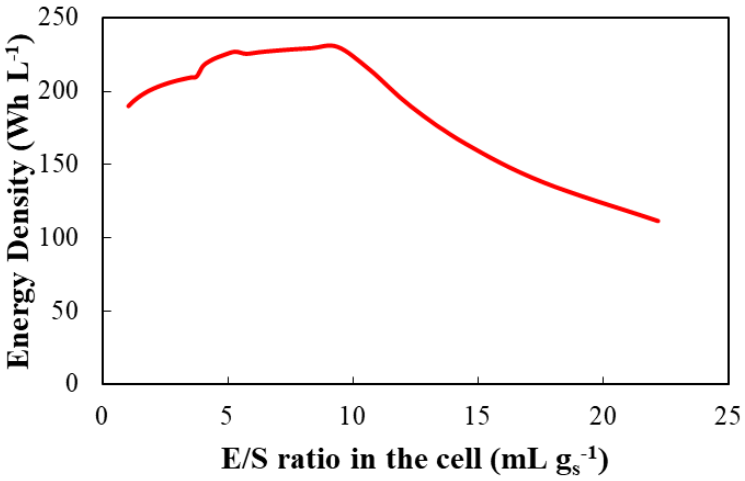

Figure 4. 9. The effect of E/S ratio in the cell on the calculated cell-level energy density of a Li-S cell. The cathode thickness is 100 μm, C/S ratio is 0.5, N/P ratio is 1.5 and current density is C/5.

Next, the effect of other critical design parameters, which are the cathode thickness, C/S ratio in the cathode, sulfur loading in the cathode, N/P ratio in the anode and current density are investigated.

4.2.1.5 The Effect of Cathode Thickness

The sulfur utilization and cell voltage of the Li-S cells are sensitive to the cathode thickness by means of the active material loading and overpotential. Therefore, the cathode thickness is an important parameter for both the cell capacity and the performance. In the model, the effect of cathode thickness on the cell level performance is investigated as discussed next.

The effect of E/S ratio in the cell on the cell voltage for different thicknesses is presented in Figure 4.10. Until approximately 3.65 mL g_s^{-1} E/S ratio, cell voltage increases sharply with increasing E/S ratio. After this point, it is seen that cell voltage stays nearly constant. The effect of thickness on the cell voltage can only be observed at low E/S ratios, where the kinetic limitations are significant within the cell. Lower thickness has higher cell voltage due to a lower overpotential in the cell

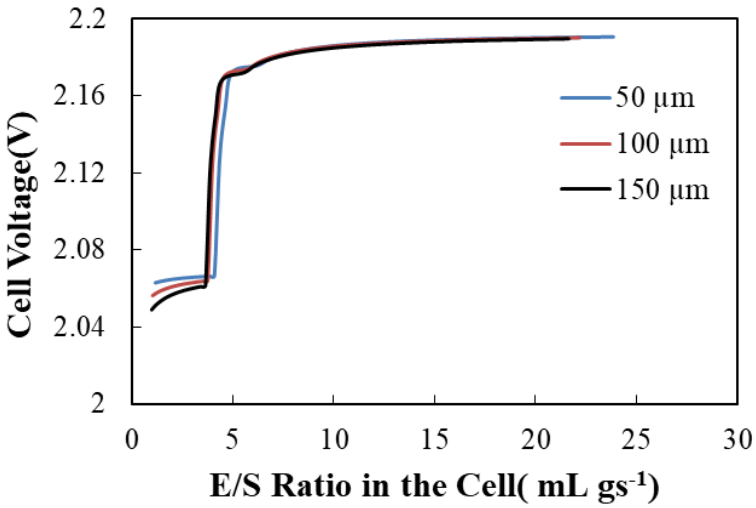

Figure 4. 10. The effect of E/S ratio in the cell on the calculated cell voltage at 60% depth of discharge of the Li-S cell for different cathode thicknesses. The C/S ratio is 0.5, N/P ratio is 1.5 and current density is C/5 for all results.

In Figure 4.11, the effect of E/S ratio on the cell-level specific energy is given for cathode thicknesses between 50-150 µm. Until around 9-10 mL g_s^{-1}, specific energy increases with increasing E/S ratio for every thickness. The highest specific energy value, which is 170 Wh kg^{-1}, is obtained at 150 µm thickness and 9 mL g_s^{-1} ratio. After the maximum point, it starts to decrease as discussed above. Increasing the cathode thickness improves the specific energy because that cell capacity rises with increasing thicknesses, or higher S loadings in other words (equation 3.37). Increasing thickness also causes higher current densities and thus lower cell voltages. However, the rise in the cell capacity compensates the decrease in the cell voltage and increase in the cell mass. As a conclusion, cell-level specific energy increases with higher thicknesses.

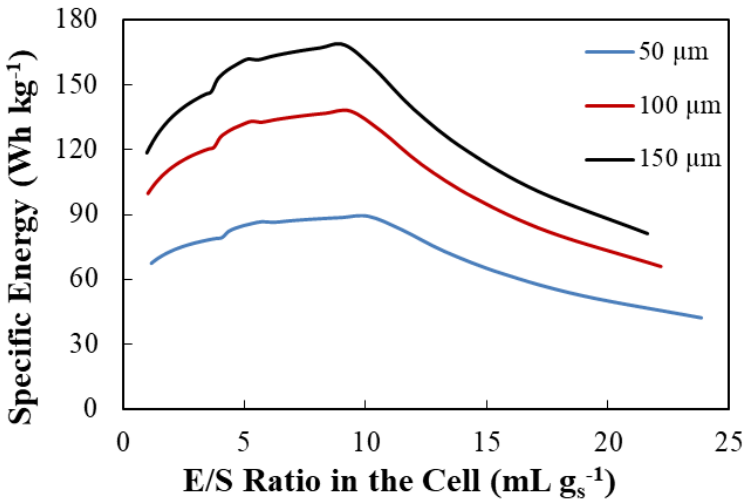

Figure 4. 11. The effect of E/S ratio in the cell on the calculated cell-level specific energy of a Li-S cell for different cathode thicknesses. The C/S ratio is 0.5, N/P ratio is 1.5 and current density is C/5 for all results.

The predicted cell-level energy density with varying E/S ratio for different cathode thicknesses is shown in Figure 4.12. The highest value, which is 255 Wh kg^{-1}, is obtained at 150 µm thickness and 9 mL g_s^{-1} E/S ratio. After the maximum point, energy density decreases continuously for all thicknesses. The energy density results show the same trend with the specific energy results; all the discussions made for Figure 4.10 is also valid for Figure 4.11. Similarly, for the energy density, increasing cell capacity with increasing thickness compensates the increase in the cell volume. Therefore, higher cathode thickness gives better energy density results.

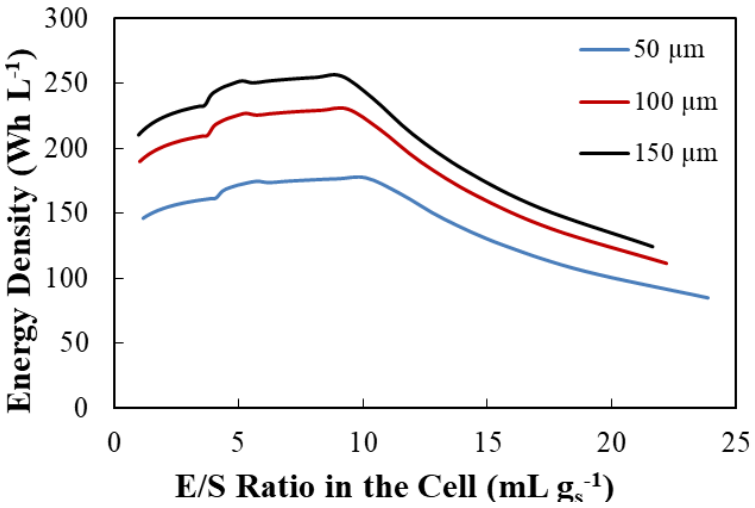

Figure 4. 12. The effect of E/S ratio in the cell on the calculated cell-level energy density of a Li-S cell for different cathode thicknesses. The C/S ratio is 0.5, N/P ratio is 1.5 and current density is C/5 for all results.

4.2.1.6 The Effect of C/S Ratio

The amount of carbon to sulfur ratio in the cathode is very important for the cell performance because for high sulfur contents the electrode conductivity and the electrochemically active area decrease. Consequently, sulfur utilization is influenced negatively [16]. However, since sulfur is the active material in the cell, too low S contents lead to low cathode capacity. Therefore, the carbon to sulfur ratio in the cathode should be optimized.

In Figure 4.13, the effect of E/S ratio on the cell voltage for different C/S ratios is shown. According to the figure, increasing electrolyte amount significantly increases the cell voltage up to a certain E/S ratio for all C/S ratios; the increase in the cell voltage is less noticeable after this point. In addition, the effect of the C/S ratio on the cell voltage can be realized. Increasing the C/S ratio results in a decrease in sulfur loading and consequently the current density. This leads to a decrease in the overpotential and thus an increase in the cell voltage. The dependence of the voltage on the E/S ratio at lower C/S ratios is more apparent; at low C/S ratios, or high sulfur loadings, increased amount of electrolyte in the cathode enhances the cell voltage

considerably. Since the electrochemical surface area and electronic conductivity are low at low C/S ratios, the cathode kinetics is more sensitive to the amount of electrolyte. However, at high C/S ratios the effect of E/S ratio on cell voltage is less pronounced as the cathode is not kinetically restricted.

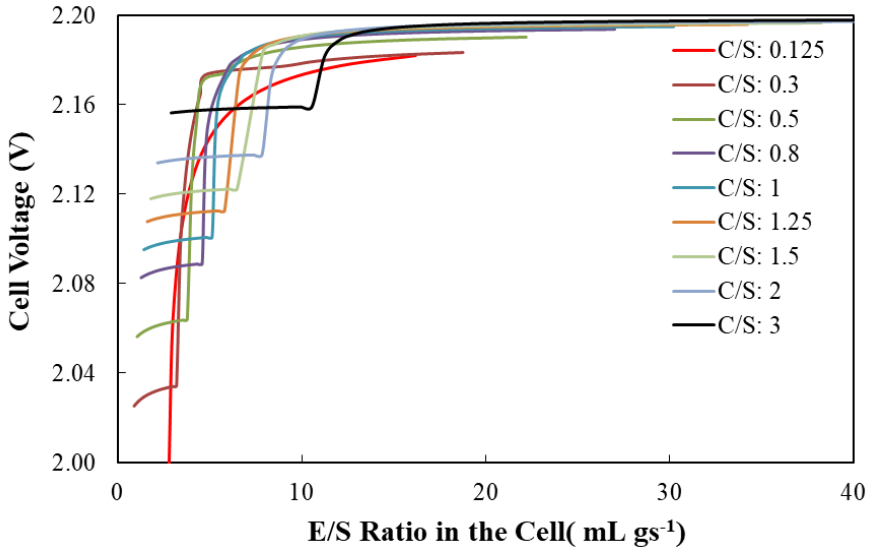

Figure 4. 13. The effect of E/S ratio in the cell on the calculated cell voltage at 60% depth of discharge of the Li-S cell for different C/S ratios. The cathode thickness is 100 µm, N/P ratio is 1.5 and current density is C/5 for all results

The effect of E/S ratio on the cell-level specific energy for C/S ratios of 0.125-3 is given in Figure 4.14. As it is seen from the figure, until an E/S ratio of 9 mL g_s^{-1} specific energy increases for every C/S ratio and after this point, specific energy starts to decrease. It can be seen that the cell is more sensitive to the C/S ratio change at lower E/S ratios; after 9 mL g_s^{-1} specific energies are very similar for every C/S ratio. At 0.125 of C/S ratio the maximum specific energy is obtained as 141 Wh kg^{-1}. Specific energy of the cell increases with decreasing C/S ratio. This is because that increasing C/S ratio decreases the cell capacity by decreasing the sulfur volume fraction in the cathode (Equation 3.37). On the other hand, cell mass decreases with increasing C/S ratio. Although increase in the cell voltage and decrease in the cell mass improve the specific energy with increasing C/S ratio, decreasing cell capacity

hinders this effect and as a result, increasing C/S ratio influences the specific energy negatively.

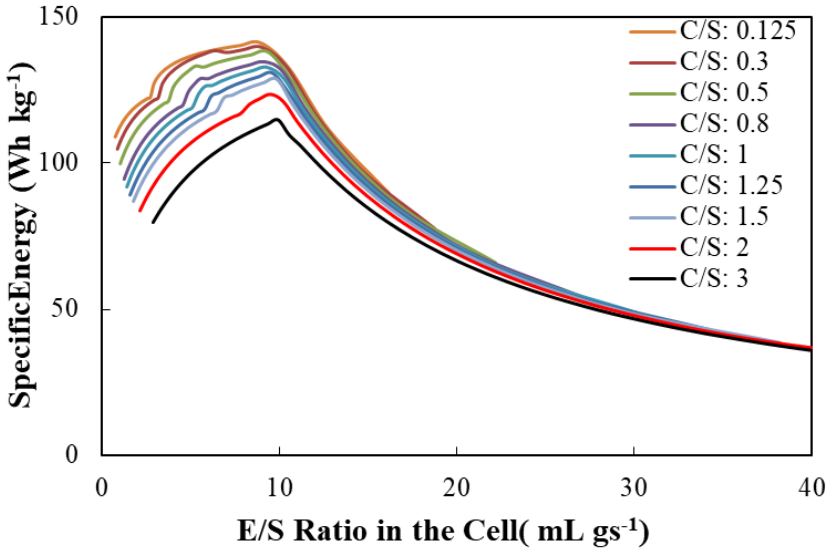

Figure 4. 14. The effect of E/S ratio in the cell on the calculated cell-level specific energy of a Li-S cell for different C/S ratios. The cathode thickness is 100 µm, N/P ratio is 1.5 and current density is C/5 for all results.

In Figure 4.15, the effect of E/S ratio in the cell on the cell-level energy density for different C/S ratios is given. The effect of C/S ratio on the energy density is not obvious for higher E/S ratios. For low E/S ratios, lower C/S ratio is better for the cell level performance because as in the specific energy results, increase in sulfur loading raises the cell capacity (with increasing sulfur utilization and sulfur volume fraction). Although, cell volume increases and cell voltage decreases with decreasing C/S ratios, higher cell capacity still provides higher energy densities. The maximum energy density, which is 234 Wh L^{-1}, is observed at 0.125 of C/S ratio.

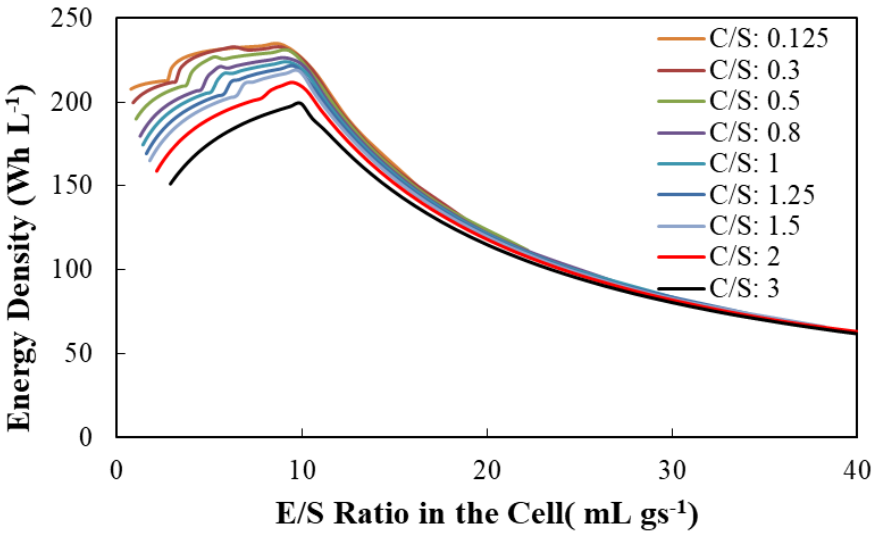

Figure 4. 15. The effect of E/S ratio in the cell on the calculated cell-level energy density of a Li-S cell for different C/S ratios. The cathode thickness is 100 μm, N/P ratio is 1.5 and current density is C/5 for all results.

4.2.1.7 The Effect of Sulfur Loading

As can be seen from Figure 4.16, increasing E/S ratio increases the cell voltage significantly up to about 4 mL g_s^{-1} for all S loadings. But at higher E/S ratios, the increase in the cell voltage is less apparent. As seen, this trend is independent of the amount of sulfur loading, but, at lower sulfur loadings increase in the cell voltage is less noticeable. Sulfur and Li_2S have low electronic conductivity and this limits the electrochemical reaction kinetics. In the model, this effect is captured as follows. The increase in the sulfur content affects the electrochemically active area and the effective electronic and ionic conductivity negatively by decreasing ε_C (carbon volume fraction in the cathode). In addition, the increase in the sulfur loading at a constant C/S ratio increases the cathode thickness, so the current density gets higher and the cell voltage decreases more.

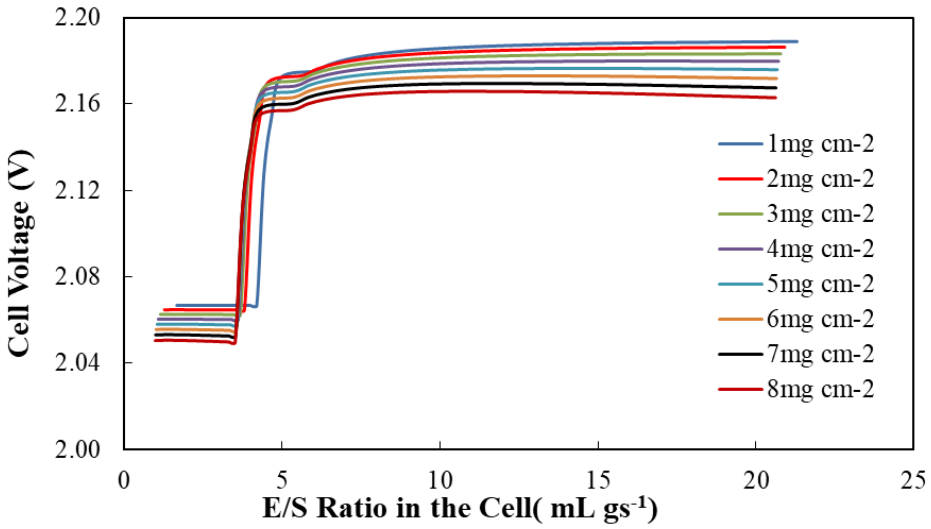

Figure 4. 16. The effect of E/S ratio in the cell on the calculated cell voltage at 60% depth of discharge of the Li-S cell for different sulfur loadings. C/S ratio is 0.5, N/P ratio is 1.5 and current density is C/5 for all results.

In Figure 4.17, the effect of E/S ratio in the cell on the specific energy of a Li-S cell for sulfur loadings of 1-8 mg cm^{-2} is determined. Until approximately 8.5 mL g_s^{-1} E/S ratio, specific energy increases for every S loading. Starting from this point, specific energy starts to decrease. Specific energy increases with increasing S loading as seen in the figure. This is because of the increasing cell capacity with increasing sulfur content in the cathode. This predicted trend about the effect of sulfur loading is consistent with the literature [43]. Moreover, it is apparent in the figure that at higher sulfur loadings (6, 7, 8 mg cm^{-2}) specific energy results become less different, especially at higher E/S ratios. As a conclusion, the maximum specific energy of 260 Wh kg^{-1} is calculated for 8 mg cm^{-2} sulfur loading with 8.5 mL g_s^{-1} E/S ratio.

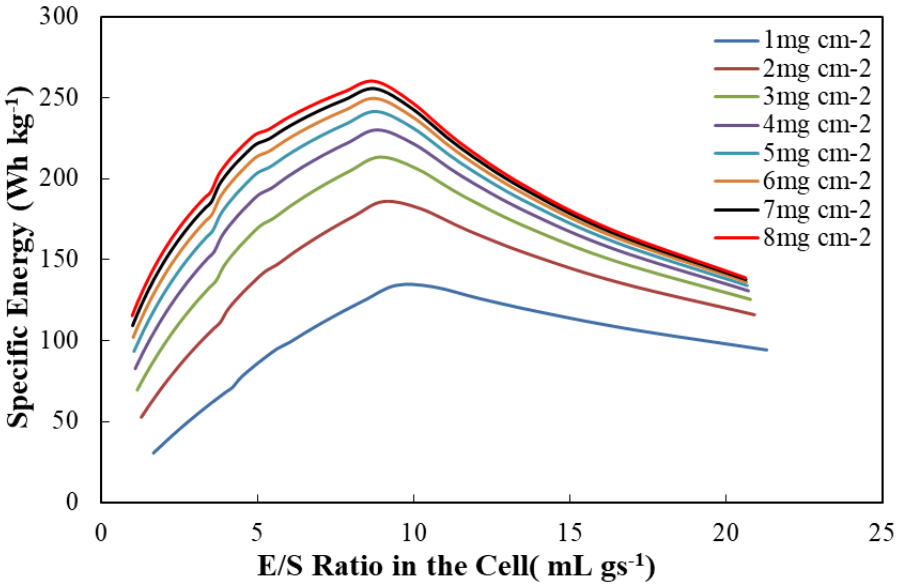

Figure 4. 17. The effect of E/S ratio in the cell on the calculated cell-level specific energy of a Li-S cell for different sulfur loadings. C/S ratio is 0.5, N/P ratio is 1.5 and current density is C/5 for all results.

As it is seen from Figure 4.18, until 8.5 mL g_s^{-1} E/S ratio energy density increases for all sulfur loadings. Higher sulfur loading increases the cell performance by means of rising cell capacity. This increase can be seen more apparently for lower sulfur loadings. In addition, at E/S ratios lower than 8.5 mL g_s^{-1}, higher sulfur loadings have more similar energy density values because that cell volume varies less at higher sulfur loadings. After the maximum point, energy density starts to decline and, at this region each sulfur loading except the lowest one has similar energy density values. According to the model predictions, for the maximum energy density, which is approximately 300 Wh L^{-1}, the cell should have 8.5 mL g_s^{-1} E/S ratio and at least 5 mg cm^{-2} sulfur loading.

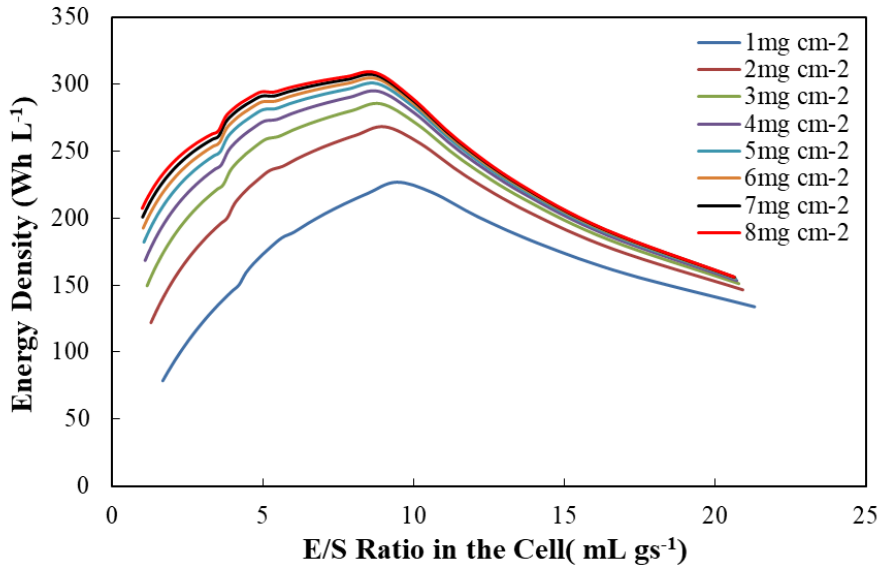

Figure 4. 18. The effect of E/S ratio in the cell on the calculated cell-level energy density of a Li-S cell for different sulfur loadings. C/S ratio is 0.5, N/P ratio is 1.5 and current density is C/5 for all results.

4.2.1.8 The Effect of N/P Ratio

As can be seen from Figure 4.19, increasing electrolyte amount up to about 6 mL g_s^{-1} E/S ratio significantly raises the cell voltage. The N/P ratio does not have an effect on the cell voltage. This is due to the fact that the N/P ratio does not affect the cathode thickness or the sulfur loading and thus the current density. Changes in the N/P ratio at a constant cathode thickness only affect the anode thickness. Since the anode thickness has no effect on the anode overpotential in the model, there is no change in the total overpotential of cell and so, no change in the cell voltage.

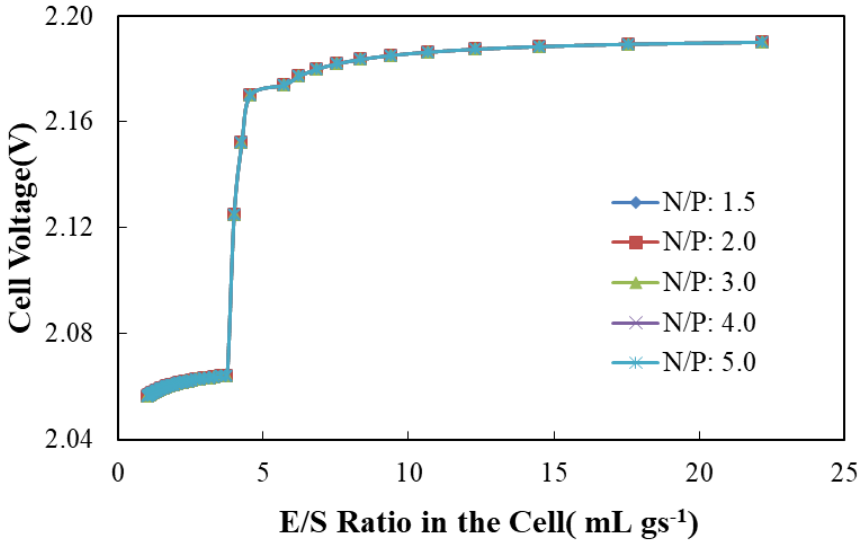

Figure 4. 19. The effect of E/S ratio in the cell on the calculated cell voltage at 60% depth of discharge of the Li-S cell for different N/P ratios. The cathode thickness 100 µm, C/S ratio is 0.5 and current density is C/5 for all results.

In Figure 4.20, the effect of E/S ratio in the cell on the specific energy for N/P ratios between 1.5 and 5 is given. Until approximately 8.5 mL g_s^{-1}, specific energy increases for every N/P ratio. At 1.5 of N/P ratio and 8.5 mL g_s^{-1} of E/S ratio the maximum specific energy value is obtained as 138 Wh kg^{-1}. After the maximum point, specific energy values start to decrease. Increasing N/P ratio reduces the specific energy but this decrease is not significant. This is because that cell mass increases with increasing N/P ratio. Therefore, the specific energy decreases. Since N/P ratio does not affect the cell capacity and just the mass and the volume of the cell, this decrease is not as significant as in the previous parameters.

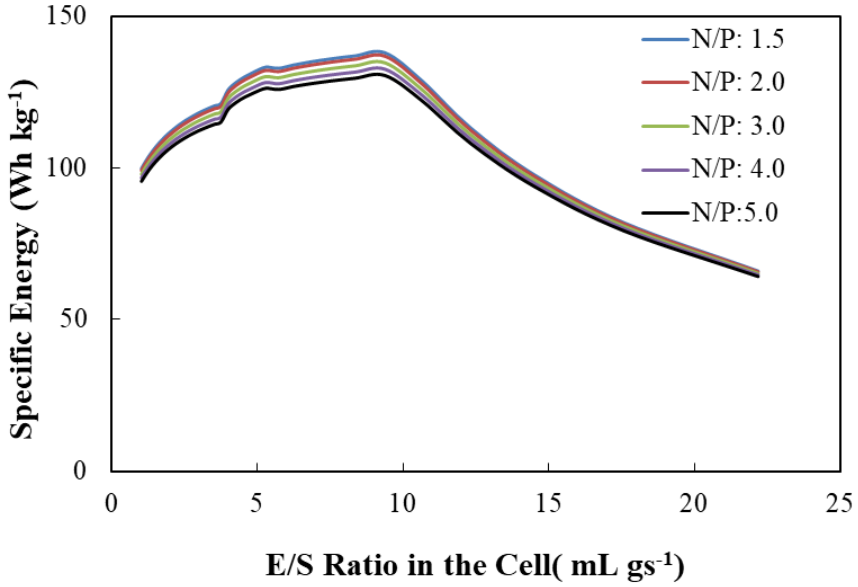

Figure 4. 20. The effect of E/S ratio in the cell on the calculated cell-level specific energy of a Li-S cell for different N/P ratios. The cathode thickness is 100 μm, C/S ratio is 0.5 and current density is C/5 for all results.

In Figure 4.21, the energy density results as a function of the E/S ratio for different N/P ratios are given. As in the specific energy results, energy density increases until approximately 8.5 mL g_s^{-1} ratio. However, the effect of N/P ratio can be seen more clearly on the energy density mainly due to the low density of the Li metal. At the lowest N/P ratio, the highest energy density, which is 230 Wh L^{-1}, is obtained. Therefore, the model predicts that lower N/P ratio provides higher energy density, which is consistent with the other modeling studies in the literature [17]. After the maximum point, energy density decreases at all N/P ratios and the difference in the energy densities becomes less obvious at higher E/S ratios.

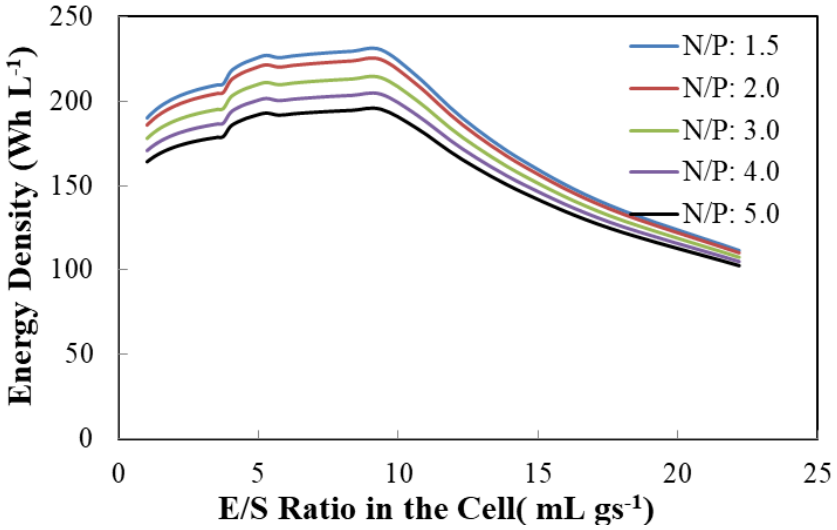

Figure 4. 21. The effect of E/S ratio in the cell on the calculated cell-level energy density of a Li-S cell for different N/P ratios. The cathode thickness is 100 µm, C/S ratio is 0.5 and current density is C/5 for all results

4.2.1.9 The Effect of Current Density

In Figure 4.22, it can be seen that the specific energy of the cell depends on the current density only at low E/S ratios. At lower current densities, overpotential is also lower so, the cell voltage becomes higher. The cell capacity and cell mass do not change with varying current density thus, only cell voltage affects the specific energy. After approximately 10 mL g_s^{-1} E/S ratio specific energy values start to decrease and the results are similar for every current density. The maximum specific energy is observed at C/50 and 10 mL g_s^{-1} E/S ratio as 139 Wh kg^{-1}.

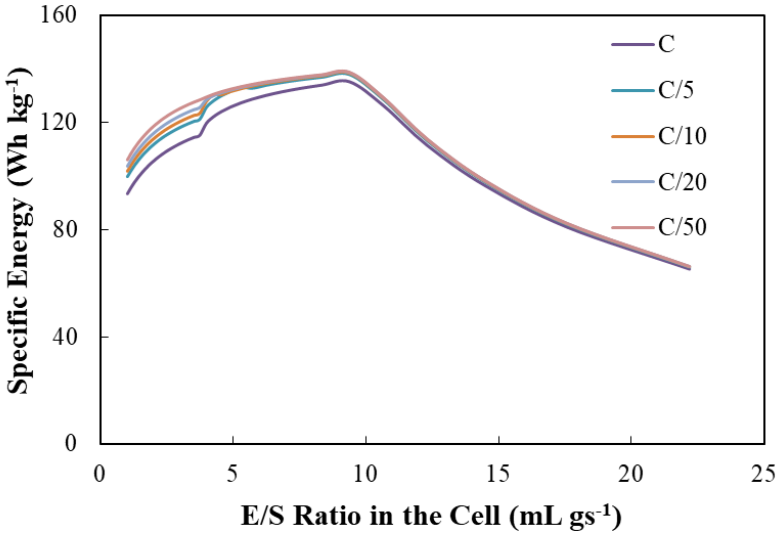

Figure 4. 22. The effect of E/S ratio in the cell on the calculated cell-level specific energy of a Li-S cell for different current densities. The cathode thickness is 100 μm, N/P ratio is 1.5 and C/S ratio is 0.5 for all results.

When energy density vs E/S ratio graph is examined in Figure 4.23, similar trends with the specific energy results in Figure 4.22 are observed. At C/50 current density and 9 mL g_s^{-1} E/S ratios, the maximum energy density value is obtained as 232 Wh L^{-1}.

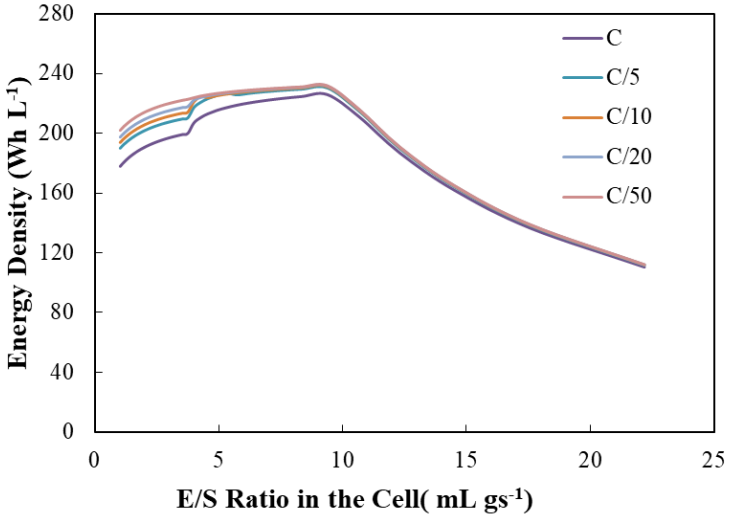

Figure 4. 23. The effect of E/S ratio in the cell on the calculated cell-level energy density of a Li-S cell for different current densities. The cathode thickness is 100 µm, N/P ratio is 1.5 and C/S is 0.5 for all results.

4.2.1.10 Mass and Volume Breakdown at the Cell Level

The mass breakdown of the Li-S cell at the maximum predicted cell level performance is given in Figure 4.24. According to the baseline calculations of the model, the maximum specific energy and energy density values are obtained at 91% porosity of the cathode (E/S ratio of 9 mL g_s^{-1}). As it is seen from the figure, inactive materials mass, which is the sum of the current collectors, separator, electrolyte, carbon and binder mass, is much higher than the active materials mass, which is the sum of sulfur and Li metal mass. The current collectors have the biggest portion of the cell mass due to their high densities. Because of the high porosity of the cathode, electrolyte also has a significant contribution to the cell mass.

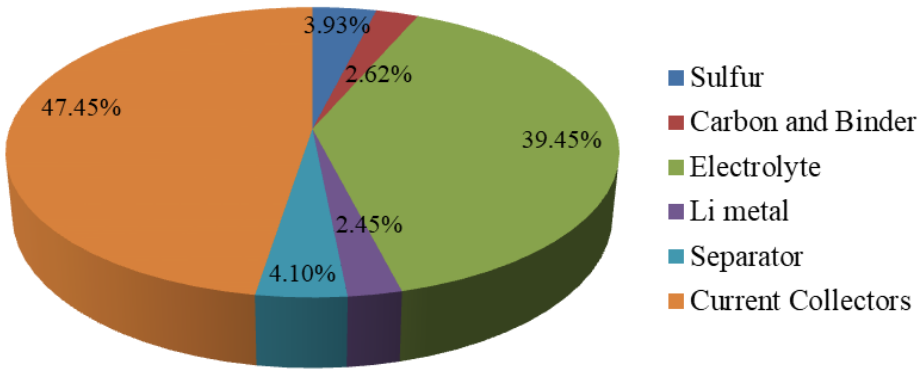

Figure 4. 24. The mass breakdown of the cell for 138 Wh kg-1 and 230 Wh L -1 Li-S cell at 91% cathode porosity (E/S ratio of 9 mL gs-1), 100 µm cathode thickness, 1.5 N/P ratio, 0.5 C/S ratio and C/5 current density.

The volume breakdown of the Li-S cell at the maximum predicted cell level performance of the baseline model is given in Figure 4.25. Because the cathode porosity is very high for this cell, the electrolyte has the highest portion in the volume breakdown of the Li-S cell. Specific capacity and energy density of the Li-S cell predicted by the model is much lower than the theoretical values. This may be explained by the low ratio of the active to inactive materials mass and volume in the cell.

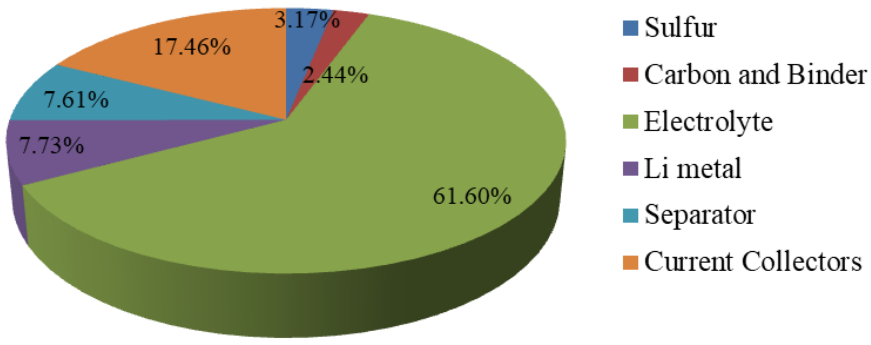

Figure 4. 25. The volume breakdown of the cell for 138 Wh kg-1 and 230 Wh L -1 Li-S cell at 91% cathode porosity (E/S ratio of 9 mL gs-1), 100 µm cathode thickness, 1.5 N/P ratio, 0.5 C/S ratio and C/5 current density

4.2.2 Cell Performance Model with Constant Cathode Specific Capacity

4.2.2.1 The Effect of Cathode Specific Capacity

In the previous section, an empirical relation between the specific capacity and E/S ratio has been used in the model to predict the cell level performance of the battery. However, higher specific capacities at lower E/S ratios maybe attained in the future with advancements in the cathode or electrolyte materials. Therefore, in this part, in order to see the effect of E/S ratio on the cell performance for stable discharge capacities, specific capacity is taken constant in the model. The effect of cathode specific capacity on the cell-level specific energy and energy density is given in Figures 4.26 and Figure 4.27, respectively.

It can be seen from Figure 4.26 that on the contrary to the previous results, increasing the E/S ratio decreases the specific energy for all specific capacities. Significantly high specific energies can be attained for high specific capacities and low E/S ratios. The figure also shows that the specific energy increases greatly with increasing specific capacity. This effect of specific capacity on the specific energy becomes less apparent after 15 mL g_s^{-1} E/S ratio. Moreover, the prediction of the model at 1000 mAh g_s^{-1} is close to an experimental study in literature presenting a specific energy of approximately 400 Wh kg^{-1} at 1 mL g_s^{-1} E/S ratio [43].

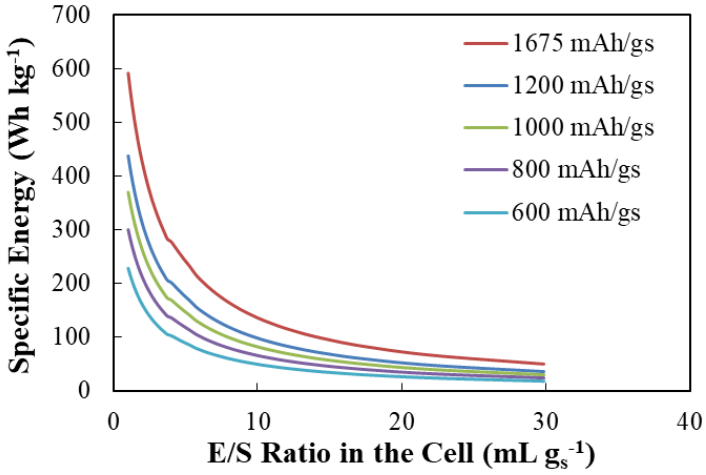

Figure 4. 26. The effect of E/S ratio in the cell on the calculated cell-level specific energy of a Li-S cell for different specific capacities. The cathode thickness is 100 µm, N/P ratio is 1.5, C/S ratio is 0.5 and current density is C/5 for all results.

Figure 4.27 shows that the energy density also decreases with increasing E/S ratios at each specific capacity. As in the specific energy results, until 15 mL g_s^{-1} specific capacity effect can be clearly seen. Also, the model predictions for 1000 mAh g_s^{-1} is similar with an experimental study in the literature; they show the same trend in the energy density based on the electrolyte amount [17].

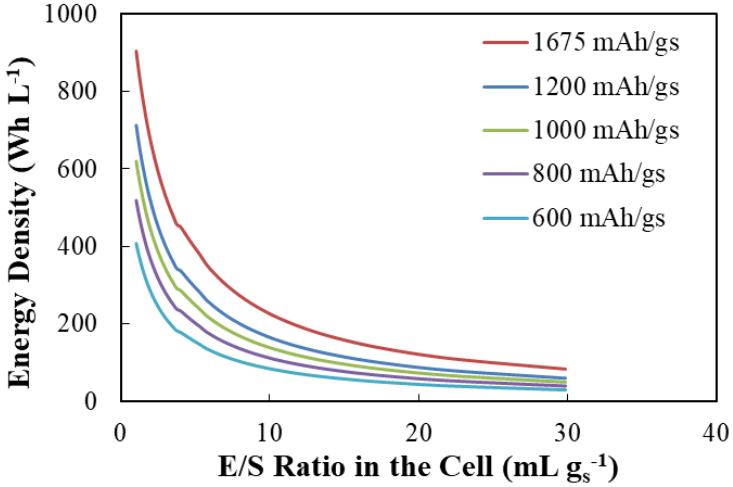

Figure 4. 27. The effect of E/S ratio in the cell on the calculated cell-level energy density of a Li-S cell for different specific capacities. The cathode thickness is 100 µm, N/P ratio is 1.5, C/S ratio is 0.5 and current density is C/5 for all results.

According to the specific energy and energy density results of the model, 1200 mAh g_s^{-1} is chosen as the specific capacity for the following studies to discuss the effect of the other design parameters. In the literature, there are various studies showing initial capacities of 1200 mAh g_S^{-1} [16, 28, 37, 43]; therefore it may be possible to retain this capacity. Since 1675 mAh g_s^{-1} is the theoretical value, 1200 mAh g S^{-1} is more realistic to be used in the model. The cell level performance based on the E/S ratio of the Li-S cell is determined for different thicknesses, C/S ratios, N/P ratios, sulfur loadings and current densities at 1200 mAh g_s^{-1}.

4.2.2.2 The Effect of Cathode Thickness

As it is seen from Figure 4.28, increasing E/S ratio decreases the specific energy for all thicknesses. According to the figure, 50µm thickness causes the lowest specific energy. The maximum specific energy is obtained as 513 Wh kg^{-1} at 0.98 mL g_s-1 E/S ratio. Since 150 µm and 100 µm thicknesses have similar specific energy values, 100 µm can be chosen for cell design to limit the performance losses associated with thicker electrodes.

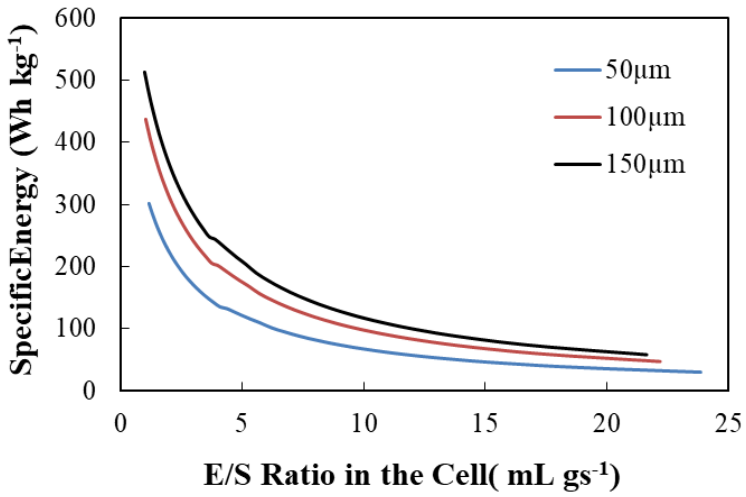

Figure 4. 28. The effect of E/S ratio in the cell on the calculated cell-level specific energy of a Li-S cell for different cathode thicknesses. The C/S ratio is 0.5, N/P ratio is 1.5, current density is C/5 and specific capacity is 1200 mAh gs-1 for all results.

As in the specific energy results, energy density decreases with rising E/S ratios in Figure 4.29. However, energy density results are closer at each thickness. Although the maximum energy density value which is 772 Wh L^{-1} is reached at 150 µm, cell resistance may be formed due to very thick cathode. Hence, using 100 µm thickness for cell design is more preferable.

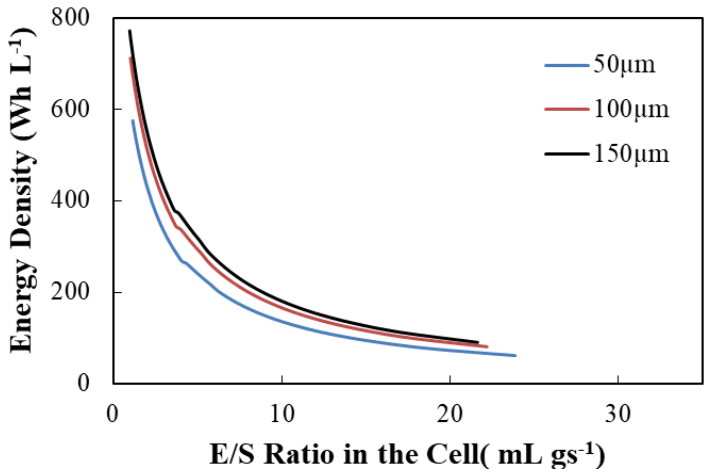

Figure 4. 29. The effect of E/S ratio in the cell on the calculated cell-level energy density of a Li-S cell for different cathode thicknesses. The C/S ratio is 0.5, N/P ratio is 1.5, current density is C/5 and specific capacity is 1200 mAh gs-1 for all results.

4.2.2.3 The Effect of C/S Ratio

In Figure 4.30., increasing E/S ratio decreases the specific energy for all C/S ratios. The effect of C/S ratio is only apparent at low E/S ratios as seen in the figure. The maximum value which is 556 Wh kg^{-1} is observed at 0.125 C/S ratio and 0. 75 mL g_s^{-1}. According to the figure, E/S ratio should be lower than 5 mL g_s^{-1} with at least a C/S ratio of 0.5 in order to reach acceptable specific energy values.

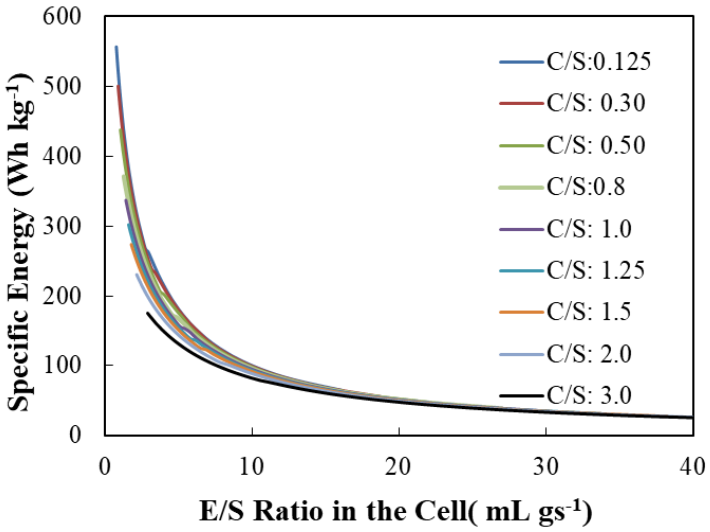

Figure 4. 30. The effect of E/S ratio in the cell on the calculated cell-level specific energy of a Li-S cell for different C/S ratios. The cathode thickness is 100µm, N/P ratio is 1.5, current density is C/5 and specific capacity is 1200 mAh gs-1 for all results.

Moreover, as shown in Figure 4.31, energy density decreases significantly with rising E/S ratio and the maximum energy density is indicated as 860 Wh L^{-1} at 0.125 C/S ratio and 0.75 mL g_s^{-1} E/S ratio. Furthermore, the impact of C/S ratio on the energy density is only significant at low E/S ratios; the results do not differ much at higher E/S ratios. Another study in the literature also discusses that increasing sulfur weight percentage, which means decreasing C/S ratio, leads to an increase in the energy density [17] and, the study shows comparable results to the proposed cell level performance model.

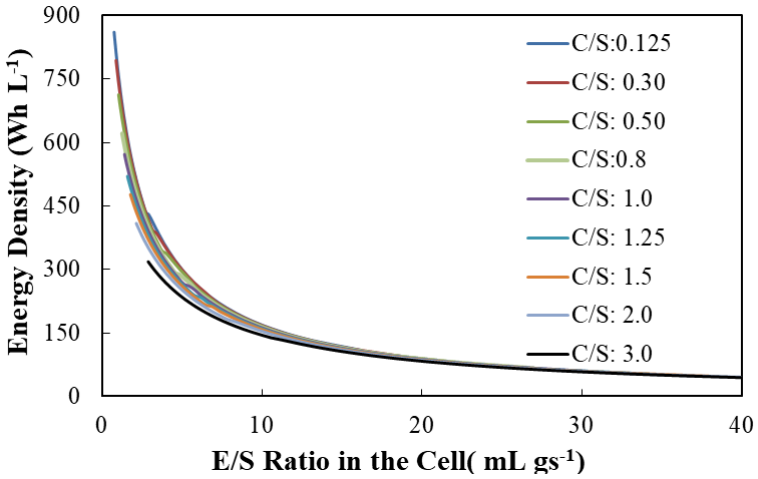

Figure 4. 31. The effect of E/S ratio in the cell on the calculated cell-level energy density of a Li-S cell for different C/S ratios. The cathode thickness is 100µm, N/P ratio is 1.5, current density is C/5 and specific capacity is 1200 mAh gs-1 for all results.

4.2.2.4 The Effect of Sulfur Loading

According to Figure 4.32, specific energy decreases with increasing E/S ratio for all sulfur loadings. It can be seen in the figure that at higher sulfur loadings high specific energies are obtained. This is because that higher sulfur loadings provide an increase in the cell capacity. At high sulfur loadings around 8, 7, 6 mg cm^{-2}, similar specific energy values which are between 450 and 500 Wh kg^{-1} are observed. There is an experimental study in the literature that determines the effect of E/S ratio on the specific energy for different sulfur loadings at a specific capacity of 1000 mAh g_s^{-1} [43]; that study acquires similar energy density results with the model predictions.

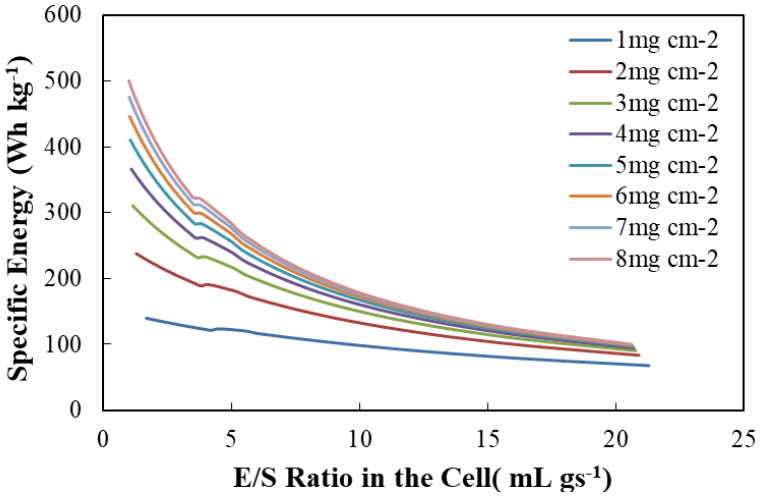

Figure 4. 32. The effect of E/S ratio in the cell on the calculated cell-level specific energy of a Li-S cell for different sulfur loadings. The cathode thickness is 100µm, N/P ratio is 1.5, C/S ratio is 0.5, current density is C/5 and specific capacity is 1200 mAh g_s^{-1} for all results.

As in the specific energy results, an increase in the E/S ratio results in decreasing energy density for all sulfur loadings in Figure 4.33. At higher E/S ratios, higher than 10 mL g_s^{-1}, all sulfur loadings (except 1 mg cm^{-2}) have similar energy densities which are between 720 and 770Wh L^{-1}.

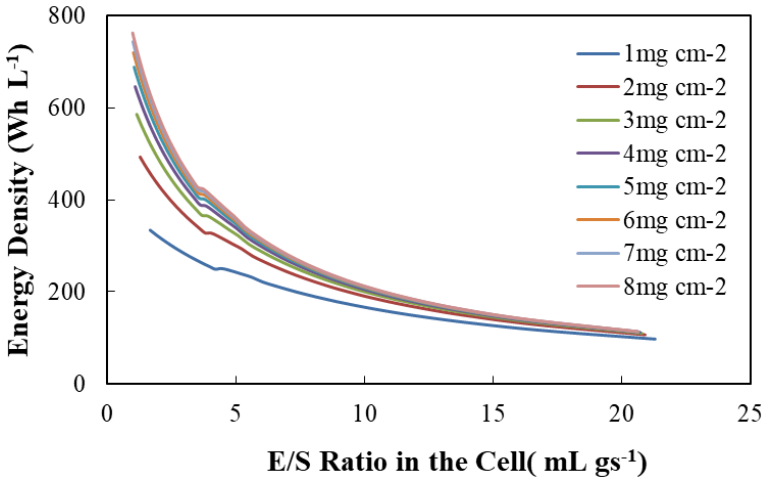

Figure 4. 33. The effect of E/S ratio in the cell on the calculated cell-level energy density of a Li-S cell for different sulfur loadings. The cathode thickness is 100µm, N/P ratio is 1.5, C/S ratio is 0.5, current density is C/5 and specific capacity is 1200 mAh g_s^{-1} for all results.

4.2.2.5 The Effect of Current Density

Figures 4.34 and 4.35 present the effect of current density on the calculated specific energy and energy density, respectively. The figures show that increasing E/S ratio affects the specific energy and energy density negatively for all C-rates. In the model, current density does not have an impact on the cell capacity and affects only the cell voltage. Because of this reason the model does not predict a significant change in the cell performance with the current density.

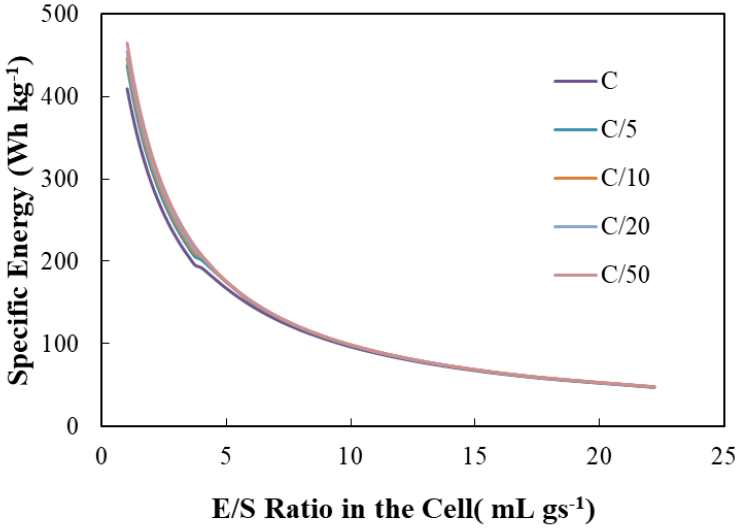

Figure 4. 34. The effect of E/S ratio in the cell on the calculated cell-level specific energy of a Li-S cell for different C-rates. The cathode thickness is 100µm, N/P ratio is 1.5, C/S ratio is 0.5 and specific capacity is 1200 mAh gs-1for all results

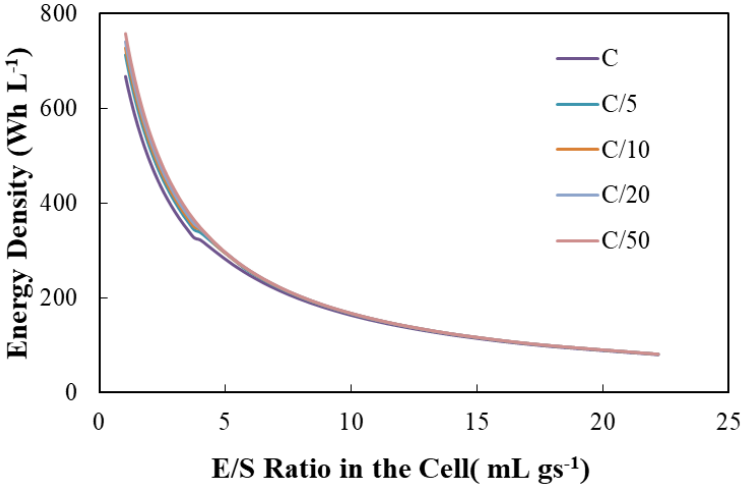

Figure 4. 35. The effect of E/S ratio in the cell on the calculated cell-level energy density of a Li-S cell for different C-rates. The cathode thickness is 100µm, N/P ratio is 1.5, C/S ratio is 0.5 and specific capacity is 1200 mAh g_s^{-1} for all results.

4.2.2.6 The Effect of N/P Ratio

Figures 4.36 and 4.37 show that at all N/P ratios, E/S ratio causes a significant decrease in the specific energy and energy density, respectively. The effect of N/P ratio on the specific energy is insignificant; similar specific energy values are obtained for all N/P ratios. This may be explained by the low density of the Li metal. On the other hand, energy density is influenced by the N/P ratio more. Until around 5 mL g_s^{-1} E/S ratio, the effect of N/P ratio can be clearly observed in Figure 4.38. Lower N/P ratios (thinner Li anodes) provide higher energy densities as expected. This result is in agreement with another model in the literature [17]. Similar energy densities are calculated at each N/P ratio after an E/S ratio of 5mL g_s^{-1}.

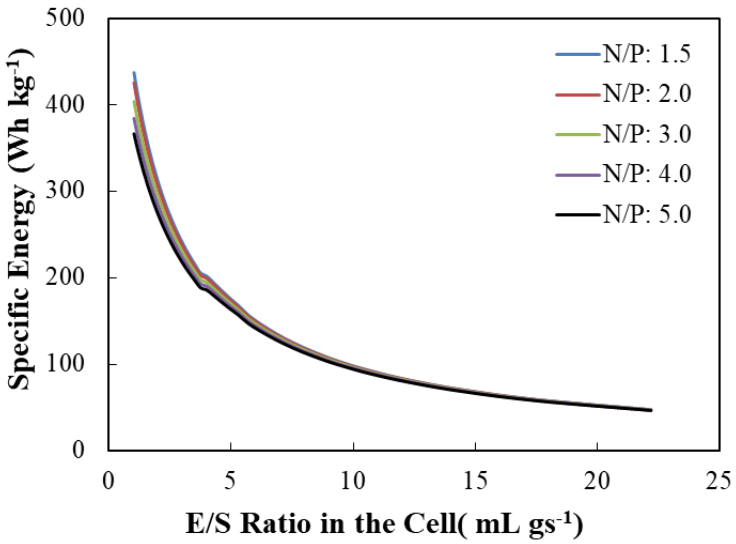

Figure 4. 36. The effect of E/S ratio in the cell on the calculated cell-level specific energy of a Li-S cell for different N/P ratios. The cathode thickness is 100µm, C/S ratio is 0.5, current density is C/5 and specific capacity is 1200 mAh gs-1 for all results.

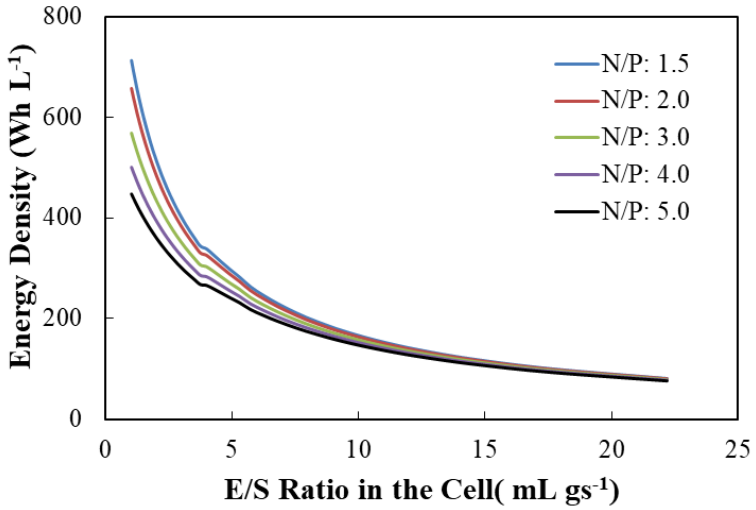

Figure 4. 37. The effect of E/S ratio in the cell on the calculated cell-level energy density of a Li-S cell for different N/P ratios. The cathode thickness is 100µm, C/S ratio is 0.5, current density is C/5 and specific capacity is 1200 mAh gs-1 for all results.

4.2.2.7 Mass and Volume Breakdown at the Cell Level

The mass breakdown of the Li-S cell at the maximum cell level performance is given in Figure 4.38. According to the model calculations, at the 51% porosity of cathode the maximum specific energy and energy density values are obtained and at this porosity the cell mass breakdown is determined. As it is seen from the figure, inactive materials mass is higher than the active materials but the distribution of each part of the cell is more uniform compared to the model with specific capacity defined as a function of E/S ratio (Figure 4.25), especially in terms of the electrolyte amount.

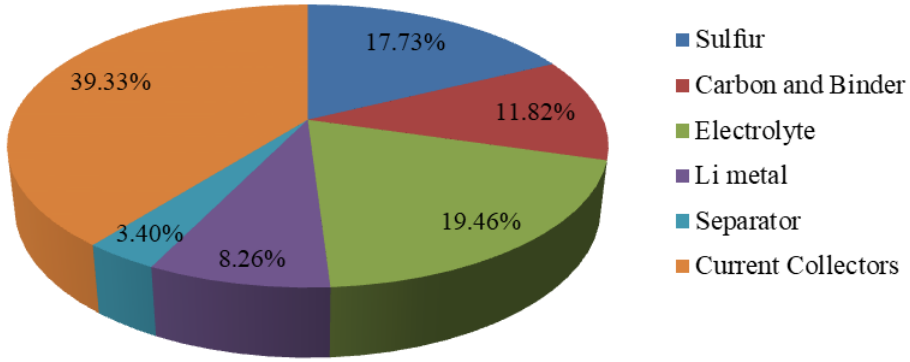

Figure 4. 38. The mass breakdown of the cell for 437 Wh kg-1 and 713 Wh L -1 Li-S cell at 51% porosity (E/S ratio of 0.89 mL gs-1), 100µm cathode thickness, 0.5 C/S ratio, C/5 current density and 1200 mAh gs-1specific capacity.

The volume breakdown of the Li-S cell at the maximum predicted cell level performance is given in Figure 4.39. It can be seen that even though the contribution of the electrolyte volume to the cell volume is much lower compared to Figure 4.25, electrolyte still occupies the largest portion in the breakdown. Because of the low density of Li metal, it has a large volume contribution to the cell even though its contribution to the cell mass is less significant.

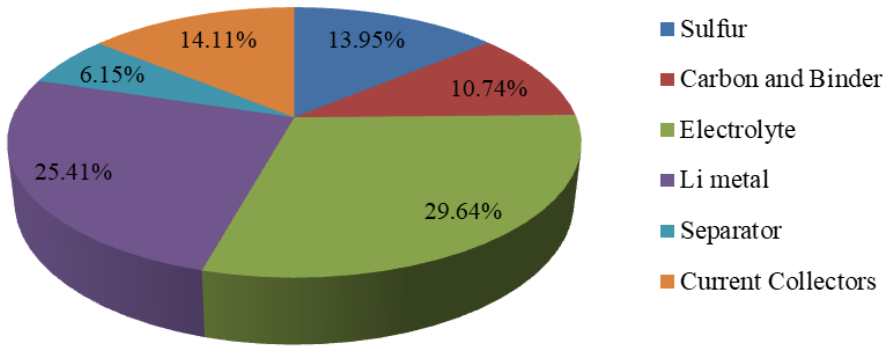

Figure 4. 39. The volume breakdown of the cell for 437 Wh kg-1 and 713 Wh L -1 Li-S cell at 51% porosity (E/S ratio of 0.89 mL gs-1), 100µm cathode thickness, 0.5 C/S ratio, C/5 current density and 1200 mAh gs-1specific capacity.

4.3 The Effect of E/S Ratio on the System Level Performance of a Li-S Battery

In the last part of this thesis, the effect of E/S ratio on the system level performance of the Li-S battery is investigated. The system level performance model is developed based on the BatPaC model. First, energy and power of the battery are chosen as 118 kWh and 80 kW, respectively, based on the requirements for EV applications [10]. Then, cell area, cell capacity and battery pack voltage are calculated. According to these energy and power requirements, specific energy and energy density of the Li-S battery are determined using the system level performance model. In the model, the maximum cathode thickness is limited to 150 μm [10]. As previously described in the Model Development part, the model uses the maximum thickness value if the calculated thickness is greater than this maximum value. Typically, the maximum electrode thickness is used in the model since increasing E/S ratio increases the calculated thickness to values greater than 150 μm. Moreover, in order to examine the effect of specific capacity on the system level performance, specific capacity is fed to the model either as a function of E/S ratio or, as a constant value.

4.3.1 System Performance Model with Cathode Specific Capacity Defined as a Function of E/S Ratio in the Cell

The effect of E/S ratio on the system-level specific energy is determined in Figure 4.40. As a baseline model, the cathode thickness, C/S ratio and N/P ratio are selected as 150 μm, 0.5 and 1.5 respectively. The system level performance shows a similar trend to the cell level results; specific energy increases with the E/S ratio until 10 mL g_s^{-1}. The maximum value which is 111 Wh kg^{-1} is lower compared to the cell level performance, as expected. After this point, specific energy starts to decrease continuously due to the theoretical specific capacity limitation. Thus, at higher E/S ratios high specific energy battery systems cannot be achieved.

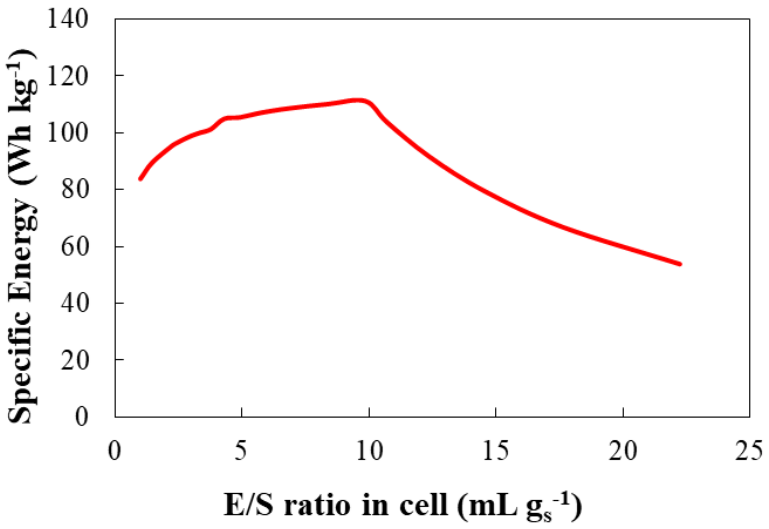

Figure 4. 40. The effect of E/S ratio in the cell on the calculated system-level specific energy of a Li-S battery. The cathode thickness is 150 µm, C/S ratio is 0.5 and N/P ratio is 1.5.

The trend seen in Figure 4.41 for the change of system-level energy density as a function of the E/S ratio is similar to the results for specific energy. The maximum value is approximately 111.2 Wh L^{-1} at 10 mL g_s^{-1} but the system level performance model does not predict high energy density values for the Li-S batter pack even at the optimum E/S ratio.

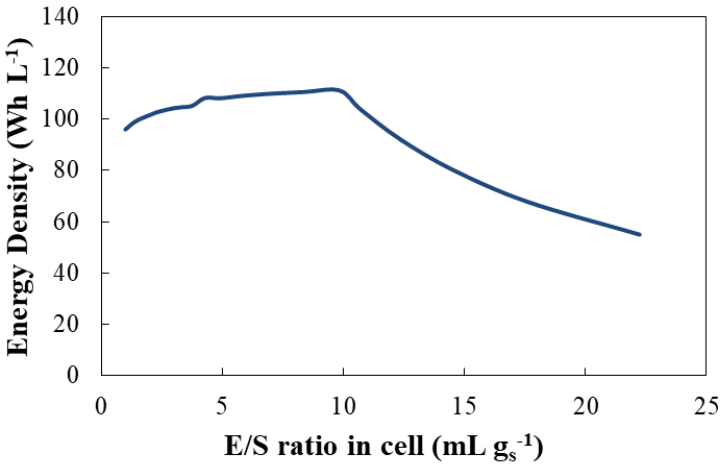

Figure 4. 41. The effect of E/S ratio in the cell on the calculated system-level energy density of a Li-S battery. The cathode thickness is 150 μm, C/S ratio is 0.5 and N/P ratio is 1.5.

Nowadays, Li-S battery prototypes can reach to 200 Wh kg^{-1} at the pack level [1]. The model predicts 111 Wh kg^{-1} specific energy with the specified conditions. In order to examine the impact of cell design more thoroughly, the effect of other critical design parameters, which are maximum cathode thickness, C/S ratio in the cathode and N/P ratio in the anode, on the system level performance is investigated with the developed model.

4.3.1.1 The Effect of Maximum Cathode Thickness

In Figure 4.42, increasing E/S ratio decreases the specific energy for different maximum cathode thicknesses. As compared to the cell-level specific energy results pack values are lower, as expected. Until approximately 10 mL g_s^{-1} E/S ratio, specific energy of battery increases for every thickness. At 200μm maximum cathode thickness the maximum specific energy is obtained as 120 Wh kg^{-1}. After the maximum point, it starts to decrease, even to values as 55-60 Wh kg^{-1}. Larger thicknesses provide higher specific energies to the battery because that the maximum

cathode thickness determines the cell area and so, cell mass changes with the thickness.

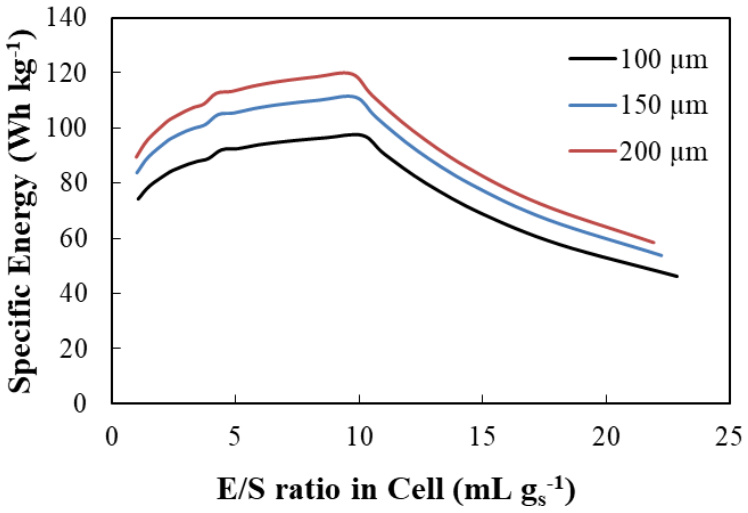

Figure 4. 42. The effect of E/S ratio in the cell on the calculated system-level specific energy of a Li-S battery for different maximum cathode thicknesses. C/S ratio is 0.5 and N/P ratio is 1.5 for all results.

In Figure 4.43, the effect of E/S ratio on the energy density for maximum cathode thicknesses between 100-200 µm is analyzed. The maximum energy density which is 116 Wh L^{-1} is observed at 200 µm thickness and 10 mL g_s^{-1} E/S ratio. As in the specific energy results, at first energy density increases and then, it starts to decrease. However, the energy density is less sensitive to the E/S ratio at ratios lower than 10 mL g_s^{-1}compared to the specific energy. When the impact of the maximum cathode thickness is considered, it can be seen in the figure that the effect is not significant especially at higher E/S ratios that decrease the energy density.

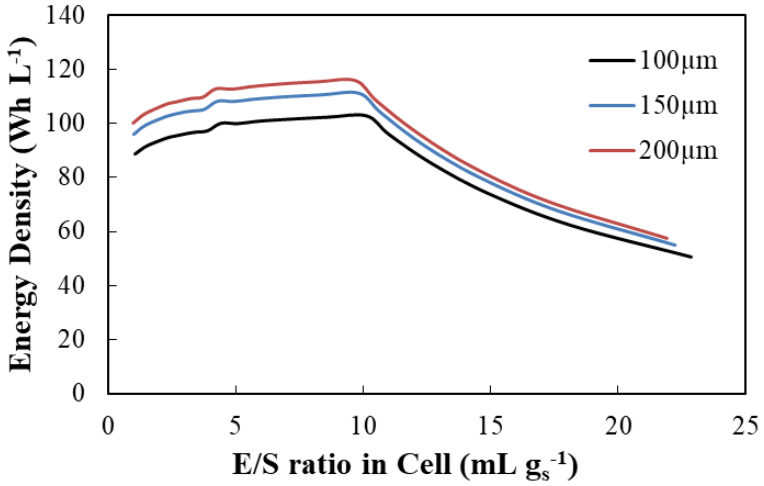

Figure 4. 43. The effect of E/S ratio in the cell on the calculated system-level energy density of a Li-S battery for different maximum cathode thicknesses. C/S ratio is 0.5 and N/P ratio is 1.5 for all results.

4.3.1.2 The Effect of C/S Ratio

Figure 4.44 shows the effect of E/S ratio on the system-level specific energy for C/S ratios between 0.125-3. Until around 9-10 mL g_s^{-1} E/S ratio, specific energy is enhanced with increasing electrolyte amount and then, it starts to diminish. At 0.125 C/S ratio, the maximum specific energy which is 115 Wh kg^{-1} is obtained. The effect of C/S ratio is clearly seen at lower E/S ratios, whereas at higher ratios there is no improvement in the specific energies by decreasing C/S ratios. Lower C/S ratios results in higher specific energy values as discussed below.

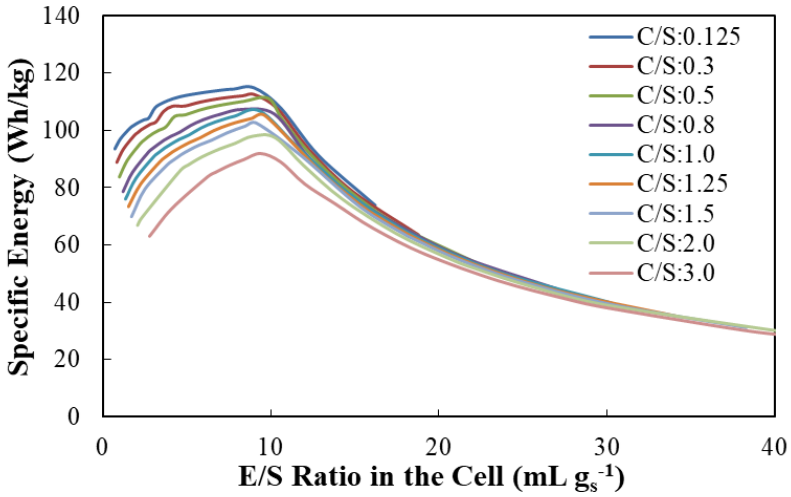

Figure 4. 44. The effect of E/S ratio in the cell on the calculated system-level specific energy of a Li-S battery for different C/S ratios. The cathode thickness is 150 µm and N/P ratio is 1.5 for all results.

The effect of E/S ratio on the system-level energy density is determined for different C/S ratios in Figure 4.45. The same trends are observed with the specific energy results and as in specific energy the maximum value, which is 114 Wh L^{-1}, is obtained at 0125 C/S ratio.

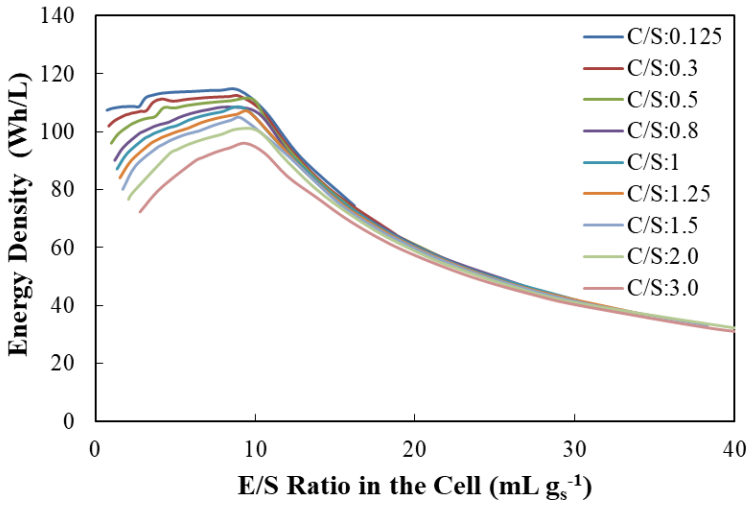

Figure 4. 45. The effect of E/S ratio in the cell on the calculated system-level energy density of a Li-S battery for different C/S ratios. The cathode thickness is 150 µm and N/P ratio is 1.5 for all results.

4.3.1.3 The Effect of N/P Ratio

The influence of the E/S ratio in the cell on the system-level specific energy for N/P ratios of 1.5-5 is shown in Figure 4.46. The N/P ratio has a more pronounced effect on the specific energy at lower E/S ratios compared to the higher ratios. N/P ratio changes cell mass via anode thickness; this effect is more obvious for N/P ratios higher than 2. At 1.5 N/P ratio the maximum value, which is 112 Wh kg^{-1}, is seen.

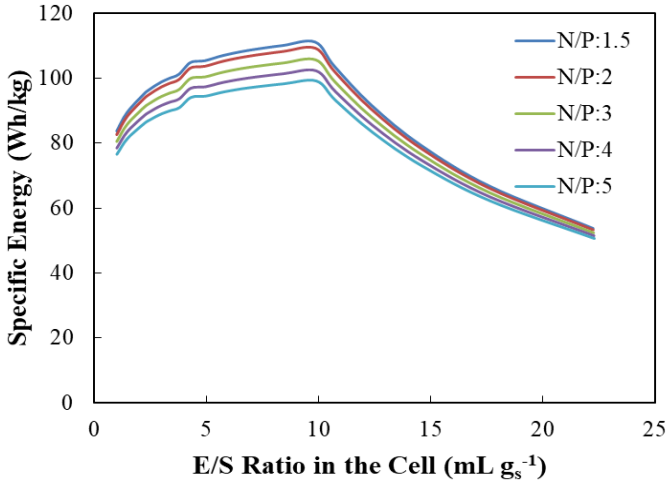

Figure 4. 46. The effect of E/S ratio in the cell on the calculated system-level specific energy of a Li-S battery for different N/P ratios. The cathode thickness is 150 µm and C/S ratio is 0.5 for all results.

The effect of E/S ratio on the system-level energy density is similar with the specific energy results. However, N/P ratio effect on the energy density is more obvious than the specific energy because that cell volume depends on the cell thickness directly.

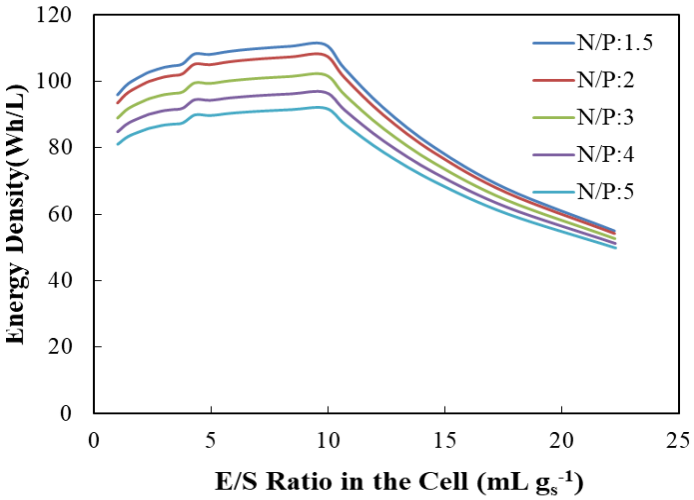

Figure 4. 47. The effect of E/S ratio in the cell on the calculated system-level energy density of a Li-S battery for different N/P ratios. The cathode thickness is 150 µm and C/S ratio is 0.5 for all results.

4.3.1.4 Mass and Volume Breakdown at System Level

The mass breakdown of the Li-S battery at the maximum system level performance predicted for the baseline case is given in Figure 4.48. According to the model calculations, the maximum specific energy and energy density values are obtained at a cathode porosity of 91.5% and the battery mass breakdown is determined at this porosity. As it is seen from the figure, electrolyte mass is the biggest contributor to the battery mass because of the high porosity of the cathode. Cell packaging, which accounts for the cell container, battery jacket etc. has also an important contribution to the mass of the pack.

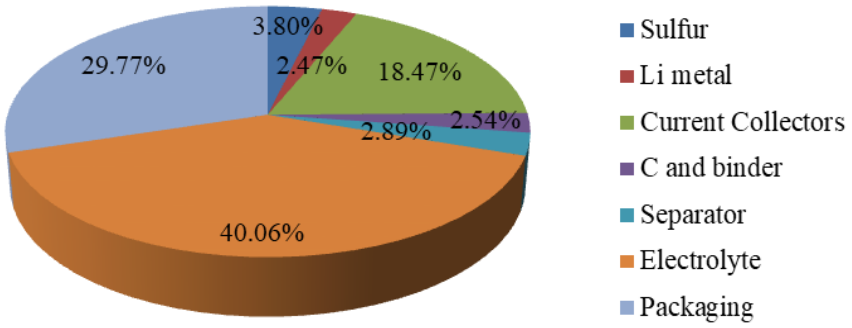

Figure 4. 48. The mass breakdown of the pack for a 118kWh use, 80 kW and 360 V Li-S battery which has 111.2 Wh kg-1 and 111 Wh L-1 at also, 150 µm cathode thickness, 10 mL gs -1 E/S ratio, 0.5 C/S ratio and 1.5 N/P ratio.

The volume breakdown of the Li-S battery at the maximum system level performance calculated for the baseline case is given in Figure 4.49. It can be seen in the figure that packaging volume is the biggest contributor to the battery volume at a cathode porosity of 91.5%. This is mainly because that the electrolyte volume also affects the packaging volume via battery jacket etc. Therefore, inactive materials volume is much higher than the active materials volume at this porosity.

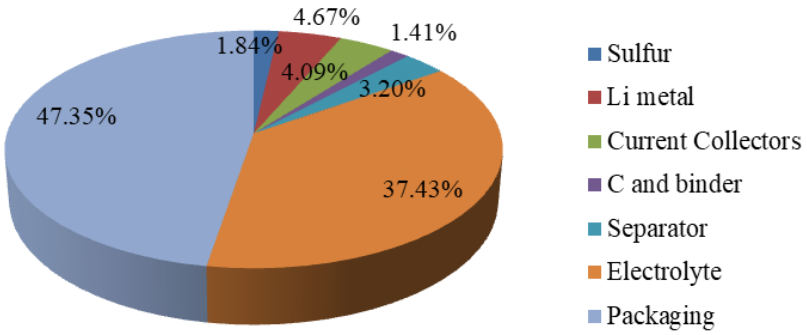

Figure 4. 49. The volume breakdown of the pack for a 118kWh use, 80 kW and 360 V Li-S battery which has 111.2 Wh kg-1 and 111 Wh L-1 also, at 150 µm cathode thickness, 10 mL gs -1 E/S ratio, 0.5 C/S ratio and 1.5 N/P ratio

4.3.2 System Performance Model with Constant Cathode Specific Capacity

4.3.2.1 The Effect of Cathode Specific Capacity

In Figure 4.50, the effect of E/S ratio on the system-level specific energy for different cathode specific capacities is given. As it is seen from the figure, increasing E/S ratio decreases specific energy because that the cell mass raises considerably with higher E/S ratios. Moreover, the calculated specific energies are much higher compared to the results presented in the previous section since specific capacities used here are significantly higher than the ones calculated as a function of the E/S ratio. This is because that sulfur mass in the cathode depends significantly on the cathode specific capacity; cell mass reduces as the specific capacity increases and so, specific energy becomes larger.

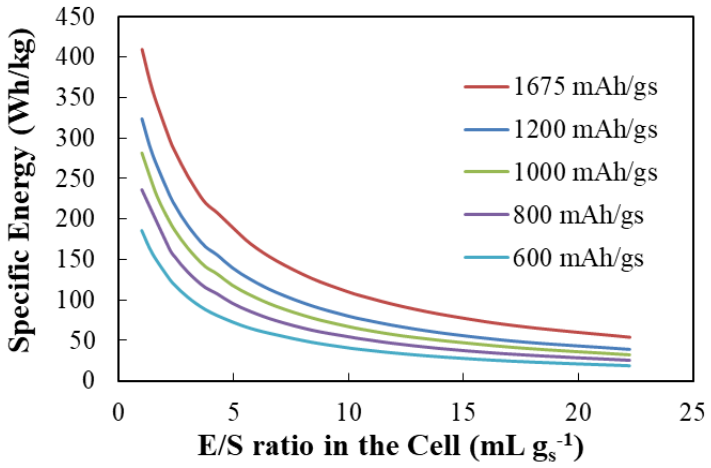

Figure 4. 50. The effect of E/S ratio in the cell on the calculated system-level specific energy of a Li-S battery for different specific capacities. The cathode thickness is 150 µm, N/P ratio is 1.5 and C/S ratio is 0.5 for all results.

As in the results reported for the specific energy, energy density also decreases with increasing E/S ratio at each specific capacity as shown in Figure 4.51. It can be seen from the figure that higher cathode specific capacity results in higher energy densities, especially at lower E/S ratios.

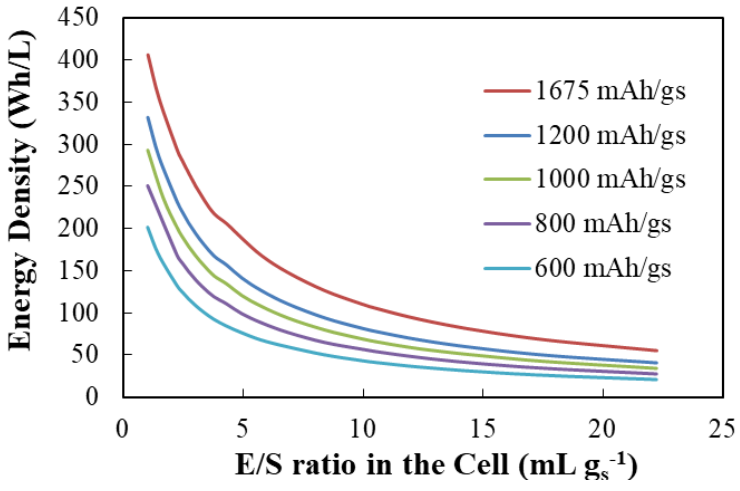

Figure 4. 51. The effect of E/S ratio in the cell on the calculated system-level energy density of a Li-S battery for different specific capacities. The cathode thickness is 150 µm, N/P ratio is 1.5 and C/S ratio is 0.5 for all results.

In order to determine the impact of cell design on the system-level performance for the model with constant specific capacity, the effect of maximum cathode thickness, C/S ratio in the cathode and N/P ratio in the anode are also investigated in this part of the model. As in the cell level performance model, a constant specific capacity of 1200 mAh g_s^{-1} is used in the model in the next part.

4.3.2.2 The Effect of Maximum Thickness

Figure 4.52 shows the effect of E/S ratio on the specific energy for different maximum cathode thicknesses. As it is seen from the figure, except at the initial E/S ratio, the results of each thickness are very similar at every E/S ratios, especially for the results obtained for 150µm and 200µm. The maximum specific energy value is obtained as 340 Wh kg^{-1} for 200 µm cathode thickness and 0.98 mL g_s^{-1} E/S ratio.

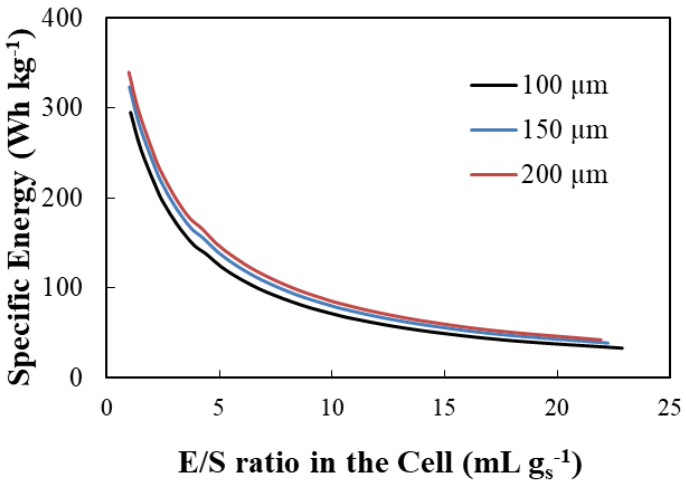

Figure 4. 52. The effect of E/S ratio in the cell on the calculated system-level specific energy of a Li-S battery for different maximum cathode thicknesses. C/S ratio is 0.5, N/P ratio is 1.5 and specific capacity is 1200 mAh gs-1 for all results.

Energy density is affected by the E/S ratio and the maximum cathode thickness in a similar manner as seen in Figure 4.53. There is no apparent difference in the energy

densities for the range of thicknesses investigated. The maximum energy density is calculated at 0.98 mL g_s^{-1} with 200 µm cathode thickness as 342 Wh L^{-1}.

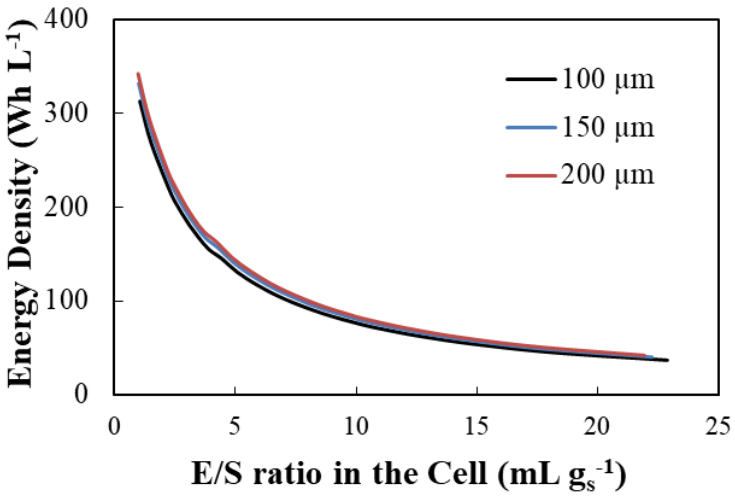

Figure 4. 53. The effect of E/S ratio in the cell on the calculated system-level energy density of a Li-S battery for different maximum cathode thicknesses. C/S ratio is 0.5, N/P ratio is 1.5 and specific capacity is 1200 mAh gs-1 for all results.

4.3.2.3 The Effect of C/S Ratio

The effect of E/S ratio on the system-level specific energy for C/S ratios between 0.125-3 is given in Figure 4.54. At low E/S ratios, about 1-2 mL g_s^{-1}, there is a substantial difference in the specific energies for each C/S ratio. Especially for C/S ratios higher than 1.5, a significant decrease can be seen in the specific energy. At higher E/S ratios, the results are much closer since cell mass is dominated by the electrolyte amount and thus does not change with changing C/S ratios significantly at these high ratios.

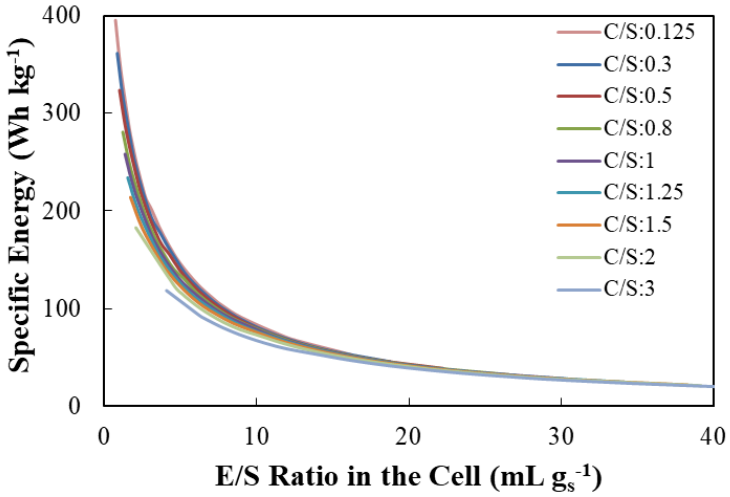

Figure 4. 54. The effect of E/S ratio in the cell on the calculated system-level specific energy of a Li-S battery for different C/S ratios. The cathode thickness is 150µm, N/P ratio is 1.5 and specific capacity is 1200 mAh gs-1 for all results.

As in the specific energy results, energy density is also reduced with increasing E/S ratio for different C/S ratios. In addition, at high E/S ratios the effect of C/S ratio on the energy density is inapparent.

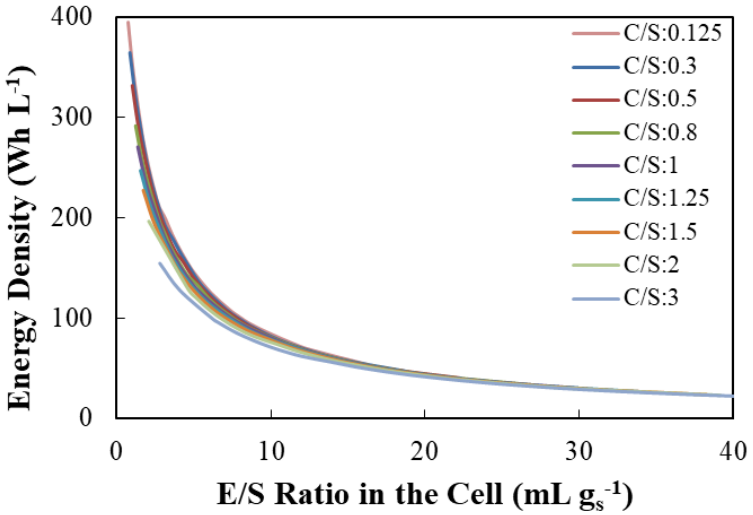

Figure 4. 55. The effect of E/S ratio in the cell on the calculated system-level energy density of a Li-S battery for different C/S ratios. The cathode thickness is 150µm, N/P ratio is 1.5 and specific capacity is 1200 mAh gs-1 for all results.

4.3.2.4 The Effect of N/P Ratio

The effect of E/S ratio on the specific energy for N/P ratios between 1.5 and 5 is discussed in Figure 4.56. According to the figure, until approximately 5 mL g_s^{-1} E/S ratio, a slight difference is observed at each N/P ratio, whereas at higher E/S ratios the results become similar.

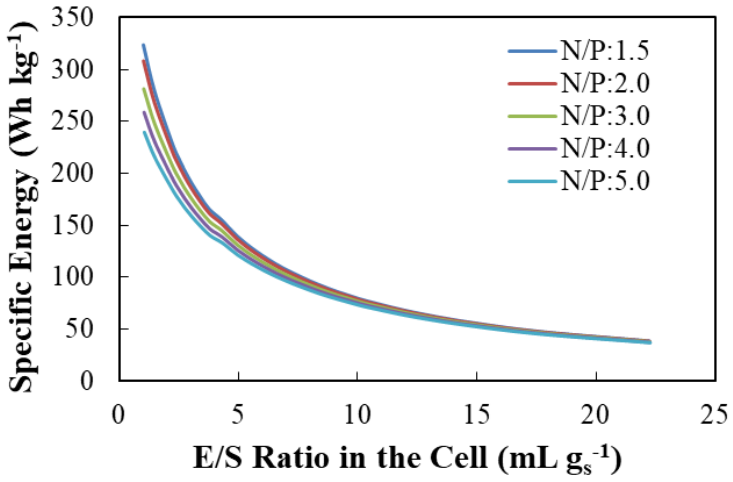

Figure 4. 56. The effect of E/S ratio in the cell on the calculated system-level specific energy of a Li-S battery for different N/P ratios. The cathode thickness is 150µm, C/S ratio is 0.5 and specific capacity is 1200 mAh gs-1 for all results.

When the energy density results (Figure 4.57) are compared with the specific energy ones, it is observed that at lower E/S ratios the importance of N/P ratio is more apparent. However, with increasing E/S ratios the effect of N/P ratio on the energy density becomes less obvious.

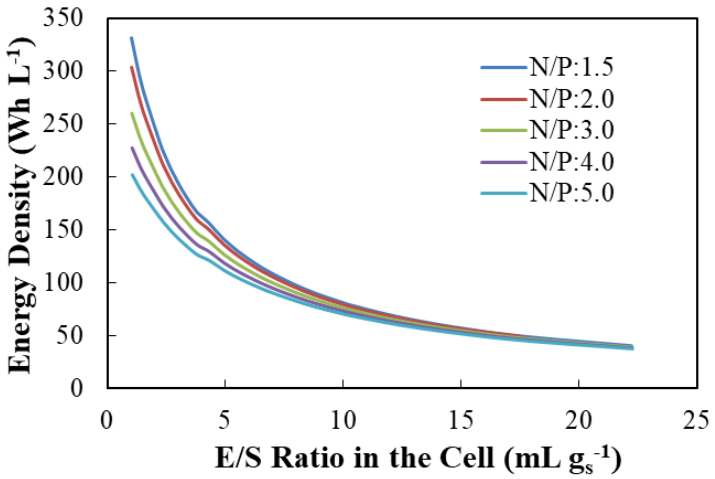

Figure 4. 57. The effect of E/S ratio in the cell on the calculated system-level energy density of a Li-S battery for different N/P ratios. The cathode thickness is 150µm, C/S ratio is 0.5 and specific capacity is 1200 mAh gs-1 for all results.

4.3.2.5 Mass and Volume Breakdown at System Level

The mass breakdown of the pack with the highest system level performance obtained for the baseline case is presented in Figure 4.58. According to the figure, electrolyte and sulfur have similar fractions in the battery mass. This is because that the highest performance values are obtained at 51% porosity, which causes a reasonable active to inactive materials mass ratio. Although the model with specific capacity defined as a function of E/S ratio has a higher percentage for the packaging due to the high inactive materials mass, the packaging is still significant in this mass breakdown.

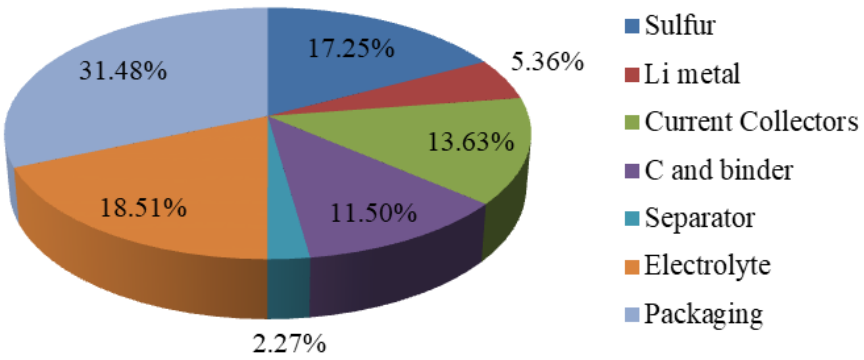

Figure 4. 58. The mass breakdown of the pack for a 118kWh use, 80 kW and 360 V Li-S battery which has 324 Wh kg-1 and 332 Wh L-1, at 150 µm the cathode thickness, 1 mL gs -1 E/S ratio, 0.5 C/S ratio and 1.5 N/P ratio.

The volume breakdown of the pack at the highest system level performance obtained for the baseline case is given in Figure 4.59. As seen in the figure, the packaging volume comprises approximately half of the battery volume. Although 51% porosity is not that high, electrolyte effect still can be seen in the battery volume; electrolyte amount affects not only the electrolyte volume but also the packaging volume.

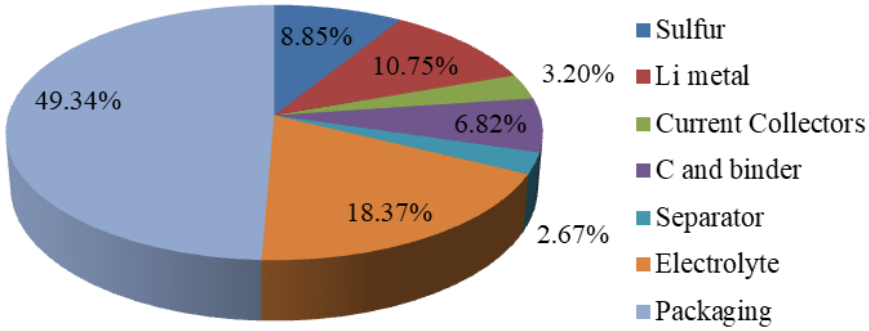

Figure 4. 59. The volume breakdown of the pack for a 118kWh use, 80 kW and 360 V Li-S battery which has 324 Wh kg-1 and 332 Wh L-1,at 150 µm the cathode thickness, 1 mL gs -1 E/S ratio, 0.5 C/S ratio and 1.5 N/P ratio.

4.3.3 Sensitivity Analysis of the System Level Performance Model

In order to analyze the effect of E/S ratio on the specific energy and energy density of the Li-S battery, the system level performance model is proposed as described above. In the electrochemical performance model, the cathode exchange current density is defined as a function of the E/S ratio. Also, at the cell level performance model specific capacity is fed into the model as a function of the E/S ratio. At the system level performance, these two inferences are fed into the model and the results are observed based on these dependencies. In order to identify the importance of the cathode exchange current density and the specific capacity for the system level performance of the battery, sensitivity analyses are done.

4.3.3.1 Sensitivity Analysis based on the Cathode Exchange Current Density

Because that the cathode exchange current density affects the cathode kinetics and thus the cell voltage significantly, the dependence of the system-level performance of the battery on this kinetic parameter is investigated by varying the slope and intercept of $i_{0,pe}$ (Equation 4.1) as shown in Figures 4.60 and 4.61. It is seen that varying the equation constants does not impact the specific energy and energy density of the battery at the system level. It can be concluded that in the battery mass and volume calculations, the influence of the cathode kinetics is relatively small. Therefore, the system-level performance is not greatly sensitive to the equation parameters in $i_{0,pe}$.

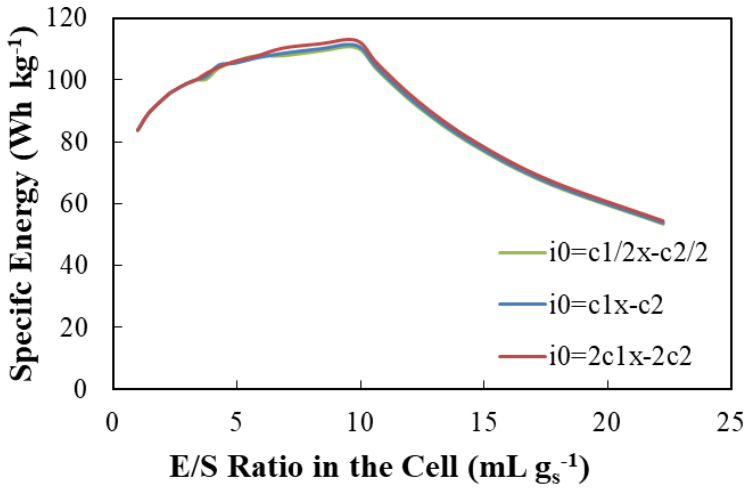

Figure 4. 60. The sensitivity analysis of the effect of the cathode exchange current density on the specific energy of the Li-S battery

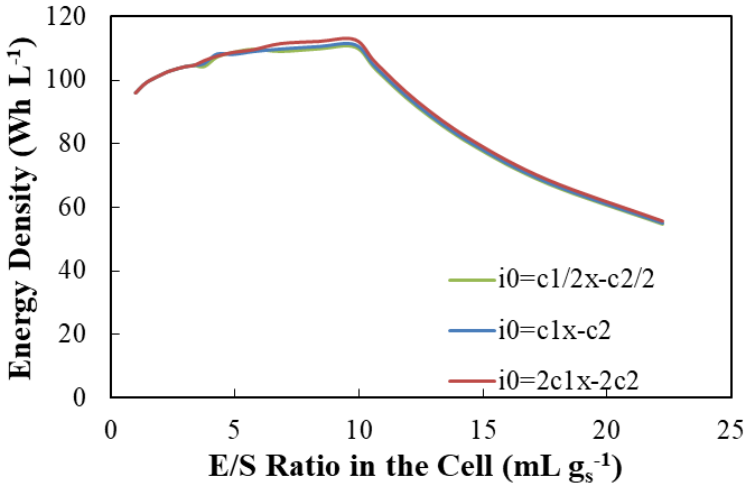

Figure 4. 61. The sensitivity analysis of the effect of the cathode exchange current density on the energy density of the Li-S battery

4.3.3.2 Sensitivity Analysis based on the Cathode Specific Capacity

Cathode specific capacity affects the positive electrode capacity and thus, the cathode thickness of the battery. In order to appoint the degree of the importance, the slope and intercept of the specific capacity equation (Equation 4.2) are altered as shown in Figures 4.62 and 4.63. From the figures, its effect can be easily seen; specific capacity influences the system level performance of the battery directly.

Specific capacity plays a critical role in determining the battery mass and volume. This is because that positive electrode and positive active material capacities are both designated via the cathode specific capacity and they determine the specific energy and energy density of the battery. The significant impact of the specific capacity equation on the system-level performance can be seen in the figures. As the E/S ratio at which the theoretical specific capacity has been reached, changes at every case, the dependence of the system level performance on the E/S ratio also changes.

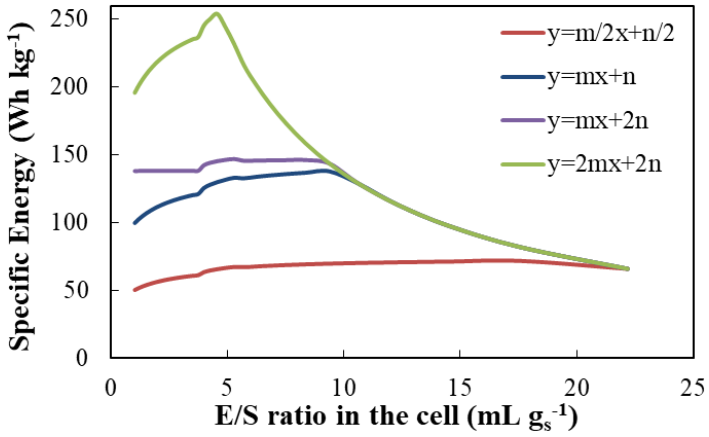

Figure 4. 62. The sensitivity analysis of the effect of the specific capacity on the specific energy of the Li-S battery

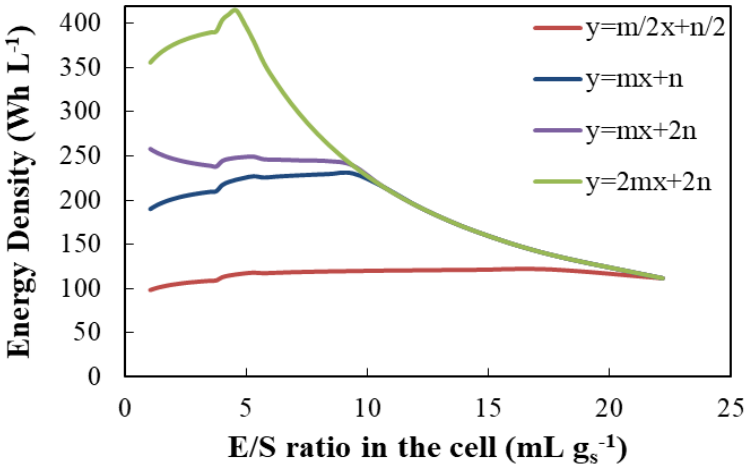

Figure 4. 63. The sensitivity analysis of the effect of the specific capacity on the energy density of the Li-S battery

Recently, Li-S battery companies have reached to 350-400 Wh kg^{-1} Li-S cells [22-25]. Especially, Oxis energy company has produced 400 Wh kg^{-1} and 321 Wh L^{-1} at the cell level; they expect that they will go beyond these values in the near future. The aim in this thesis is to develop models that can simply direct the researchers to reach the performance goals of the Li-S batteries by optimizing the cell design. At the cell level, the model with specific capacity defined as a function of the E/S ratio predicts a Li-S battery with138 Wh kg^{-1} and 230 Wh L^{-1}. This is the baseline condition for the model with cell design parameters as 9 mL g_s^{-1} E/S ratio, C/5 current density, 0.5 C/S ratio, 100 μm cathode thickness and 1.5 N/P ratio. As seen from the results, the baseline model does not reach the current Li-S cell performances; better performances can only be achieved with lower C/S ratios and higher S loadings. For example, with 8.3 mL g_s^{-1} E/S ratio, 150 μm cathode thickness, 0.125 C/S and 1.5 N/P ratio the best performance results predicted by the model is 172.5 Wh kg^{-1} and 260 Wh L^{-1}. On the other hand, the model with constant specific capacity has higher specific energy and energy density results. As a baseline 0.5 C/S ratio, 1.5 N/P ratio, C/5 current density, 100 μm cathode thickness and 0.89 mL g_s^{-1} E/S ratio are selected and at this point the model can reach up to 437 Wh kg^{-1} and 712 Wh L^{-1}. This clearly shows that in order to obtain high performance Li-S cells, high specific capacities should be attained at low E/S ratios. For example, one experimental study [33] from the literature presents a 400 Wh kg^{-1} Li-S cell with the following design parameters: 75% sulfur utilization, C/S ratio of 0.26 C/S ratio, N/P ratio of 1.5 and a current density of C/2. It is discussed that in order to exceed 500 Wh kg^{-1} specific energy with these design parameters, sulfur loading should be higher than 4 mg cm^{-2} and E/S ratio should be lower than 2.

For the system level performance model, the same discussions are valid. At the system level, the model with the specific capacity defined as a function of the E/S ratio predicts the maximum performance values for the baseline case as 111 Wh kg^{-1} and 111.2 Wh L^{-1} with 10 mL g_s^{-1} E/S ratio, 0.5 C/S ratio, 150 μm cathode thickness

and 1.5 N/P ratio. However, the best performance values predicted for the entire design parameters are 122.2 Wh kg^{-1} and 117.8 Wh L^{-1} reached at 8.87 mL g_s^{-1} E/S ratio, 200 μm cathode thickness and 0.125 C/S ratio. When the model has constant

specific capacity, the performance values increase to 324 Wh kg^{-1} and 332 Wh L^{-1} with 1 mL g_s^{-1} E/S ratio, 150 μm cathode thickness and 0.125 C/S ratio parameters. The system level model can reach the desired Li-S performance with constant specific capacity value at low E/S ratios. As a conclusion, the most critical issue in achieving high specific energy and energy density Li-S batteries (>400 Wh kg^{-1} and >400 Wh L^{-1}) is attaining high specific capacities (>1200 mAh g_S^{-1}) at low E/S ratios (< 3 mL g_S^{-1}) and low C/S ratios (<0.125).

CHAPTER 5

CONCLUSIONS

In this study, the effect of E/S ratio on the electrochemical performance and cell- and system-level energy density and specific energy of a Li-S battery is investigated. A 1-D concentration independent electrochemical model is proposed at isothermal, constant current discharge condition in order to observe the relation of current and voltage. The first assumption in the model is that there is no polysulfide shuttle mechanism in the cell. In addition, the model assumes that there is a single electrochemical reaction in the cathode for each of the two discharge plateaus. With this simplification, the cathode kinetics is defined with a single kinetic model parameter, cathode exchange current density ($i_{0,pe}$), for each of the discharge plateau. The model predicts the electrochemical performance by calculating the cell voltage at 60% depth of discharge. For the estimation of cell voltage, overpotential values are found at each E/S ratio. In the overpotential calculations, Butler-Volmer equation is used for the anode, Ohm's Law is used for the separator and the Porous Electrode Theory is used for the cathode. In the model, $i_{0,pe}$ is estimated by comparing the model predictions for the area-specific impedance with the experimental resistance measurements in the literature; therefore, $i_{0,pe}$ can capture the electrochemical and physical changes occurring within the cell. It is found that if $i_{0,pe}$ is fed into the model as a function of the electrolyte volume fraction in the cathode, the model can capture the experimental trends for the effect of E/S ratio on the electrochemical performance; cell voltage increases significantly with the E/S ratio up to a certain point and then slightly changes. In order to determine the dependency of $i_{0,pe}$ on the electrolyte amount, an experimental study in the literature, which observes the resistance responses of a cell to the changes in the electrolyte amount, is used. It is found that $i_{0,pe}$ is a linear function of the electrolyte volume fraction and so, increasing E/S ratio raises the cell voltage.

Next, the proposed electrochemical model is extended to predict the cell level performance of the cell. In the performance model, the cathode specific capacity is

either defined as a linear function of the E/S ratio based on the experimental trends or taken as a constant value. The model, in which the cathode specific capacity is dependent on the E/S ratio, predicts that the specific energy and energy density at the cell level increase until 10 mL g_s^{-1} with increasing E/S ratio and then, increasing ratio diminishes the cell level performance. The effect of other design parameters are also taken into account in the model. As a result, it is concluded that high thicknesses (>100μm), low C/S ratios (<C/S:0.5), and high sulfur loadings (>5 mg cm^{-2}) in the cathode, and low N/P ratios (<1.5) in the anode give the best cell level performances. Moreover, in order to understand the importance of the cathode specific capacity, it is taken as a constant value in the model. It is seen that at 1200 mAh g_s^{-1} of specific capacity, specific energy and energy density values are much higher. When the specific capacity is independent of the electrolyte amount in the model, increasing E/S ratio drops the cell level performance continuously. On the other hand, the effect of other design parameters are the same with the previous model that defines the specific capacity as a function of the E/S ratio.

After the investigation of the cell-level performance, the system-level performance of the battery is also studied with varying E/S ratios. The system-level performance model is based on the BatPac model, which is used for battery configuration and pack-level design. In the model, according to the specified energy and power values, required pack area and cell capacity are found. As in the cell level performance, 10 mL g_s^{-1} of E/S ratio gives the maximum specific energy and energy density at the system level and after this point, system performance starts to decrease when the cathode specific capacity is defined as a linear function of the E/S ratio in the model. However, when the cathode specific capacity is constant for all E/S ratios, the system-level energy density and specific energy decrease continuously with increasing electrolyte amount. The effect of maximum cathode thickness, C/S ratio and N/P ratio are also considered for both cases. Similar to the cell level performance model, higher thicknesses, lower C/S ratios and lower N/P ratios give better system-level performance. Mass and volume breakdown analysis are also done at both cell and system level. Finally, sensitivity analyses of $i_{0,pe}$ and specific capacity showed that the influence of $i_{0,pe}$ on the pack performance is less significant

than the influence of the cathode specific capacity. It can be concluded that the electrochemical, cell and system performance models proposed in this study can capture the impact of critical cell design parameters on the Li-S battery performance successfully.

For future studies, firstly, the electrochemical model can be improved with additional considerations. As known, E/S ratio affects the reaction kinetics in the cell and so, polysulfide shuttle mechanism (PSS) changes with changing E/S ratio. In the model, PSS effect is ignored to simplify the study. When this mechanism is added to the model, the changes in the reaction kinetics will be captured better. For observing the PSS effect, additional redox reactions that are caused by the polysulfides can be considered in the model. Therefore, multiple reaction rate constants will be used and overpotential calculations will be done based on each rate constant. Alternatively, in order to capture the polysulfide shuttle mechanism, a shuttle constant can be fed to the model as in the study of Mikhaylik and Akridge [30]. In addition, the electrochemical model can be enhanced by considering the accumulation of Li_2S on the cathode surface. As known, Li_2S is an insulating solid product and its precipitation influence the cell resistance and so the cell performance. In the model, it is not considered in the overpotential and ASI calculations. If the precipitation reaction is added to the model, Li_2S effect can be also captured. In addition to these recommendations on the improvement in the model assumptions about reaction kinetics, the model can also be improved with addition experimental data. The model contains two empirical equations which are the cathode exchange current density and specific capacity equations. They are obtained from the experimental studies in the literature. By a smart experimental design, these empirical equations can be obtained. For example, cathode exchange current density is determined by using cell resistance data. If the effect of E/S ratio on the cell resistance is obtained with the EIS method experimentally, cathode exchange current density equation in the model can be improved. Moreover, the cell voltage measurements with varying E/S ratio can be done and so, the cathode specific capacity equation will be also improved.

REFERENCES

[1] Y. Deng, J. Li, T. Li, X. Gao, C. Yuan, Life cycle assessment of lithium sulfur battery for electric vehicles, J. Power Sources. 343 (2017) 284–295. doi:10.1016/j.jpowsour.2017.01.036.

[2] N. Ding, S.W. Chien, T.S.A. Hor, Z. Liu, Y. Zong, Key parameters in design of lithium sulfur batteries, J. Power Sources. 269 (2014) 111–116. doi:10.1016/j.jpowsour.2014.07.008.

[3] S.H. Chung, C.H. Chang, A. Manthiram, Progress on the Critical Parameters for Lithium–Sulfur Batteries to be Practically Viable, Adv. Funct. Mater. 28 (2018) 1–20. doi:10.1002/adfm.201801188.

[4] J. Yan, X. Liu, B. Li, Capacity fade analysis of sulfur cathodes in lithium–sulfur batteries, Adv. Sci. 3 (2016). doi:10.1002/advs.201600101.

[5] M.K. Song, Y. Zhang, E.J. Cairns, A long-life, high-rate lithium/sulfur cell: A multifaceted approach to enhancing cell performance, Nano Lett. 13 (2013) 5891–5899. doi:10.1021/nl402793z.

[6] J.B. Dunn, L. Gaines, J. Sullivan, M.Q. Wang, Impact of recycling on cradle-to-gate energy consumption and greenhouse gas emissions of automotive lithium-ion batteries, Environ. Sci. Technol. 46 (2012) 12704–12710. doi:10.1021/es302420z.

[7] X. Ji, L.F. Nazar, Advances in Li-S batteries, J. Mater. Chem. 20 (2010) 9821–9826. doi:10.1039/b925751a.

[8] Y.X. Yin, S. Xin, Y.G. Guo, L.J. Wan, Lithium-sulfur batteries: Electrochemistry, materials, and prospects, Angew. Chemie - Int. Ed. 52 (2013) 13186–13200. doi:10.1002/anie.201304762.

[9] N. Erisen, N.B. Emerce, S.C. Erensoy, D. Eroglu, Modeling the effect of key cathode design parameters on the electrochemical performance of a lithium-sulfur battery, Int. J. Energy Res. 42 (2018) 2631–2642. doi:10.1002/er.4045.

[10] D. Eroglu, K.R. Zavadil, K.G. Gallagher, Critical Link between Materials Chemistry and Cell-Level Design for High Energy Density and Low Cost Lithium-Sulfur Transportation Battery, J. Electrochem. Soc. 162 (2015) A982–A990. doi:10.1149/2.0611506jes.

[11] J. Brückner, S. Thieme, H.T. Grossmann, S. Dörfler, H. Althues, S. Kaskel, Lithium-sulfur batteries: Influence of C-rate, amount of electrolyte and sulfur loading on cycle performance, J. Power Sources. 268 (2014) 82–87. doi:10.1016/j.jpowsour.2014.05.143.

[12] P.G. Bruce, S.A. Freunberger, L.J. Hardwick, J.M. Tarascon, Li-O_2 and Li-S batteries with high energy storage, Nat. Mater. 11 (2012) 19–29. doi:10.1038/nmat3191.

[13] M. Barghamadi, A. Kapoor, C. Wen, A Review on Li-S Batteries as a High Efficiency Rechargeable Lithium Battery, J. Electrochem. Soc. 160 (2013) A1256–A1263. doi:10.1149/2.096308jes.

[14] Y. Zhang, Y. Zhao, K.E. Sun, P. Chen, Development in Lithium/Sulfur Secondary Batteries, Open Mater. Sci. J. 5 (2011) 215–221. doi:10.2174/1874088X01105010215.

[15] M.K. Song, E.J. Cairns, Y. Zhang, Lithium/sulfur batteries with high specific energy: Old challenges and new opportunities, Nanoscale. 5 (2013) 2186–2204. doi:10.1039/c2nr33044j.

[16] S. Urbonaite, T. Poux, P. Novák, Progress Towards Commercially Viable Li-S Battery Cells, Adv. Energy Mater. 5 (2015) 1–20. doi:10.1002/aenm.201500118.

[17] W. Xue, L. Miao, L. Qie, C. Wang, S. Li, J. Wang, J. Li, Gravimetric and volumetric energy densities of lithium-sulfur batteries, Curr. Opin. Electrochem. 6 (2017) 92–99. doi:10.1016/j.coelec.2017.10.007.

[18] S.H. Kang, X. Zhao, J. Manuel, H.J. Ahn, K.W. Kim, K.K. Cho, J.H. Ahn, Effect of sulfur loading on energy density of lithium sulfur batteries, Phys. Status Solidi Appl. Mater. Sci. 211 (2014) 1895–1899. doi:10.1002/pssa.201330569.

[19] F.Y. Fan, M.S. Pan, K.C. Lau, R.S. Assary, W.H. Woodford, L.A. Curtiss, W.C. Carter, Y.-M. Chiang, Solvent Effects on Polysulfide Redox Kinetics and Ionic Conductivity in Lithium-Sulfur Batteries, J. Electrochem. Soc. 163 (2016) A3111–A3116. doi:10.1149/2.1181614jes.

[20] V.S. Kolosnitsyn, E. V. Karaseva, E. V. Kuzmina, A.L. Ivanov, Reasons for the effect of the amount of electrolyte on the performance of lithium–sulfur cells, Russ. J. Electrochem. 52 (2016) 273–282. doi:10.1134/S1023193516030071.

[21] A.F. Hofmann, D.N. Fronczek, W.G. Bessler, Mechanistic modeling of polysulfide shuttle and capacity loss in lithium-sulfur batteries, J. Power Sources. 259 (2014) 300–310. doi:10.1016/j.jpowsour.2014.02.082.

[22] Y. Mikhaylik, I. Kovalev, R. Schock, K. Kumerasan, J. Xu, J. Affinito, High Energy Rechargeable Li-S Cells for EV Application. Status, Remaining Problems and Solutions, Ecs Trans. 25 (2010) 23–34. doi: 10.1149/1.3414001.

[23] Y. Mikhaylik, I. Kovalev, J. Xu, R. Schock, Rechargeable Li-S Battery with Specific Energy 350 Wh/kg and Specific Power 3000 W/kg., Ecs Trans. 13 (2008) 53–59. doi: 10.1149/1.3018749.

[24] S.H. Chung, A. Manthiram, Rational Design of Statically and Dynamically Stable Lithium–Sulfur Batteries with High Sulfur Loading and Low Electrolyte/Sulfur Ratio, Adv. Mater. 30 (2018) 1–9. doi:10.1002/adma.201705951.

[25] T. Cleaver, P. Kovacik, M. Marinescu, T. Zhang, G. Offer, Perspective—Commercializing Lithium Sulfur Batteries: Are We Doing the Right Research?, J. Electrochem. Soc. 165 (2018) A6029–A6033. doi:10.1149/2.0071801jes.

[26] P. Sources, S. Zhang, Liquid Electrolyte Lithium / Sulfur Battery : Fundamental Chemistry , Problems , and Solutions ", 231 (2016) 153–162. doi:10.1016/j.jpowsour.2012.12.102.

[27] S. Urbonaite, P. Novák, Importance of “unimportant” experimental parameters in Li-S battery development, J. Power Sources. 249 (2014) 497–502. doi:10.1016/j.jpowsour.2013.10.095.

[28] K. Sun, A.K. Matarasso, R.M. Epler, X. Tong, D. Su, A.C. Marschilok, K.J. Takeuchi, E.S. Takeuchi, H. Gan, Effect of Electrolyte on High Sulfur Loading Li-S Batteries, J. Electrochem. Soc. 165 (2018) A416–A423. doi:10.1149/2.0071803jes.

[29] D. Lv, J. Zheng, Q. Li, X. Xie, S. Ferrara, Z. Nie, L.B. Mehdi, N.D. Browning, J.G. Zhang, G.L. Graff, J. Liu, J. Xiao, High Energy Density Lithium-Sulfur Batteries: Challenges of Thick Sulfur Cathodes, Adv. Energy Mater. 5 (2015) 1–8. doi:10.1002/aenm.201402290.

[30] Y. V. Mikhaylik, J.R. Akridge, Polysulfide Shuttle Study in the Li/S Battery System, J. Electrochem. Soc. 151 (2004) A1969. doi:10.1149/1.1806394.

[31] G. Xu, B. Ding, J. Pan, P. Nie, L. Shen, X. Zhang, High performance lithium-sulfur batteries: Advances and challenges, J. Mater. Chem. A. 2 (2014) 12662–12676. doi:10.1039/c4ta02097a.

[32] J. Gao, H.D. Abruña, Key parameters governing the energy density of rechargeable Li/S batteries, J. Phys. Chem. Lett. 5 (2014) 882–885. doi:10.1021/jz5001819.

[33] P. Bonnick, E. Nagai, J. Muldoon, Perspective—Lithium-Sulfur Batteries, J. Electrochem. Soc. 165 (2018) A6005–A6007. doi:10.1149/2.0031801jes.

[34] J.S. Newman, C.W. Tobias, Theoretical Analysis of Current Distribution in Porous Electrodes, J. Electrochem. Soc. 109 (1962) 1183. doi:10.1149/1.2425269.

[35] J.W. Choi, J.K. Kim, G. Cheruvally, J.H. Ahn, H.J. Ahn, K.W. Kim, Rechargeable lithium/sulfur battery with suitable mixed liquid electrolytes, Electrochim. Acta. 52 (2007) 2075–2082. doi:10.1016/j.electacta.2006.08.016.

[36] S.S. Zhang, Improved cyclability of liquid electrolyte lithium/sulfur batteries by optimizing electrolyte/sulfur ratio, Energies. 5 (2012) 5190–5197. doi:10.3390/en5125190.

[37] J. Zheng, D. Lv, M. Gu, C. Wang, J.-G. Zhang, J. Liu, J. Xiao, How to Obtain Reproducible Results for Lithium Sulfur Batteries?, J. Electrochem. Soc. 160 (2013) A2288–A2292. doi:10.1149/2.106311jes.

[38] M. Hagen, P. Fanz, J. Tübke, Cell energy density and electrolyte/sulfur ratio in Li-S cells, J. Power Sources. 264 (2014) 30–34. doi:10.1016/j.jpowsour.2014.04.018.

[39] F.Y. Fan, Y.-M. Chiang, Electrodeposition Kinetics in Li-S Batteries: Effects of Low Electrolyte/Sulfur Ratios and Deposition Surface Composition, J. Electrochem. Soc. 164 (2017) A917–A922. doi:10.1149/2.0051706jes.

[40] M.J. Lacey, Influence of the Electrolyte on the Internal Resistance of Lithium−Sulfur Batteries Studied with an Intermittent Current Interruption Method, ChemElectroChem. 4 (2017) 1997–2004. doi:10.1002/celc.201700129.

[41] S.-E. Cheon, K.-S. Ko, J.-H. Cho, S.-W. Kim, E.-Y. Chin, H.-T. Kim, Rechargeable Lithium Sulfur Battery, J. Electrochem. Soc. 150 (2003) A796. doi:10.1149/1.1571533.

[42] S. Chen, Y. Gao, Z. Yu, M.L. Gordin, J. Song, D. Wang, Nano Energy High capacity of lithium-sulfur batteries at low electrolyte / sulfur ratio enabled by an organosul fi de containing electrolyte, Nano Energy. 31 (2017) 418–423. doi:10.1016/j.nanoen.2016.11.057.

[43] D. Lu, Q. Li, J. Liu, J. Zheng, Y. Wang, S. Ferrara, J. Xiao, J.G. Zhang, J. Liu, Enabling High-Energy-Density Cathode for Lithium-Sulfur Batteries, ACS Appl. Mater. Interfaces. 10 (2018) 23094–23102. doi:10.1021/acsami.8b05166.

[44] K. Kumaresan, Y. Mikhaylik, R.E. White, A Mathematical Model for a Lithium–Sulfur Cell, J. Electrochem. Soc. 155 (2008) A576. doi:10.1149/1.2937304.

[45] M. Marinescu, T. Zhang, G.J. Offer, A zero dimensional model of lithium-sulfur batteries during charge and discharge, Phys. Chem. Chem. Phys. 18 (2016) 584–593. doi:10.1039/c5cp05755h.

[46] D.N. Fronczek, W.G. Bessler, Insight into lithium-sulfur batteries: Elementary kinetic modeling and impedance simulation, J. Power Sources. 244 (2013) 183–188. doi:10.1016/j.jpowsour.2013.02.018.

[47] M. Ghaznavi, P. Chen, Analysis of a Mathematical Model of Lithium-Sulfur Cells Part III: Electrochemical Reaction Kinetics, Transport Properties and Charging, Electrochim. Acta. 137 (2014) 575–585. doi:10.1016/j.electacta.2014.06.033.

[48] M. Ghaznavi, P. Chen, Sensitivity analysis of a mathematical model of lithium-sulfur cells part I: Applied discharge current and cathode conductivity, J. Power Sources. 257 (2014) 394–401. doi:10.1016/j.jpowsour.2013.10.135.

[49] M. Ghaznavi, P. Chen, Sensitivity analysis of a mathematical model of lithium-sulfur cells: Part II: Precipitation reaction kinetics and sulfur content, J. Power Sources. 257 (2014) 402–411. doi:10.1016/j.jpowsour.2013.12.145.

[50] K. Yoo, M.K. Song, E.J. Cairns, P. Dutta, Numerical and Experimental Investigation of Performance Characteristics of Lithium/Sulfur Cells, Electrochim. Acta. 213 (2016) 174–185. doi:10.1016/j.electacta.2016.07.110.

[51] T. Zhang, M. Marinescu, S. Walus, G.J. Offer, Modelling transport-limited discharge capacity of lithium-sulfur cells, Electrochim. Acta. 219 (2016) 502–508. doi:10.1016/j.electacta.2016.10.032.

[52] S. Risse, S. Angioletti-Uberti, J. Dzubiella, M. Ballauff, Capacity fading in lithium/sulfur batteries: A linear four-state model, J. Power Sources. 267 (2014) 648–654. doi:10.1016/j.jpowsour.2014.05.076.

[53] T. Zhang, M. Marinescu, L. O'Neill, M. Wild, G. Offer, Modeling the voltage loss mechanisms in lithium-sulfur cells: The importance of electrolyte resistance and precipitation kinetics, Phys. Chem. Chem. Phys. 17 (2015) 22581–22586. doi:10.1039/c5cp03566j.

[54] Y.X. Ren, T.S. Zhao, M. Liu, P. Tan, Y.K. Zeng, Modeling of lithium-sulfur batteries incorporating the effect of Li_2S precipitation, J. Power Sources. 336 (2016) 115–125. doi:10.1016/j.jpowsour.2016.10.063.

[55] S.M. Al-Mahmoud, J.W. Dibden, J.R. Owen, G. Denuault, N. Garcia-Araez, A simple, experiment-based model of the initial self-discharge of lithium-sulphur batteries, J. Power Sources. 306 (2016) 323–328. doi:10.1016/j.jpowsour.2015.12.031.

[56] V. Thangavel, K.-H. Xue, Y. Mammeri, M. Quiroga, A. Mastouri, C. Guéry, P. Johansson, M. Morcrette, A.A. Franco, A Microstructurally Resolved Model for Li-S Batteries Assessing the Impact of the Cathode Design on the Discharge Performance, J. Electrochem. Soc. 163 (2016) A2817–A2829. doi:10.1149/2.0051614jes.

[57] B.D. McCloskey, Attainable Gravimetric and Volumetric Energy Density of Li-S and Li Ion Battery Cells with Solid Separator-Protected Li Metal Anodes, J. Phys. Chem. Lett. 6 (2015) 4581–4588. doi:10.1021/acs.jpclett.5b01814.

[58] M. Cuisinier, P.E. Cabelguen, B.D. Adams, A. Garsuch, M. Balasubramanian, L.F. Nazar, Unique behaviour of nonsolvents for polysulphides in lithium-sulphur batteries, Energy Environ. Sci. 7 (2014) 2697–2705. doi:10.1039/c4ee00372a.

[59] K.G. Gallagher, S. Goebel, T. Greszler, M. Mathias, W. Oelerich, D. Eroglu, V. Srinivasan, Quantifying the promise of lithium-air batteries for electric vehicles, Energy Environ. Sci. 7 (2014) 1555–1563. doi:10.1039/c3ee43870h.

[60] P. A. Nelson, K.G. Gallagher, I. Bloom, D.W. Dees, Modeling the Performance and Cost of Lithium-Ion Batteries for Electric-Drive Vehicles Chemical Sciences and Engineering Division, Second Edition, Next Gener. Energy Storage Conf. (2017) 116. doi:http://dx.doi.org/10.3133/fs20143035.

[61] D. Eroglu, S. Ha, K.G. Gallagher, Fraction of the theoretical specific energy achieved on pack level for hypothetical battery chemistries, J. Power Sources. 267 (2014) 14–19. doi:10.1016/j.jpowsour.2014.05.071.

[62] K.G. Gallagher, P.A. Nelson, D.W. Dees, Simplified calculation of the area specific impedance for battery design, J. Power Sources. 196 (2011) 2289–2297. doi:10.1016/j.jpowsour.2010.10.020.

[63] N.A. Cañas, K. Hirose, B. Pascucci, N. Wagner, K.A. Friedrich, R. Hiesgen, Investigations of lithium-sulfur batteries using electrochemical impedance spectroscopy, Electrochim. Acta. 97 (2013) 42–51. doi:10.1016/j.electacta.2013.02.101.

[64] L. Yuan, X. Qiu, L. Chen, W. Zhu, New insight into the discharge process of sulfur cathode by electrochemical impedance spectroscopy, J. Power Sources. 189 (2009) 127–132. doi:10.1016/j.jpowsour.2008.10.033.

APPENDICES

A. The Electrochemical Model for the Porous Cathode Electrode

For porous cathode in the Li-S cell, the Porous Electrode Theory developed by Newman and Tobias is used [34]. When the theory is applied to the model, the following assumptions are made: (1) In the lower discharge plateau, there is a single electrochemical reaction, (2) there is no change in the concentrations within the cell, (3) there is no velocity in the cathode, (4) the discharge-charge reactions are symmetric and (5) there is no double layer charging. According to Ohm's Law, currents of matrix and electrolyte are defined as in Equations A.1 and A.2. In addition, conservation of charge is shown in Equation A.3. The polarization equation for the charge transfer, which is from the matrix phase to the electrolyte phase, is given in Equation A.4. Boundary conditions are chosen as Equation A.5 and Equation A.6 based on Figure A.1.

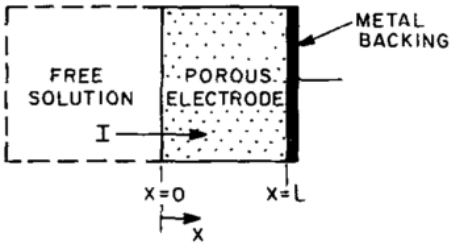

Figure A. 1. 1-D Porous Cathode Electrode [34]

$$i_1 = -\sigma_{eff} \frac{d\phi_1}{dx} \tag{A.1}$$

$$i_2 = -\kappa_{eff} \frac{d\phi_2}{dx} \tag{A.2}$$

$$\frac{di_1}{dx} + \frac{di_2}{dx} = 0 \tag{A.3}$$

$$\nabla.i_2=ai_{0,pe}\left[\exp\left(\frac{\alpha_a F}{RT}(\phi_1-\phi_2)\right)-\exp\left(\frac{\alpha_c F}{RT}(\phi_1-\phi_2)\right)\right] \quad (A.4)$$

$$\text{At } x=0\ ,\ i_2=I \ \text{ and } \ \phi_2=0 \quad (A.5)$$

$$\text{At } x=L\ ,\ i_1=I \quad (A.6)$$

In order to determine the current and voltage relation, overpotential of the cathode is derived based on either Tafel or Linear kinetics. The model is studied at the cathodic case of the polarization curve as discussed below.

Tafel Kinetics: $|I|>a\ i_{0,pe}L_{pe}$

Equation A.4 is simplified for the cathodic Tafel case as in Equation A.7. By defining dimensionless parameters (Equation A.8) and their boundary conditions(Equations A.10 and A.11), a dimensionless differential equation and its analytical solution are obtained as given in Equations A.9 and A.12, respectively.

$$\frac{di_2}{dx}=-a\ i_{0,pe}\ \exp\left[-\frac{\alpha_{pe,c}F}{RT}(\phi_1-\phi_2)\right] \quad (A.7)$$

$$y=\frac{x}{L_{pe}},\quad j=\frac{i_1}{-I}\ ,\ \beta=\frac{\alpha_{pe,c}F}{RT},\quad \delta=L_{pe}|I|\beta\left(\frac{1}{\kappa_{eff}}+\frac{1}{\sigma_{eff}}\right),\ \epsilon=\frac{L_{pe}|I|\beta}{\kappa_{eff}} \quad (A.8)$$

$$\frac{d^2j}{dy^2}=\frac{dj}{dy}(\delta j-\epsilon) \quad (A.9)$$

$$\text{At } y=0,\quad j=0 \quad (A.10)$$

$$\text{At } y=1,\quad j=1 \quad (A.11)$$

$$\phi_1(L)-\phi_2(0)=\ \frac{1}{\beta}\left\{(\delta-\epsilon)\left[\frac{\epsilon}{\delta}+\frac{2}{\delta}\ln\sec(\theta-\psi)\right]+\frac{2\epsilon}{\delta}\ln\sec\psi+\ln\left(\frac{2|I|\theta^2}{ai_{0,pe}L_{pe}\delta}\right)\right\} \quad (A.12)$$

where $\theta=\arctan\frac{2\delta\theta}{4\theta^2-\epsilon(\delta-\epsilon)}$ and $\psi=\arctan\frac{\epsilon}{2\theta}$

Linear Kinetics: $|I|<a\, i_{0,pe} L_{pe}$

For the linear kinetics, Equation A.4 is simplified into Equation A.13. The overpotential calculated for the linear kinetics by defining the following dimensionless parameters and the boundary conditions (Equations A.14-A.16) is given in Equation A.17.

$$\frac{di_2}{dx}=\left(\alpha_{pe,a}+\alpha_{pe,c}\right)\frac{a\, i_{0,pe}\, F}{RT}(\phi_1-\phi_2) \tag{A.13}$$

$$y=\frac{x}{L_{pe}},\ j=\frac{i_1}{-I}\ ,\ \nu^2=\left(\alpha_{pe,a}+\alpha_{pe,c}\right)\frac{F\times a\times i_{0,pe}\times L_{pe}^{\ 2}}{RT}\left(\frac{1}{\kappa_{eff}}+\frac{1}{\sigma_{eff}}\right) \tag{A.14}$$

$$\frac{d^2j}{dy^2}-\nu^2\left(j-\frac{\sigma_{eff}}{\sigma_{eff}+\kappa_{eff}}\right)=0 \tag{A.15}$$

$$\begin{aligned}&\text{At } y=0,\quad j=0\\&\text{At } y=1,\quad j=1\end{aligned} \tag{A.16}$$

$$\phi_1(L)-\phi_2(0)=\frac{I\times Lpe}{\kappa_{eff}+\sigma_{eff}}\left[1+\frac{2+\left(\frac{\sigma_{eff}}{\kappa_{eff}}+\frac{\kappa_{eff}}{\sigma_{eff}}\right)\cosh\nu}{\nu\sinh\nu}\right] \tag{A.17}$$

B. I-V Relations for System Level Performance Model

In the system level performance model, based on Bat-Pac and Eroglu's study Ip and Ve are calculated by iterations in the VBA code as shown in Equations B.1 and B.2 [10, 60]. First, an initial guess is given for both Ip and Ve, and the overpotential and ASI for the cell is calculated using Equations B.3-B.8 accordingly. Then, using the total overpotential and the ASI estimated by the electrochemical model, the model recalculates the Ip and Ve values by Equations B.1 and B.2.

$$Ip=Ipnew=\frac{0.2\times U}{ASI_{total,p}} \tag{B.1}$$

$$Ve=Venew=U-\eta_{total,e} \tag{B.2}$$

$$\eta_{total\ p,e}=\eta_{pe,p,e}+\eta_{ne,p,e}+\eta_{sep,p,e}+\eta_{cc-,p,e}+\eta_{cc+,p,e} \tag{B.3}$$

$$ASI_{total\ ,p,e}=ASI_{pe,p,e}+ASI_{ne,p,e}+ASI_{sep,p,e}+ASI_{cc-,p,e}+ASI_{cc+,p,e} \tag{B.4}$$

Positive Electrode

For power calculation;

Tafel Kinetics; $|Ip|>a\times i_o\times L_{pe}$

$$\eta_{pe,p}=\frac{1}{\beta}\left\{(\delta-\epsilon)\left[\frac{\epsilon}{\delta}+\frac{2}{\delta}\ln\sec(\theta-\psi)\right]+\frac{2\epsilon}{\delta}\ln\sec\psi+\ln\left(\frac{2|I_p|\theta^2}{ai_{0,pe}L_{pe}\delta}\right)\right\} \tag{B.5}$$

Linear Kinetics; $|Ip|<a\times i_o\times L_{pe}$

$$\eta_{pe,p}=\frac{I_p\times Lpe}{\kappa_{eff}+\sigma_{eff}}\left[1+\frac{2+\left(\frac{\sigma_{eff}}{\kappa_{eff}}+\frac{\kappa_{eff}}{\sigma_{eff}}\right)\cosh\nu}{\nu\sinh\nu}\right] \tag{B.6}$$

$$ASI_{pe,p}=\frac{\eta_{pe}}{Ip} \tag{B.7}$$

For energy calculation;

Tafel Kinetics; $|Ie|>a\times i_o\times L_{pe}$

$$\eta_{pe,e}=\frac{1}{\beta}\left\{(\delta-\epsilon)\left[\frac{\epsilon}{\delta}+\frac{2}{\delta}\ln\sec(\theta-\psi)\right]+\frac{2\epsilon}{\delta}\ln\sec\psi+\ln\left(\frac{2|Ie|\theta^2}{ai_{0,pe}L_{pe}\delta}\right)\right\} \quad (B.8)$$

Linear Kinetics; $|Ie|<a\times i_o\times L_{pe}$

$$\eta_{pe,e}=\frac{I_e\times Lpe}{\kappa_{eff}+\sigma_{eff}}\left[1+\frac{2+\left(\frac{\sigma_{eff}}{\kappa_{eff}}+\frac{\kappa_{eff}}{\sigma_{eff}}\right)\cosh\nu}{\nu\sinh\nu}\right] \quad (B.9)$$

$$ASI_{pe,e}=\frac{\eta_{pe}}{Ie} \quad (B.10)$$

Negative Electrode

$$\eta_{ne,p}=\frac{R\times T}{\alpha_{li}\times F}\times\operatorname{asinh}\left(\frac{I_p}{2i_o}\right) \quad (B.11)$$

$$ASI_{ne,p}=\frac{\eta_{ne,p}}{|I_p|} \quad (B.12)$$

$$\eta_{ne,e}=\frac{R\times T}{\alpha_{li}\times F}\times\operatorname{asinh}\left(\frac{I_e}{2i_o}\right) \quad (B.13)$$

$$ASI_{ne,e}=\frac{\eta_{ne,e}}{|I_e|} \quad (B.14)$$

Separator

$$ASI_{sep,p}=\frac{L_{sep}}{\kappa_{sep}} \quad (B.15)$$

$$\eta_{sep,p}=ASI_{sep,p}\times|I_p| \quad (B.16)$$

$$ASI_{sep,e}=\frac{L_{sep}}{\kappa_{sep}} \quad (B.17)$$

$$\eta_{sep,e}=ASI_{sep,e}\times|I_e| \quad (B.18)$$

Negative Current Collector

$$ASI_{cc-,p}=\text{resistance}\times A_{layer} \tag{B.19}$$

$$\eta_{cc-,p} = ASI_{cc^-,p}\times I_p \tag{B.20}$$

$$ASI_{cc-,e}=\text{resistance}\times A_{layer} \tag{B.21}$$

$$\eta_{cc-,e} = ASI_{cc^-,e}\times I_e \tag{B.22}$$

Positive Current Collector

$$ASI_{cc+,p}=\text{resistance}\times A_{layer} \tag{B.23}$$

$$\eta_{cc+,p} = ASI_{cc^+,p}\times I_p \tag{B.24}$$

$$ASI_{cc+,e}=\text{resistance}\times A_{layer} \tag{B.25}$$

$$\eta_{cc+,e} = ASI_{cc^+,e}\times I_e \tag{B.26}$$

C. I-V Relations with Maximum Thickness Limitation

In this part, the same electrochemical equations with Appendix B are used based on Bat-Pac model and Eroglu's study [10, 60]. However, when the calculated cathode thickness exceeds the maximum allowed thickness in the model, cathode thickness is set as a constant value at the maximum thickness. Consequently, the model recalculates the cell area, I_p and V_e accordingly. The revised equations with the maximum thickness limitation are given below. In addition, in the VBA code, only the Ip value is iterated. V_E is already set because cell capacity is calculated by the set cathode thickness.

$$\text{Ipnew} = \frac{\text{P}}{\text{Ncell}\times\ \text{Acell}\ \times\text{Vp}} \tag{C.1}$$

$$\text{Vp}=\text{U}-\eta_{\text{total,p}} \tag{C.2}$$

$$\text{A}_{\text{cell}}=\frac{\text{Q}}{\text{L}_{\text{pos.electrode at adj OCV\%}}\times\text{c}_{\text{pe}}} \tag{C.3}$$

$$\text{A}_{\text{layer}}=\frac{\text{A}_{\text{cell}}}{\text{Number of layers per cell}} \tag{C.4}$$

$$\text{A}_{\text{pack}}=\text{A}_{\text{cell}}\times\text{number of cell} \tag{C.5}$$

D. Battery Configuration

In the battery configuration part, there are some parameters that are used for the model [10, 60] and they are given in Table D1. Each part of the battery pack is designed separately. Therefore, cell, module and battery design are explained below step by step.

Table D.1. Parameters for battery configuration.

Target % OCV at full power	80%
OCV at full power cell (OCV at 20% SOC)	2.2V
Open circuit voltage average for discharge (OCV at 50% SOC)	2.2V
Limiting current density(mA/cm2)	85
Limiting C-rate(A/Ah)	100
Cell terminal contact voltage loss % of cell OCV	0.01

Cell Design

For the cell design, a prismatic cell in a stiff-pouch container, which is a commonly used type, is chosen [60]. There are positive and negative electrodes which have aluminum and copper current collector foils, respectively. Terminals of the cell have approximately similar size with the cell and they are welded to current collector tabs. The cell container has tri-layers, which are polyethylene terephthalate (PEP), 0.1-mm aluminum and polypropylene (PP). Moreover, aluminum conduction channel is used for liquid based thermal management of heat rejection. The size and mass of the cell are determined using below equations.

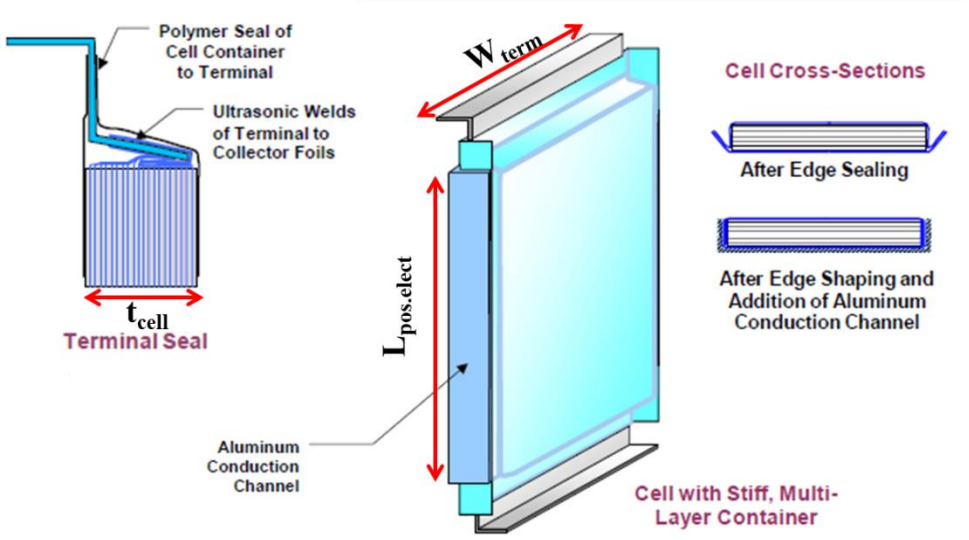

Figure D. 1.The cell configuration (adapted from [60])

$$\text{Length of current collector tabs (mm)} = t_{cell} + 8 \quad \text{(D.1)}$$

$$\text{Length of terminals(mm)} = 2\, t_{cell} + 10 \quad \text{(D.2)}$$

$$\text{Thickness of terminals(mm)} = 1 \quad \text{(D.3)}$$

$$\text{Width of terminals(mm)} = W_{pos.elect.} - 8 \quad \text{(D.4)}$$

$$\text{Pouch thickness (mm)} = 0{,}1 \quad \text{(D.5)}$$

$$\text{Thickness of cell container aluminum layer } (\mu m)=100 \tag{D.6}$$

$$\text{Thickness of cell container(PET-Al-PP)}(\mu m)=30+t_{\text{cell container Al layer}}+20 \tag{D.7}$$

$$\text{Density of cell container } \left(\frac{g}{cm^3}\right)=2.2 \tag{D.8}$$

$$\text{Length-to-width ratio for positive electrode}\left(\frac{L}{W}\right)=3 \tag{D.9}$$

$$\text{Thickness of cell edge from pos. elect to outside of fold } (mm)=1 \tag{D.10}$$

$$\text{Top of positive electrode to top of terminal } (mm)=15 \tag{D.11}$$

$$\text{Number of bicell layers}=\frac{\text{Number of layers}}{2} \tag{D.12}$$

$$\text{Width of positive electrode } (mm)=\sqrt{\frac{A_{layer}}{\left[\frac{L}{W}\right]_{\text{pos. electrode}}}} \tag{D.13}$$

$$\text{Length of positive electrode } (mm)=\frac{A_{layer}}{W_{pos.elect.}} \tag{D.14}$$

$$\text{Width of cell } (mm)=W_{pos.elect.}+2(t_{\text{cell edge from pos. eletrode to outside of fold}}) \tag{D.15}$$

$$\text{Length of cell } (mm)=L_{pos.elect.}+2(L_{\text{top of pos.elect. to top of term}}) \tag{D.16}$$

$$\begin{aligned}\text{Thickness of cell } (mm)=&(\text{Number of bicell layers}+1)\times t_{neg.foil}\\&+(\text{Number of bicell layers})\times t_{pos.foil}\\&+(2\text{Number of bicell layers})\times\left(t_{\text{pos. elect. at adj. OCV}}+t_{\text{neg. elect. at adj. OCV}}+t_{sep}\right)\\&+2\,t_{pouch}\end{aligned} \tag{D.17}$$

$$\text{Volume of cell } (cm^3)=W_{cell}\times L_{cell}\times t_{cell} \tag{D.18}$$

$$\text{Positive foil area}(m^2)=\text{Number of bicell layer}\times(W_{pos.elect.})\times \tag{D.19}$$

$$(L_{pos.elect.}+L_{cc\ tabs})$$

$$\text{Negative foil area}(m^2)=(\text{Number of bicell layer}+1)\times(W_{pos.elect.}+2)\times(L_{pos.elect.}+L_{cc\ tabs}+2) \quad (D.20)$$

$$\text{Separator area}(m^2)=(2\text{Number of bicell layers})\times((W_{pos.elect.}+4)\times(L_{pos.elect.}+6) \quad (D.21)$$

$$\text{Electrolyte volume (L)}=\frac{m_{ne}}{\rho_{ne,total}}\times v_e+\frac{m_{pe}}{\rho_{pe,total}}\times v_e+A_{sep}\times L_{sep}\times \text{void vol}+t_{cell}\times L_{pos.elect.}\times W_{pos.elect.}\times\frac{0.02}{1000} \quad (D.22)$$

$$\text{Positive terminal assembly mass (g)}=\rho_{pos.\ foil}\times L_{term}\times t_{term}\times W_{term} \quad (D.23)$$

$$\text{Negative terminal assembly mass (g)}=\rho_{neg.\ foil}\times L_{term}\times t_{term}\times W_{term} \quad (D.24)$$

$$\text{Cell container (PET-Al-PP)mass(g)}=(W_{cell}+2t_{cell}+6)\times(L_{cell}-6)\times 2t_{cell\ container}\times\rho_{cell\ container} \quad (D.25)$$

$$\text{Active material mass in pos. elect.(g)}=\frac{\text{cell capacity}}{\text{positive active material capacity}} \quad (D.26)$$

$$\text{Carbon and binder mass in pos. elect. (g)}=w_{c,b}\times\text{total mass} \quad (D.27)$$

$$\text{Total mass of positive electrode (g)}=\frac{\text{active material mass}}{w_{pe,act}} \quad (D.28)$$

$$\text{S loading in the electrode}\left(\frac{mg}{cm^2}\right)=\frac{\text{active material mass}}{A_{cell}} \quad (D.29)$$

$$\text{Electrolyte in pos. elect. (g)}=\frac{\text{total mass}}{\rho_{total}}\times Ve\times\rho_{electrolyte} \quad (D.30)$$

$$\text{Active material in neg. elect. (g)}=\frac{\text{cell capacity}}{\text{neg. act. material capacity}}\times\frac{N}{P} \quad (D.31)$$

$$\text{Total mass of negative electrode (g)}=\frac{\text{active material mass}}{w_{ne,act}} \quad (D.32)$$

$$\text{Cell mass (g)} = m_{pe} + m_{ne} + \left(A_{neg.foil} \times L_{neg\ foil} \times \rho_{neg.\ foil}\right) + (A_{pos.foil} \times L_{pos.\ foil} \times \rho_{pos.\ foil}) + (L_{sep} \times \rho_{sep} \times A_{sep}) + V_{electrolyte} \times \rho_e + m_{pos.\ terminal\ assembly} + m_{neg.\ terminal\ assembly} + m_{cell\ container} \quad \text{(D.33)}$$

$$\frac{E}{S}\text{ratio}\ \left(\frac{mL}{g}\right) = \frac{V_{electrolyte}}{m_{active\ material\ in\ pos.\ electrode}} \quad \text{(D.34)}$$

$$\text{Electrolyte mass\% in the cell} = \frac{V_{electrolyte} \times \rho_e}{\text{cell mass}} \quad \text{(D.35)}$$

Module Design

For the module design 0.5-mm thick aluminum is used and the entrance of water vapor and electrolyte losses from the cell are prevented with the sealing of the module. The size and mass of the module are determined using the following equations.

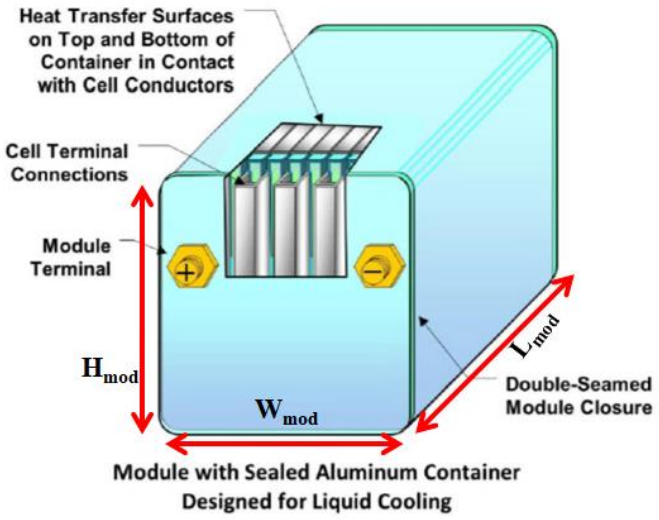

Figure D. 2. The module configuration (adapted from [60])

$$\text{Module capacity (Ah)} = \text{cell group capacity} \quad \text{(D.36)}$$

$$\text{Rate of terminal temperature rise at full power} = 0.05\ C^0/s \tag{D.37}$$

$$\text{Terminal heating factor (W/g)} = \text{rate of term. temp. rise at full power x } Cp_{\text{copper}} \tag{D.38}$$

$$\text{Terminal resistance factor (A-ohms/cm)} = \left(\frac{\text{terminal heating factor x } \rho_{Cu}}{\sigma_{Cu}}\right)^{0.5} \tag{D.39}$$

$$\text{Module terminal resistance both terminal (ohms)} = \begin{cases} \text{if number of modules per battery pack} = 1\ ; \\ 0x\ \dfrac{2}{\text{max current at full power}}\ x\ \text{terminal resistance factor} \\ \text{if not}\ ; \\ 2x\ \dfrac{2}{\text{max current at full power}}\ x\ \text{terminal resistance factor} \end{cases} \tag{D.40}$$

$$\text{Mass of each cell group interconnect (g)} = \begin{cases} \text{if number of cells in parallel} = 1\ ;\ 0 \\ \text{if not}\ ; = \text{number of cells in parallel} \times t_{cell} \times \dfrac{t_{term}}{2} \times W_{term} \times 1.5 \times \rho_{Cu} \end{cases} \tag{D.41}$$

$$\text{Module SOC regulator assembly (g)} = \frac{8 \times \text{number of cells per module}}{\text{number of cells in parallel}} \tag{D.42}$$

$$\text{Module terminals (g)} = \begin{cases} \text{if Number of modules per battery pack} = 1\ ;\ 0 \\ \text{if not}\ ; \\ 2x\ \dfrac{2 \times \text{max current at full power} \times \text{terminal resistance factor}}{\text{terminal heating factor}}\ x1{,}2 \end{cases} \tag{D.43}$$

$$\text{Length of cooling fin (mm)} = L_{\text{pos.elect.}} \tag{D.44}$$

$$\text{Thickness of cooling fin} = 1\ \text{mm} \tag{D.45}$$

$$\text{Total mass of cooling fin(g)}=\frac{\text{number of cell per module}}{2}\times L_{\text{cooling fin}}\ x\ \left(W_{\text{cell}}+2t_{\text{cooling fin}}\right)\times t_{\text{cooling fin}}\times\rho_{Al}\times 0.5 \quad \text{(D.46)}$$

$$\text{Balance of module materials (g)}=\rho_{Al}xt_{\text{module wall}}\ x\ \left(L_{\text{module}}\ x\ W_{\text{module}}+L_{\text{module}}x\ H_{\text{module}}+W_{\text{module}}\ x\ H_{\text{module}}\right)x2 \quad \text{(D.47)}$$

$$\text{Module length(mm)}=L_{\text{cell}}+2\ t_{\text{module wall}} \quad \text{(D.48)}$$

$$\text{Module width(mm)}=\left(t_{\text{cell}}+\frac{t_{\text{cooling fin}}}{2}\right)\times(\text{number of cells per module}+1)+2\ t_{\text{mod. wall}} \quad \text{(D.49)}$$

$$\text{Module height(mm)}=W_{\text{cell}}+2\ t_{\text{module wall}}+2\ t_{\text{cooling fin}} \quad \text{(D.51)}$$

$$\text{Module volume (L)}=L_{\text{module}}\ x\ W_{\text{module}}xH_{\text{module}} \quad \text{(D.52)}$$

$$\text{Module mass (kg)}=\left(\frac{\text{mass of each cell group interconnect}\times\text{number of cells per module}}{\text{number of cells in parallel}}+1\right)+\text{number of cells per module}\times m_{\text{cell}}+m_{\text{module SOC regulator assembly}}+m_{\text{module terminals}}+m_{\text{total mass of cooling fin}}+m_{\text{balance of module materials}} \quad \text{(D.53)}$$

Battery Design

In the battery pack, interconnection between the negative and positive terminals of the modules is provided with the help of copper connectors. Also, compression force is exerted to the modules via steel bands. In order to ensure the flow capability of heat transfer fluid which is ethylene glycol-water solution, a tray that is on the top and bottom of the battery jacket is used. Furthermore, the battery jacket is made of

aluminum sheet and with 10 mm thickness. All size and mass calculations of the battery pack is given below.

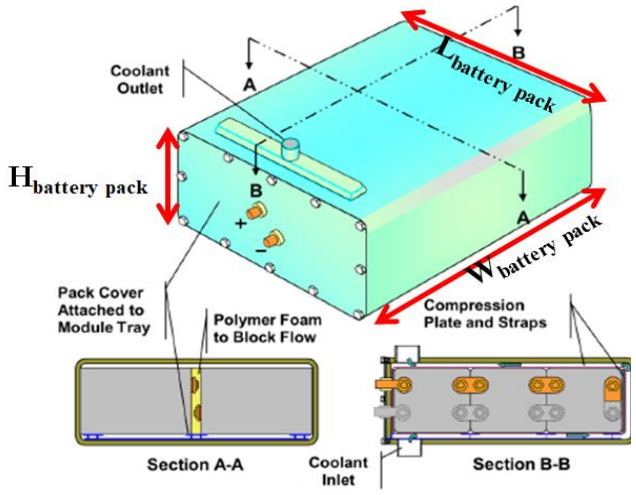

Figure D. 3. The battery configuration (adapted from [60])

$$\text{Battery pack capacity(Ah)} = \text{module capacity x number of modules in parallel} \tag{D.54}$$

$$\text{Total battery pack energy storage (kWh)} = \text{cell group capacity} \times \text{number of modules in parallel} \times \left(\text{nominal battery voltage-cells per battery pack} \times \frac{\text{cell capacity}}{5} \times \frac{ASI_{\text{total cell energy}}}{A_{cell} \times \text{number of(cells in parallel} \times \text{modules in parallel)}}\right) \tag{D.55}$$

$$\text{Useable battery energy storage(kWh)} = \text{total pack energy x selected energy \%} \tag{D.56}$$

$$\text{Thickness of module compression plates (steel)} = 1.5 \text{ mm} \tag{D.57}$$

$$\text{Coolant space above and below modules} = 20 \text{ mm} \tag{D.58}$$

$$\text{Battery pack insulation thickness} = 10 \text{ mm} \tag{D.59}$$

$$\text{Battery jacket total thickness (mm)} = t_{\text{battery pack insulation}} + 2 \text{ if module volume x Number of modules per battery pack} < 20 ; 1 , \text{ if module volume x number of modules per battery pack} < 40; 1{,}5 \text{ if not; } 2 \tag{D.60}$$

$$\text{Pack integration unit (BMS \& disconnects)} = 4L \tag{D.61}$$

$$\text{Battery pack length (A dimension) (mm)} = 2t_{\text{module compression plates (steel)}} + L_{\text{coolant space above and below modules}} + 2t_{\text{total battery jacket}} + W_{\text{module}} \text{ x number of modules in row} \tag{D.62}$$

$$\text{Battery pack width (B dimension) (mm)} = L_{\text{module}} \text{ x number of rows of m (if (number of rows of modules per pack = 1; 8, if = 2 ; 10 , "if =4 ; 20)} + 2x\ t_{\text{total battery jacket}} \tag{D.63}$$

$$\text{Battery pack height (C dimension) (mm)} = 2t_{\text{total battery jacket}} + 2\ L_{\text{coolant space above and below modules}} + H_{\text{module}} \tag{D.64}$$

$$\text{Volume of battery pack and integration unit (L)} = (L_{\text{Battery pack}} \text{ x } H_{\text{Battery pack}} \text{x } W_{\text{Battery pack}}) + V_{\text{Pack integration unit}} \tag{D.65}$$

$$\text{Mass of each module inter-connect (5-cm long)(g)} = \frac{5 \times \text{terminal resist. factor} \times \text{max curr. at full power}}{\text{terminal heating factor}} \times 1.2 \tag{D.66}$$

$$\text{Mass of module compression plates and steel straps (g)} = 2t_{\text{module compression plates}} \text{ x } (W_{\text{Battery pack}} - 2t_{\text{total battery jacket}}) \text{x } (H_{\text{Battery pack}} - 2t_{\text{total battery jacket}}) \text{x } \rho_{\text{stainless steel}} \tag{D.67}$$

$$\text{Power of battery heaters} = 3\ \text{kW} \tag{D.68}$$

$$\text{Mass of battery pack heaters (0.1 kg/kW)} = \text{Power of battery heaters} \times 0.1\ \text{kg} \tag{D.69}$$

$$\text{Battery coolant mass within jacket (kg)} = L_{\text{coolant space above and below modules}} \times L_{\text{module}} \times \frac{2}{3} \times W_{\text{module}} + \left(\left(\frac{\text{number of cells per module}}{2} \right) \times L_{\text{cooling fin}} \times \left(W_{\text{cell}} + 2t_{\text{cooling fin}} \right) \times t_{\text{cooling fin}} \times 0.5 \right) \times \text{number of modules per battery pack} \times \rho_{\text{coolant}} \tag{D.71}$$

$$\text{Battery jacket mass parameter (g/cm2)} = (t_{\text{battery pack insulation}} \times \rho_{Cu}) + (t_{\text{total battery jacket}} - t_{\text{battery pack insulation}}) \times \rho_{Al} \tag{D.72}$$

$$\begin{aligned}\text{Battery jacket mass (kg)} = {} & 2\left(L_{\text{battery pack}} - L_{\text{total battery jacket}}\right) \times \left(W_{\text{battery pack}} - L_{\text{total battery jacket}}\right) + \\ & 2\left(L_{\text{battery pack}} - L_{\text{total battery jacket}}\right) \times \left(H_{\text{battery pack}} - L_{\text{total battery jacket}}\right) + \\ & 2\left(W_{\text{battery pack}} - L_{\text{total battery jacket}}\right) \times \left(H_{\text{battery pack}} - L_{\text{total battery jacket}}\right) \times \\ & \text{battery jacket mass parameter} + \\ & (\text{number of modules per battery pack} + 1) \times \\ & m_{\text{each module interconnect}} + m_{\text{module compression plates and steel straps}}\end{aligned} \tag{D.73}$$

$$\text{Pack integration unit (BMS \& disconnects, ave. density = 1.0)} = \text{Pack integration unit (BMS \& disconnects) kg} \tag{D.74}$$

$$\text{Mass of battery pack and integration unit (kg)} = m_{\text{battery coolant within jacket}} + m_{\text{Battery jacket}} + \text{Pack integration unit} + \text{number of modules per battery pack} \times \text{module mass} \tag{D.75}$$

$$\text{Battery mass (kg)} = \text{Mass of battery pack and integration unit} \tag{D.76}$$

$$\text{Battery volume (L)} = \text{Volume of battery pack and integration unit} \tag{D.77}$$

$$\text{Nominal battery voltage (OCV at 50\% SOC) (V)} = \frac{\text{cells per battery pack}}{\text{number of cells in parallel}} \times \frac{\text{OCV average for discharge (OCV at 50\% SOC)}}{\text{number of modules in parallel}} \tag{D.78}$$

$$\text{OCV at full power battery (OCV at 20\% SOC) (V)} = \frac{\text{cells per battery pack}}{\text{number of cells in parallel}} \times \frac{\text{OCV at full power cell}}{\text{number of modules in parallel}} \tag{D.79}$$

$$\text{Maximum current at full power (A)} = \frac{\text{total pack power}}{\frac{\text{Vp}}{\text{U}} \times \text{OCVat full power battery}} \tag{D.80}$$

where $\rho_{\text{stainless steel}}$, ρ_{Cu} and ρ_{Al} are the stainless steel, copper and aluminum density in g cm^{-3}, σ_{Cu} is the copper conductivity in $\Omega^{-1}\text{cm}^{-1}$.

For determining the nominal battery voltage of the battery, OCV is a good approximation so, OCV average for the discharge of the cell can be used as given in Equation D.78. Likewise, cell OCV at full power is used for the OCV at full power battery as shown in Equation D.79. Maximum current at full power of the battery is obtained with Equation D.80 in order to calculate the ASI of the battery.

ASI Calculation

In the battery, many physical and electrochemical processes that affect the resistance of the battery occur simultaneously. ASI is the measure of total resistances in a battery pack; it is calculated for all pack components such as cell, module and battery terminals, and module interconnects resistances. ASI calculations are shown in Equations from D.81 to D.91. Moreover, cooling system requirements are

determined via heat generation rate calculations that are given in Equations D.92 and D.93.

$$\text{Electrode system ASI for power at SOC for vehicle type(ohm-cm2)} = \text{ASIp} - \text{cell hardware and battery ASI} \tag{D.81}$$

$$\text{Current collector resistance parameter(ohms)} = \frac{2}{\sigma_{Al} \times t_{Al\ CC}} + \frac{2}{\sigma_{Cu} \times t_{Cu\ CC}} \tag{D.82}$$

$$\text{Current collector ASI (ohmscm2)} = \text{CC resistance parameter} \times \frac{L_{pos.elect.}^{2}}{3} + L_{pos.elect.} \times L_{cc\ tabs.} \tag{D.83}$$

$$\text{Cell terminal and connection ASI (ohms-cm2)} = \frac{\frac{10}{\sigma_{Al}} + \frac{10}{\sigma_{Cu}}}{t_{term}} \times \frac{L_{term.}}{W_{term.}} \times A_{cell} + \text{cell terminal contact voltage loss} \times \frac{\text{OCV at full power cell}}{\text{max current at full power}} \times A_{cell} \tag{D.84}$$

$$\text{Resistance of module interconnects if more than one module (ohms)} = (\text{Number of modules per battery pack} - 1) \times 2 \times \left(\frac{3 \times \text{terminal resistance factor}}{\text{max. current at full power}}\right) \tag{D.85}$$

$$\text{Resistance of battery pack terminals (ohms)} = 2 \times \frac{3 \times \text{terminal resistance factor}}{\text{max. current at full power}} \tag{D.86}$$

$$\text{Resistance of module and pack per module (ohms)} = \text{Module terminal resistance both terminal} + \text{Resistance of module interconnects if more than one module} + \frac{\text{Resistance of battery pack terminals}}{\text{Number of}(\text{modules per battery pack} \times \text{modules in parallel}^2)} \tag{D.87}$$

$$\text{Resistance of module and pack hardware per cell (ohms)} = \frac{\text{Resistance of module and pack per module}}{\text{Number of cells per module} \times \text{number of cells in parallel}^2} \tag{D.88}$$

$$\text{Total cell hardware and battery ASI (ohm-cm2)} = \text{Current collector ASI} + \text{Cell terminal and connection ASI} + \text{Resistance of module and pack hardware per cell} \times A_{cell} \tag{D.89}$$

$$\text{Total cell ASI for power (ohm-cm2)} = ASI_p \tag{D.90}$$

$$\text{Total cell ASI for energy (C/5 rate)(ohm-cm2)} = \text{Total cell hardware and battery ASI} + ASI_e \tag{D.91}$$

Battery Cooling System

$$\text{Resistance, sustained power (W)} = \frac{\frac{\text{Total cell ASI for energy (C/5 rate)}}{A_{cell}} \times \text{Cells per battery pack}}{\text{number of cells in parallel}^2 \times \text{number of modules in parallel}^2} \tag{D.92}$$

$$\text{Heat generation rate for battery system (W)} = \text{Resistance, sustained power (W)} \times \left(\frac{\text{Battery pack capacity}}{5}\right)^2 \tag{D.93}$$